THE CHARACTERIZATION OF THE ROLE OF MYELOID TRANSLOCATION GENE 16 IN HEMATOPOIETIC PROGENITOR AND STEM CELL FUNCTIONS

By

Melissa Ann Fischer

Dissertation

Submitted to the Faculty of the

Graduate School of Vanderbilt University

in partial fulfillment of the requirements

for the degree of

DOCTOR OF PHILOSOPHY

in

Biochemistry

December, 2011

Nashville, Tennessee

Approved:

Professor Scott Hiebert

Professor David Cortez

Professor Bruce Carter

Professor Stephen Brandt

Professor Christine Eischen

This dissertation is dedicated to the memory of my friend, Michelle Gronendyke. She and I were best friends from the time we were in the nursery together at church. I always looked up to Michelle as we were growing up, but I never could have imagined how much I would learn from her after she was diagnosed with leukemia as her life was supposed to be just beginning. I remember during one of my visits to see her in the hospital, she asked me what I wanted to do with my degree. I knew the answer, but I felt so guilty telling her I wanted to go into cancer research, because I knew there was nothing I could do to help her. However, instead of a response of self-pity and bitterness I was expecting, she told me that was great because we needed people like that. The fact that she could sit there and think of how that would help other people, while she herself was so sick, became a defining moment for me. Remembering how she faced her too early death with courage and faith, her example has given me the extra motivation I needed during the tough times in graduate school.

In loving memory,

Michelle Jean Gronendyke

July 11, 1980- July 6, 2001

ACKNOWLEDGEMENTS

If I may quote Charles Dickens (A Tale of Two Cities), I think the best way to describe my graduate student career is with the saying, "It was the best of times, it was the worst of times." I have found that graduate school is not for the faint of heart, but I can also look back and realize how much I have grown and learned over the years throughout this process. I would be remiss however if I did not acknowledge the people who have been there for me along the way.

I must start by thanking my mentor, Dr. Scott Hiebert, for taking a chance on me five years ago when I was a budding IGP student. Over the last five years, I have been afforded the ability to grow as a scientist by being able to perform almost any experiment I could imagine, attend national conferences, and be entrusted to train numerous rotation students. These opportunities have shaped me into the scientist I am today, who can design informative experiments, present my data, and mentor future students. These skills will benefit me no matter what career path I decide to take. I must also thank my committee members, Dr. Stephen Brandt, Dr. Bruce Carter, Dr. David Cortez, and Dr. Christine Eischen, for all of their support over the years and helpful comments that have guided my project along the way. I must especially thank Dr. Brandt and Dr. Eischen for their kind words of encouragement that gave me the extra boost of confidence that I needed at times. Dr. Eischen was an especially great mentor to me these past few years that always had an open door for me when I needed advice or someone to talk to, and for that, I am beyond grateful.

This experience would not have been the same without all of the current and past members of the Hiebert Lab. For starters, I am greatly indebted to Dr. Isabel Moreno-Miralles for both bringing humor to the lab, and for taking me under her wing and teaching me everything I know about flow cytometry and bone marrow transplants. By learning these skills so early in my graduate career, I was able to progress some really fun projects as I built more techniques on top of the basics she taught me. Additionally, Dr. Srividya Bhaskara and I shared many late nights together in the lab over the years discussing a lot about science and life. From these discussions, she has been such a great mentor and has become a really close friend. I would also like to thank Dr. Chris Williams, Dr. Amy Moore, and Dr. Alyssa Summers for their guidance and support even after they left the lab. Dr. Laura DeBusk has done a great job filling their shoes; she is such a great encourager. And of course I am most thankful for the graduate students I have had the privilege of sharing this journey with. Dr. Tiffany Ellis-Farmer and Dr. Sarah Knutson were here when I started and gave such great advice about quals, dissertation writing, dealing with lab issues, and even general life issues! I was lucky to start this rollercoaster ride along with Dr. Aubrey Hunt. We've shared quals, conferences, rejected papers, and even dissertation writing together, and let me tell you, it would not have been the same without a friend to go through each new hurdle along with you. Finally, I never knew that offering to take on a rotation student would lead to me finding one of my best friends that I get to work with everyday. Christina Wells, I don't know what I would have done without you to confide in and I wish you the very best in whatever your life brings you. You have all been such great colleagues, and I look forward to the life-long friendships we will share!

Due to unique circumstances, I must give a special acknowledgement to Dr. Aubrey Hunt and Christina Wells. I know everyone always thanks their fellow lab members, but you both deserve special recognition for going above and beyond the duties of normal lab mates. After the car accident, I experienced at least 5 months of complete physical and emotional distress from barely being able to walk and feeling like my career as a scientist was getting stripped away from me. On top of your own experiments and everything else you each had going on, you both helped me on a daily basis get through both the physical and emotional pain I was enduring by harvesting mice for me, carrying ice buckets that I couldn't hold, or simply talking to me to encourage me. You both exemplified true friendship and really being there to pick someone up when they've fallen. Words could never describe how much that meant to me, and I don't think I could have gotten through those months in the lab without you.

In addition to lab mates, graduate school has brought me into contact with many great people. Dave Flaherty and Brittany Matlock are two amazing people that work in the flow core, and since I pretty much spent half of my graduate career running samples down there, we have really became such great friends. Thank you both for your humor and helping me keep my spirits high even on crazy, stressful days when I had to start at 5AM to get ready for my sort! Though we met late in our graduate careers on our trip together to St. Jude, Laura Gordy-Kees and Dr. Mandy Linkous and I quickly became great friends and have been there for each other during some important times at the end of graduate school.

Outside of work, I have been lucky to be involved in two great churches that have fostered really great friendships to help me on this journey. I have enjoyed so many

times with John and Megan Kellis, Jeremy and Sarah Skiles, and Danielle Kizzire. The fun times we have shared definitely helped take my mind off the science when I needed it and made me feel a little less lonely as I was away from my family. Though there were miles between us, Christine Woerner, Christy Singleton, and Dave Southern were only a phone call away and have always had my back.

Last, but not least, I must thank all of my wonderful family. To know that I have so many people who love and support me has been such a comfort. To my sister and brother-in-law, Megan and Damian, thank you for making it a point to come down each July to celebrate my birthday with me. Having that to look forward to each summer helped me push through a lot of long work days. I love you both, and especially my little niece, Maddie, who has brought such joy to my life. To my parents, John and Diane, thank you for always believing in me, and even more so, teaching me to believe in myself. Thank you for showing me the meaning of hard work and dedication, and for bringing me up on the foundations of faith. Most importantly, thank you for loving me unconditionally, and for being the best parents a girl could ask for. To my husband, Daniel, thank you for supporting me in my career, even if you don't always understand it. As you continually say, 'we are a team', so thank you for standing by me and carrying this team when I am overloaded. We have been through a lot, and I look forward to all of the years we have ahead of us as we go through this journey of life together. Finally, I would like to thank God for blessing me with such amazing people in my life who have helped get me where I am today, and who keep making me a better person with each new day.

TABLE OF CONTENTS

LIST OF FIGURES

LIST OF TABLES

LIST OF ABBREVIATIONS

AML	Acute myeloid leukemia
AML1/ETO	Fusion protein formed by the t(8;21)
AOM	Azoxymethane
B220	CD45R/B220 B cell antigen
Bcl2	B-cell CLL/lymphoma 2
BCL6	B-cell lymphoma 6 protein
BM	Bone marrow
BMT	Bone marrow transplant
BrdU	Bromodeoxyuridine
c-Kit	CD117 antigen, stem cell factor receptor
c-Myc	v-myc myelocytomatosis viral oncogene homolog
C/EBP	CCAAT/enhancer binding protein
C/EBP α	CCAAT/enhancer binding protein, alpha
C/EBP δ	CCAAT/enhancer binding protein, delta
C/EBP ε	CCAAT/enhancer binding protein, epsilon
CAFC	Cobblestone area-forming cell assay
CBF	Core binding factor
Ccnd1	Cyclin D1
CD150	Signaling lymphocytic activation molecule family member 1 (Slamf1)
CD34	Hematopoietic progenitor cell antigen CD34
CD48	CD48 Antigen

CD52	CD52 molecule
CD69	CD69 molecule
CD71	Transferrin receptor (p90, CD71)
Cdc25b	Cell division cycle 25 homolog B
CDK	Cyclin dependent kinase
Cdk2	Cyclin-dependent kinase 2
cDNA	Complimentary DNA
CFC	Colony forming cell
CFSE	Carboxyfluorescein diacetate, succinimidyl ester
CFU-S	Colony forming unit-spleen assay
$CFU\text{-}S_{12}$	Colony forming unit-spleen day 12 assay
$CFU\text{-}S_{8}$	Colony forming unit-spleen day 8 assay
ChIP	Chromatin immunoprecipitation
CMP	Common myeloid progenitor
CRA	Competitive repopulation assay
Cxcr4	Chemokine (C-X-C motif) receptor 4
DNA	Deoxyribonucleic acid
DSS	Dextran sodium sulfate
E2A	Transcription factor 3 (E12/E47)
E2F	E2F transcription factor
E2F2	E2F transcription factor 2
E47	E2A immunoglobulin enhancer binding factors E12/E47
Ela2	Elastase, neutrophil expressed

ENU	N-ethyl-N-nitrosurea
EPO	Erythropoietin
EpoR	Erythropoietin receptor
ES cells	Embryonic stem cells
Eto2	Eight Twenty One 2, also known as MTG16
FACS	Fluorescence activated cell sorting
FCγR	Fc gamma receptor
Fli1	Friend leukemia virus integration 1
Flt3	Fms-related tyrosine kinase 3
Fos	FBJ murine osteosarcoma viral oncogene homolog
Gadd45β	Growth arrest and DNA-damage-inducible, beta
Gata1	GATA binding protein 1
Gata3	GATA binding protein 3
GEO	Gene expression omnibus database
Gfi1	Growth factor independent 1 transcription factor
Gfi1β	Growth factor independent 1B transcription factor
GMP	Granulocyte monocyte progenitor
Gr-1	Myeloid differentiation antigen Gr-1
H & E	Hematoxylin & Eosin
HDAC	Histone deacetylase
Hes1	Hairy and enhancer of split 1, (Drosophila)
Hes5	Hairy and enhancer of split 5
HO	Hoechst

HoxB2	Homeobox B2
HSC	Hematopoietic stem cell
HSPC	Hematopoietic stem and progenitor cell
Id1	Inhibitor of DNA binding 1
Id2	Inhibitor of DNA binding 2
IL	Interleukin
Klf5	Kruppel-like factor 5
KO	Knockout
LIC	Leukemia-initiating cell
Lmo2	LIM domain only 2
LMPP	Lymphoid-primed multipotent progenitor
LSC	Leukemia stem cell
LSK	Lineage Negative/Sca-1+/c-Kit+
LT-HSC	Long-term hematopoietic stem cell
LTC-IC	Long-term culture- initiating cell assay
Lyl1	Lymphoblastic leukemia derived sequence 1
Mac-1	Antigen CD11b
MDS	Myelodysplastic syndrome
Mef2c	Myocyte enhancer factor 2C
MEL	Murine erythroleukemia
MEP	Myeloid erythroid progenitor
MPP	Multipotent progenitor
mRNA	Messenger RNA

MSCV	Murine stem cell virus
MTG	Myeloid translocation gene
Mtg16	Myeloid translocation gene on chromosome 16 protein
MTG8	Myeloid translocation gene on chromosome 8 protein
Mtgr1	Myeloid translocation gene-related protein 1
N-CoR	Nuclear receptor corepressor
N-myc	v-myc myelocytomatosis viral related oncogene, neuroblastoma derived
N-myc	v-myc myelocytomatosis viral related oncogene, neuroblastoma derived (avian)
NHR	Nervy homology region
$p18^{ink4}$	Cyclin-dependent kinase inhibitor 2C (p18, inhibits CDK4)
p21	Cyclin-dependent kinase inhibitor 1A
p27	Cyclin-dependent kinase inhibitor 1B
Pax2	Paired box 2
PB	Peripheral blood
PCR	Polymerase chain reaction
PHZ	Phenylhydrazine
PLCγ	Phospholipase C, gamma
PLZF	Promyelocytic leukemia zinc finger protein
PU.1	Spi1 transcription factor
PY	Pyronin
Q-RT-PCR	Quantitative real-time PCR
Raf	v-raf-1 murine leukemia viral oncogene homolog

RNA	Ribonucleic acid
RT-PCR	Real-Time PCR
RUNX1	also known as AML1
Sca1	Stem cell antigen 1 (Ly6a)
SCF	Stem cell factor (c-Kit ligand)
SCL	Stem cell leukemia (also know as Tal1)
SLAM	Signaling lymphocyte activating molecule
Socs2	Suppressor of cytokine signaling 2
Socs3	Suppressor of cytokine signaling 3
SP	Side population
ST-HSC	Short-term hematopoietic stem cell
Stat1	Signal transducer and activator of transcription 1
Tal1	T-cell acute lymphocytic leukemia protein 1 (also known as SCL)
TCF4	Transcription factor 4
Ter119	TER-119 erythroid antigen
TF	Transcription factor
Tif1γ	Tripartite motif-containing 33
TPO	Thrombopoietin
Wnt	Wingless-type MMTV integration site family
WT	Wild typ

CHAPTER I

INTRODUCTION

Chromosomal translocations disrupt master regulatory genes that control cellular proliferation, apoptosis, and the lineage decisions of progenitor cells [1, 2]. Indeed, a critical component in the development of acute leukemia is the shunting of stem cells or multipotent progenitor cells towards a specific lineage, which also must acquire the ability to self-renew, to give rise to a specific form of acute myeloid leukemia. The Myeloid Translocation Gene on chromosome 16 (MTG16, also known as ETO-2 or *CBFA2T3*) and Myeloid Translocation Gene on chromosome 8 (MTG8, also known as Eight-Twenty-one or ETO) are disrupted by the t(16;21) and t(8;21), respectively. In addition to mutations in acute leukemia, *MTG8* and *MTG16* have also been identified as candidate cancer genes in other tissues [3-5]. Although a great deal of information has been gathered about the molecular interactions of the MTG family members through the analysis of the leukemia-related fusion proteins, less is known about the physiological functions of this gene family. Thus, the analysis of the normal functions of the MTG family is critical to our understanding of the development of acute leukemia, and how mutations of MTG family members contribute to tumorigenesis in other organ systems.

Acute Myeloid Leukemia (AML)

Description of the disease

Acute myeloid leukemia (AML) is a heterogeneous disease of the blood-forming cells in the bone marrow (BM) and is the most common type of leukemia in adults. The age-adjusted incidence rate for 2010 was 3.5 per 100,000 men and women per year, and the associated death rate was 2.8 per 100,000 men and women per year. Upon onset of disease, immature leukemic cells rapidly accumulate in the myeloid lineage, usually with a block in their maturation, and prevent the normal blood cells from performing their regular functions. Due to this replacement of normal BM cells with the leukemic cells, the signs of AML consist of a decrease in red blood cells, platelets, and normal white blood cells, which results in symptoms such as fever, weakness and fatigue, loss of weight and appetite, aches and pains in the bones or joints, and easy bruising and bleeding [6]. As an acute leukemia, the disease progresses quickly and can be fatal within weeks or months if it is not treated. However, depending on the genetic abnormality that is present in the leukemic cells, a potential cure is attainable with continued research into future therapies.

Approximately 55% of adult patients with *de novo* AML typically contain non-random chromosome translocations and/or gene rearrangements [7]. Several of these known gene rearrangements involve the juxtaposition of a transcriptional activator that retains its DNA binding motif with a protein that is capable of recruiting a corepressor complex [8]. Thus, a commonly accepted model for disease formation is that the fusion protein aberrantly recruits corepressor complexes to the DNA binding regions of the

coactivators. This in turn alters expression of target genes necessary for myeloid development and thereby lays the foundation for leukemic transformation. A total of 749 recurrent translocations have been identified to date; however, the four most common recurrent fusion proteins are PML-RARα, AML1-ETO, CBFβ-MYH11, and MLL-fusions, which together account for approximately 30% of AML cases [8]. It is commonly believed that the translocation fusion proteins target key hematopoietic regulators and thereby disrupt the normal differentiation program. Although these translocations are very common and therefore important for disease formation, they are in fact weak oncogenes and are insufficient to cause leukemia by themselves. This has led to the idea of a 'two-hit' hypothesis for leukemogenesis [7]. In general, the chromosomal translocations are often accompanied by mutations that affect receptor tyrosine kinases (RTKs), such as FLT3 and c-KIT, or N-RAS or K-RAS, which are downstream of the kinases [7].

Core binding factor leukemias

Two of the most common translocations in AML disrupt the core binding factor (CBF) transcription factor, which is comprised of two subunits (Figure 1). The CBFα subunit, AML1 (also known as RUNX1) is part of the RUNT family of TFs that possesses the RUNT DNA binding domain in its N-terminus [9]. The CBFβ subunit is a smaller protein that interacts with RUNX1 to enhance its binding to DNA. The two most common translocations that disrupt these CBF proteins are the t(8;21) and inv(16), which produce the AML1-ETO and CBFβ-MYH11 fusion proteins, respectively [7].

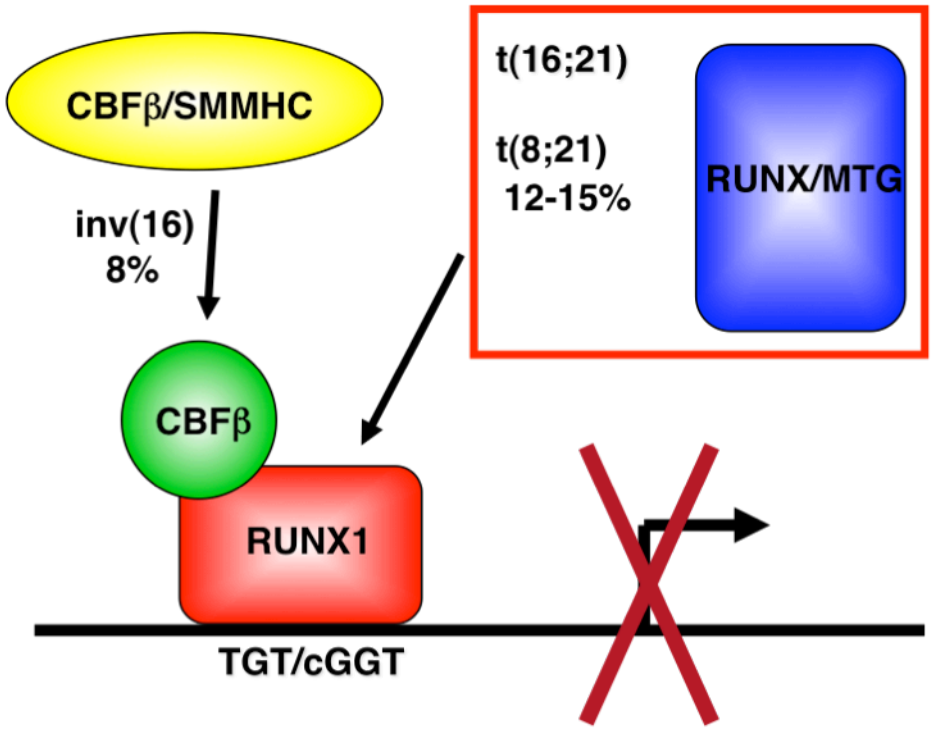

Figure 1. Core binding factor leukemias. Graphical representation of two of the most common translocations in AML that form fusion proteins with the CBF transcription factor, which is comprised of two subunits. The t(8;21) disrupts the CBFα subunit (RUNX1), and inv(16) disrupts the CBFβ subunit.

AML1-ETO, t(8;21)

The fusion protein AML1-ETO is formed by the t(8;21) translocation, accounts for 10-12% of d*e novo* AML [10-16], and is generally associated with a favorable prognosis [8]. This fusion protein links the N-terminal DNA binding domain of AML1 (also known as RUNX1) to almost all of the Myeloid Translocation Gene on chromosome 8, MTG8 (also known as ETO or RUNX1T1) protein [13]. The t(8;21) translocation is found in approximately 40% of the French-American-British (FAB) subtype M2 AML, but it is not restricted to this subtype [6]. The FAB subtype M2 classifies it as an AML with maturation. As with other translocations in AML, AML1-ETO requires cooperating mutations to promote leukemia. Two of the most common genetic abnormalities that are associated with AML1-ETO are mutations in c-Kit and Flt3 signaling molecules [7]. It is worth noting that a similar, yet rare, translocation exists between RUNX1 and a related family member of MTG8. The t(16;21) translocation links RUNX1 with Myeloid Translocation Gene on chromosome 16, MTG16 (also known as ETO2 or CBFA2T3), and is associated with therapy-related AML [17].

RUNX1 is a transcription factor that activates transcription by recruiting coactivators to enhancer core motifs (TGT/cGGT), which are present in a number of genes involved in myeloid and lymphoid development [9]. It has been confirmed to be a master regulator of hematopoiesis, as *RUNX1*$^{-/-}$ embryos die due to hemorrhage and a complete lack of definitive hematopoiesis [18, 19]. To bypass the embryonic lethality, conditional deletions of *RUNX1* have also been generated to determine the effects of RUNX1 on adult hematopoiesis. Loss of *RUNX1* in the adult mouse resulted in marked reductions in common lymphoid progenitors and mature B cells and maturation defects in

T cells and platelet production [20, 21]. Conversely, *RUNX1*-deficient mice contained an increase in myeloid progenitors and peripheral blood neutrophils, which resulted in a mild myeloproliferative phenotype. Therefore, in addition to its requirement for definitive hematopoiesis, RUNX1 is important for hematopoietic differentiation of multiple lineages in adult hematopoiesis.

The MTG family interacts with repressor proteins such as histone deacetylases (HDACs) and nuclear receptor corepressor (N-CoR) to act as transcriptional corepressors. The AML1-ETO fusion protein contains the RUNX1 DNA binding domain such that it retains the ability to bind to RUNX1 target genes; however, the corepressor activity of the MTG moiety results in a dominant repression of RUNX1-regulated genes [22, 23]. This has been confirmed in various reporter assays that show how AML1-ETO functions as a dominant repressor of wild-type RUNX1 transcriptional activation, which in turn leads to the repression of tumor suppressor genes and genes that are required for hematopoietic differentiation such as $p14^{ARF}$, *Neurofibromatosis-1*, *PU.1*, and *C/EBP*α [24-27].

Due to the importance of AML1-ETO in the pathogenesis of human AML, numerous attempts have been made to design a mouse model to study the biological effects of this fusion protein and learn how it could lead to AML. The first attempts tried to create a chimeric murine/human hybrid of AML1-ETO by mimicking the t(8;21) in the mouse germline [28, 29]. Similar to $AML1^{-/-}$ mice, the knock-in mice that were heterozygous for the AML1-ETO allele died from lethal hemorrhage in the embryos. To bypass the embryonic lethality from the AML1-ETO fusion protein, transgenic mice with conditional expression of the fusion protein in BM cells were created, but yielded only

modest phenotypes [30]. In addition, bone marrow (BM) or hematopoietic stem and progenitor cells (HSPCs) that had been retrovirally transduced to express the AML1-ETO fusion protein were used to reconstitute lethally irradiated mice to create a tissue-specific transgenic allele [31]. Though these approaches led to high expression of the fusion protein in the BM cells, this was not sufficient for the mice to develop spontaneous AML.

Taking into account the fact that the translocation fusion proteins in AML usually require cooperating mutations to cause disease, a number of labs began testing this theory in their murine models. At first, AML1-ETO-positive mice were treated with N-ethyl-N-nitrosurea (ENU), which efficiently induces single base mutations [31, 32]. These studies supported the notion that more than one mutation is required for development of leukemia, because in contrast to untreated AML1-ETO mice, 30-55% of those mice that received ENU treatment developed AML with many features mimicking that of human t(8;21) AML. However, since ENU is a non-specific DNA damaging agent, a small percentage of the mice came down with T-cell leukemias in both the wild-type and AML1-ETO expressing animals. This implies that while AML1-ETO is not solely sufficient to cause disease, it was required for the development of myeloid disease in this model.

Numerous labs have built upon the ENU studies by combining AML1-ETO expression with specific additional mutations, such as activating mutations in the receptor kinases TEL-PDGFRβ [33], c-Kit [34], or FLT3 [35], overexpression of Wilms' tumor gene [36], or deficiencies of ICSBP (interferon consensus sequence-binding protein) [37] or p21/waf1 [38]. All of these mutations facilitated leukemia formation in the recipients,

which further corroborates the two-hit hypothesis for leukemogenesis, and provide excellent backgrounds to study the development of AML by the t(8;21) translocation.

Most recently, a truncated form of AML1-ETO that does not require additional mutations to form leukemia has been discovered [39, 40]. More importantly, alternately spliced isoforms of t(8;21) in AML were also found to exist in human patient samples. This truncation lacks amino acids 576-752 in MTG8, which deletes a domain for N-CoR/SMRT interaction, and resulted in a rapid onset of leukemia in transplant recipients. This truncated form of AML1-ETO was termed AML1-ETO9a [39]. Later experiments showed that co-expression of the truncated form with full-length AML1-ETO resulted in an even earlier onset of leukemia with a block in myeloid differentiation at a more immature stage [39]. In addition, these authors also found that the oligimerization domain was crucial for AML1-ETO9a leukemogenesis [41]. This requirement of the NHR2 domain for leukemogenesis insinuates that the normal function of MTG family members could be important for the development of leukemia, as binding to the fusion protein would diminish their ability to bind to their normal transcription factors. Hence, the study of the normal functions of MTG proteins would garner key information about how the AML1-ETO fusion protein leads to the formation of leukemia.

Myeloid Translocation Gene (MTG) Family

Identification and functions

As previously mentioned, this family was first recognized by the discovery of the t(8;21) translocation, which resulted in the AML1-ETO fusion protein [13]. Although

MTG8 was a novel protein at the time this translocation was discovered, it is the founding member of a family of proteins that include MTG16 and Myeloid Translocation Gene-Related Protein 1 (MTGR1, also known as CBFA2T2). The ability of the t(8;21) fusion protein to repress transcription suggested that the MTG family members act as transcriptional corepressors. Since this family does not directly bind to DNA, they function by linking DNA-binding transcription factors to class I HDACs and other corepressors, such as mSin3 and N-CoR/SMRT (Figure 2). As expected for transcriptional corepressors, MTG family members are recruited by many site-specific DNA binding proteins, including Gfi1, Gfi1B, TAL1/SCL, the "E proteins" E2A and HEB, BTB-POZ domain factors BCL6 and PLZF, and mediators of Wnt and Notch signaling (TCF4 and CSL) [42-50]. Thus, MTG family members play a pivotal function during hematopoiesis to link DNA binding transcription factors to chromatin modifying enzymes and other corepressors to influence gene expression.

The MTG family shares four evolutionarily conserved domains with the *Drosophila* protein, Nervy, which are called Nervy Homology Regions (NHR) 1-4 (See Figure 3A). NHR1 has homology to human TBP-associated factor 130 (hTAF130), hTAF105, and *Drosophila* TAF 110, and is therefore sometimes called the TAF110 domain. This region is most well characterized as the region that binds to various transcription factors with which the MTG family interacts. NHR2 contains a hydrophobic heptad repeat and is the oligimerization domain that can form homo- or heterodimers between family members as well as bind other proteins. The function of NHR3 is currently undefined, but may mediate protein interactions. Finally, NHR4 is in the MYND class of zinc finger proteins that are involved in protein interactions. All

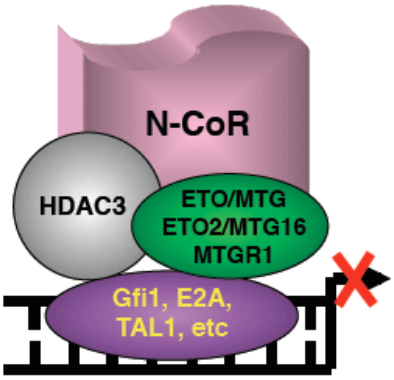

Figure 2. MTG family members form co-repressor complexes. Schematic diagram of the corepressor complexes that are formed by MTG family members. Gfi1, E2A, and TAL1 are examples of transcription factors that MTG proteins interact with to repress transcription of the genes they bind.

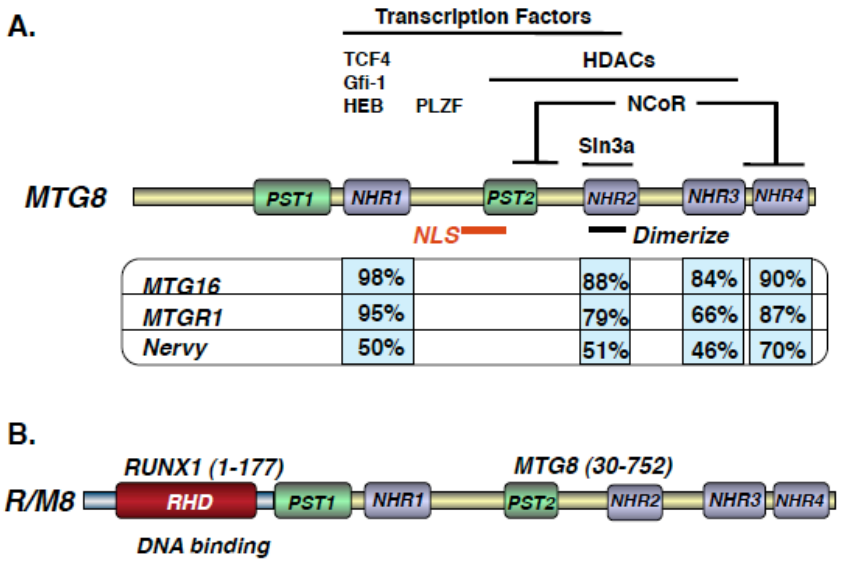

Figure 3. MTG family members and leukemogenic translocations. (A) Schematic diagram of MTG8 showing corepressor and transcription factor binding sites. Also shows homology among MTG family members within the four conserved Nervy Homology Regions (NHR). (B) Schematic diagram of the RUNX1-MTG8 fusion protein.

four of these conserved domains are present in the full-length version of the AML1-ETO fusion protein (Figure 3B). The binding locations of a few of the corepressors, HDACs, and transcription factors that bind MTG8 are shown in Figure 3A [51-53]. Given their high sequence identity, it is not surprising that each family member binds to many of the same proteins and in similar locations. However, unlike MTG8, MTG16 does not bind mSin3a, and MTG16 binds to more HDAC family members than MTG8 [54]. This suggests that these proteins may perform similar yet distinct functions, and that it is important to determine which protein interactions are unique to each MTG family member.

Roles in stem cells

In addition to being linked to hematopoiesis, MTG family members may contribute to the function of stem cells in multiple organs. Gene targeting studies of *Mtg8* indicated that it is required for the development of the gut, as many of the pups died due to deletion of the mid-gut [55]. Even in mice that retained the mid-gut, there was a dramatic loss of architecture, which could be due to defective stem cells. Similarly, mice with a deletion of *Mtgr1* failed to maintain the secretory lineage cells in the small intestine [56]. Furthermore, after treatment with the ulcerative agent dextran sodium sulfate (DSS), the *Mtgr1-null* colonic epithelium failed to correctly regenerate, also suggesting altered stem cell functions [57]. In addition, *Mtg16* has been detected in proteomic screens of key regulatory DNA binding transcription factors that regulate hematopoiesis and stem cell functions (e.g., Heb, Gfi1, TAL1/SCL, TCF4) [46, 47]. Collectively, these data suggest MTG family members play key roles in multiple tissue-

specific stem cells. Thus, deregulation of these proteins could alter stem cell functions and lead to cancer in the corresponding tissue.

Roles in cancer

Although *MTGR1* has not been identified in a direct chromosomal translocation as already described for MTG8 and MTG16, it does map to chromosome 20q11, which is frequently deleted in myelodysplastic syndromes (MDS) and in 3-10% of AML [58]. Thus, the cumulative data suggest that the MTG/ETO family members function as transcriptional corepressors whose activities are co-opted by chromosomal translocations or deletions to induce leukemia. The involvement of these proteins in chromosomal translocations highlights the important role this family must play in key cellular functions, since many translocations target master regulatory genes.

In addition to their involvement in chromosomal translocations and leukemia, deletion of MTG family members have been observed in other types of cancers as well. *MTG16* is deleted in approximately 40% of the most common form of breast cancer and, *MTG8* was marked as a candidate colon cancer gene through a recent screen of human tumor samples [3]. Interestingly, although the authors did not highlight *MTG16* in their mutational analysis, it is important to note that mutations in *MTG16* were also found in the initial screen of colorectal carcinoma samples. Thus, 5 of the original 11 samples had mutations in MTG family members. Furthermore, sequencing of 1507 genes in 441 lung, ovarian, breast, and prostate tumors identified *MTG8* was mutated in 6 lung cancers and 2 breast cancer samples, whereas *MTG16* was mutated in an ovarian cancer sample (Figure 4) [5]. MTG family members also have the ability to form

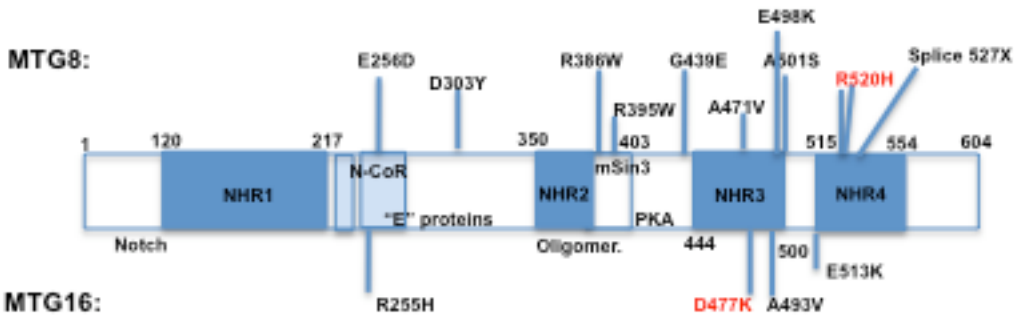

Figure 4. MTG family members are mutated in cancer. Schematic diagram of mutations that were found in MTG8 (above) or MTG16 (below) when 441 lung, ovarian, breast and prostate tumors were sequenced. This study found that MTG8 was mutated in 6 lung cancers and 2 breast cancer samples, whereas they identified MTG16 was mutated in one ovarian cancer sample. Mutations in red depict residues conserved in all family members and in the Drosophila homologue, *Nervy*. Note that the R520H mutation is was recurrent.

oligomers, and the fusion proteins associated with leukemia bind to the wild type MTGs that remain. This suggests an intriguing hypothesis that loss of function of wild-type MTG proteins could contribute to leukemogenesis, yet the mechanism by which this might occur remains obscure. Taken together, these findings suggest that *MTG* family members may act as tumor suppressors. Conversely, loss of *Mtgr1* has recently been described to have had an anti-tumorigenic effect in the murine azoxymethane (AOM)/DSS colitis-associated carcinoma model [59]. In this model, *Mtgr1*$^{-/-}$ mice were protected from tumorigenesis when subjected to AOM/DSS treatment, which was in part due to an increase in apoptosis of the tumor cells and an increase in the amount of tumor infiltrating immune cells. Nonetheless, MTG family members are plausible important regulators for tumor formation, but whether they are activators or repressors of carcinogenesis may turn out to be cell type dependent.

Myeloid Translocation Gene on Chromosome 16

Of the MTG family members, MTG16 is the most highly expressed member in bone marrow cells [60, 61], particularly in the hematopoietic stem cells (HSCs) and early progenitors [61]. In accordance with this, microarray profiling of normal and leukemic stem cells suggests that *Mtg16* is expressed in these cells [60, 62]. Taken together, this would imply that MTG16 would be important for the regulation of hematopoietic development and cell fate decisions. Given that MTG16 does not bind DNA itself, its regulation of hematopoiesis would be imparted by the transcription factors it binds. Although this list is not conclusive, some of the major hematopoietic regulators that interact with MTG16 are Gfi1, Gfi1b, Tal1/SCL, and E proteins (E2A and HEB) [43, 46,

47]. Their roles in hematopoiesis will be discussed, as this knowledge will help delineate how MTG16 could act as such a vital regulator of hematopoiesis by orchestrating the transcriptional events of each of these transcription factors.

Effects on hematopoietic lineages based on specific transcription factor interactions

Gfi1/Gfi1b

Growth factor independent 1 and growth factor independent 1b (Gfi1 and Gfi1b, respectively) encode two nuclear zinc finger proteins that act as transcriptional repressors, in part through their interaction with MTG family members. *Gfi1* knockout studies indicated that Gfi1 is important for neutrophil differentiation and more importantly for HSC functions [63-65]. *Gfi1*$^{-/-}$ mice had increased numbers of HSCs that were hyperproliferative, compared to WT HSCs. Although *Gfi1*$^{-/-}$ HSCs were able to reconstitute all lineages in a straight bone marrow transplant (BMT), they were defective in both serial transplants and in a competitive repopulation assay (CRA), with only partial reconstitution of peripheral blood cells even at high cell doses. Given these results, it can be concluded that *Gfi1*$^{-/-}$ HSCs are not completely impaired, but are deficient when compared to WT HSCs. In contrast, *Gfi1b* inactivation revealed only a minor role in regulating HSC dormancy and pool size, but this is likely explained by compensation by Gfi1 [66]. However, Gfi1b is necessary for the development and differentiation of the erythroid and megakaryocytic lineages through its cooperation with GATA1 [67].

SCL/Tal1

The stem cell leukemia (SCL) gene, also known as T-cell acute lymphoblastic leukemia 1 (Tal1), is a basic helix-loop-helix transcription factor that regulates erythroid and megakaryocytic development. In addition, *SCL/Tal1* inactivation resulted in embryonic lethality due to a complete failure of hematopoiesis [68-71]. Despite its clear importance for the development of hematopoiesis, there is controversy in the field about its role in HSCs. Originally, conditional deletion of *SCL/Tal1* in the adult hematopoietic compartment showed that it was dispensable for the long-term repopulating activity and multipotency of the HSC, but that it was essential for proper differentiation of erythroid and megakaryocytic precursors [72]. However, SCL/Tal1 is highly expressed in long term (LT)-HSCs and heterozygous deletion of *SCL/Tal1* resulted in increased cycling of the HSCs [73]. Therefore, SCL/Tal1 seems to be required to maintain the quiescence and long-term repopulating ability of HSCs. In addition to its roles in erythropoiesis and HSCs, it has also been linked to monocyte differentiation [74]. When *SCL/Tal1* was deleted in myeloid precursors, the cells displayed decreased entry and progression through the G1 and S phases of the cell cycle, which resulted in impaired proliferation.

E-proteins (E2A and HEB)

MTG16 interacts with members of the E protein family (E2A and HEB). A major function of E protein signaling is to direct T-cell development, which suggested that Mtg16 plays a pivotal role in lymphopoiesis. $E2A^{-/-}$ mice display decreased numbers of thymocytes and various T-cell progenitors, and were further impaired in their ability to produce T-cells in an *in vitro* assay that drives T-cell development from a strong Notch

signal [75]. Indeed, deletion of *Mtg16* in mice phenocopied the defects seen in the *E2A*-null mice. Loss of *Mtg16* impaired the development of thymocyte T-cells with almost a complete loss of T-cells after competitive bone marrow transplantation [61]. This defect was recapitulated *in vitro* where *Mtg16*$^{-/-}$ cells (LSK stem and progenitor cells or Double Negative 1 thymocyte progenitors) were unable to make CD4^{+}/CD8^{+} T-cells in response to a Notch signal. The *in vitro* assay permitted the re-expression of *Mtg16* to complement the loss of T-cell development, which made it possible to test deletion constructs to determine which regions of Mtg16 were responsible for proper T-cell development. This analysis showed that the ability for Mtg16 to bind to E-proteins was required for the establishment of T-cell fate specification. In addition to their roles in T-cell development, E-proteins also play a role in HSCs in that deletion of *E2A* leads to decreased numbers of LT-HSCs, multipotent progenitors, and erythroid progenitors. Not only are the HSC numbers decreased, but the HSCs are also hyperproliferative [76], which causes diminished functional capacity in competitive repopulation assays.

Hematopoiesis

Given the number of hematopoietic defects that are seen when any of the proteins that interact with Mtg16 are deleted, it would be assumed that the loss of Mtg16 would also impair hematopoiesis. In order to study the role of Mtg16 in hematopoiesis, one must first understand this process. Hematopoiesis is a term that describes the formation of all of the blood cells in the body, which are all derived from the hematopoietic stem cell.

Definition of a stem cell

Stem cells are set apart from other cell types based on two main features: (1) their ability to self-replicate and continue to make copies of themselves (self-renewal), and (2) their ability to differentiate and generate all of the progeny of their given system (multipotency) [77]. Their ability to do this is through a process called asymmetric cell division, in which they produce one differentiated daughter cell (progenitor) and another daughter that still retains the stem cell properties. Due to these unique properties, stem cells have been a subject of intense research over the last 40 years due to their potential use in medical therapies.

Although the first 'hematopoietic stem cell' concept was proposed in 1961 [78], the field has greatly expanded since then and now covers stem cells that give rise to many organ/tissue types (tissue-specific stem cells) or embryonic stem (ES) cells that give rise to all of the cells of the growing embryo [77]. Recent work has also discovered that adult cells can be genetically reprogrammed to an embryonic-like stem cell state by the forced expression of specific genes and factors that are crucial for those phenotypes. Given all of these different stem cell types and definitions, a standard nomenclature has evolved to define what type of differentiation potential each type of stem cell population possesses (Table 1) [77].

Hematopoietic stem cells

Given that the idea of a stem cell in the bone marrow compartment was first discovered over 40 years ago, the HSC has become the most well-characterized adult stem cell population, both in terms of cell surface markers used for purification and

Table 1. Common nomenclature used to define the differentiation potential of stem cell populations

Designation	Differentiation potential implied by designation	Examples of stem/ progenitors with these properties
Totipotent	All embryonic and extraembryonic tissues	Zygote
Pluripotent	All embryonic tissues	ICM, ES cell, iPS cell
Multipotent	All lineages of a tissue/ organ	HSC, NSC
Oligopotent	Several but not all lineages of a tissue/ organ	CMP, CLP
Unipotent	Single lineage of a tissue/organ	MacP

CLP, common lymphoid progenitor; CMP, common myeloid progenitor; ES, embryonic stem; HSC, hematopoietic stem cell; ICM, inner cell mass; iPS, induced pluripotent stem; MacP, macrophage progenitor; NSC, neural stem cell.

assays to test for functional capacity. The study of the HSC began when limited numbers of BM cells were injected into irradiated recipient mice and cellular colonies were observed that formed in the spleens of recipient mice [78]. After detailed analysis of these colonies, they concluded that a small subpopulation of the donor BM cells had the ability to produce multiple types of myeloerythroid cells and the ability to self-replicate. These findings were the initial defining criteria for 'stem cells'.

In accordance with the stem cell properties, HSCs are the only cells in the bone marrow that are able to differentiate into more than 10 distinct functional mature blood cells, while still retaining the ability to self-renew and give rise to identical HSCs [79]. A schematic of hematopoiesis is depicted in Figure 5, where the long-term (LT-) HSC maintains self-renewal, and also yields a short-term (ST-) HSC and other lineage-restricted progenitor cells that rapidly differentiate into all of the mature lineages that are found in the peripheral blood. While the frequency of HSCs is only about 0.01% of the total nucleated cells in the bone marrow, they are able to persist for the lifespan of the animal to continually replenish the hematopoietic system at a rate of more than one million cells per second in the adult human [80].

Hematopoietic stem and progenitor cell isolation and purification schemes

In 1988, a major advancement in HSC biology was attained when mouse multipotent progenitor cells were isolated by using flow cytometry to define the Thy-1^{lo} Sca-1^{+} Lineage^{-} population [81]. This new Sca-1 (stem cell antigen-1) marker is a member of the Ly6 family and is also known as the Ly6A/E antigen. It was discovered that on average, 1 out of every 20 Thy-1^{lo} Sca-1^{+} Lineage^{-} cells intravenously injected

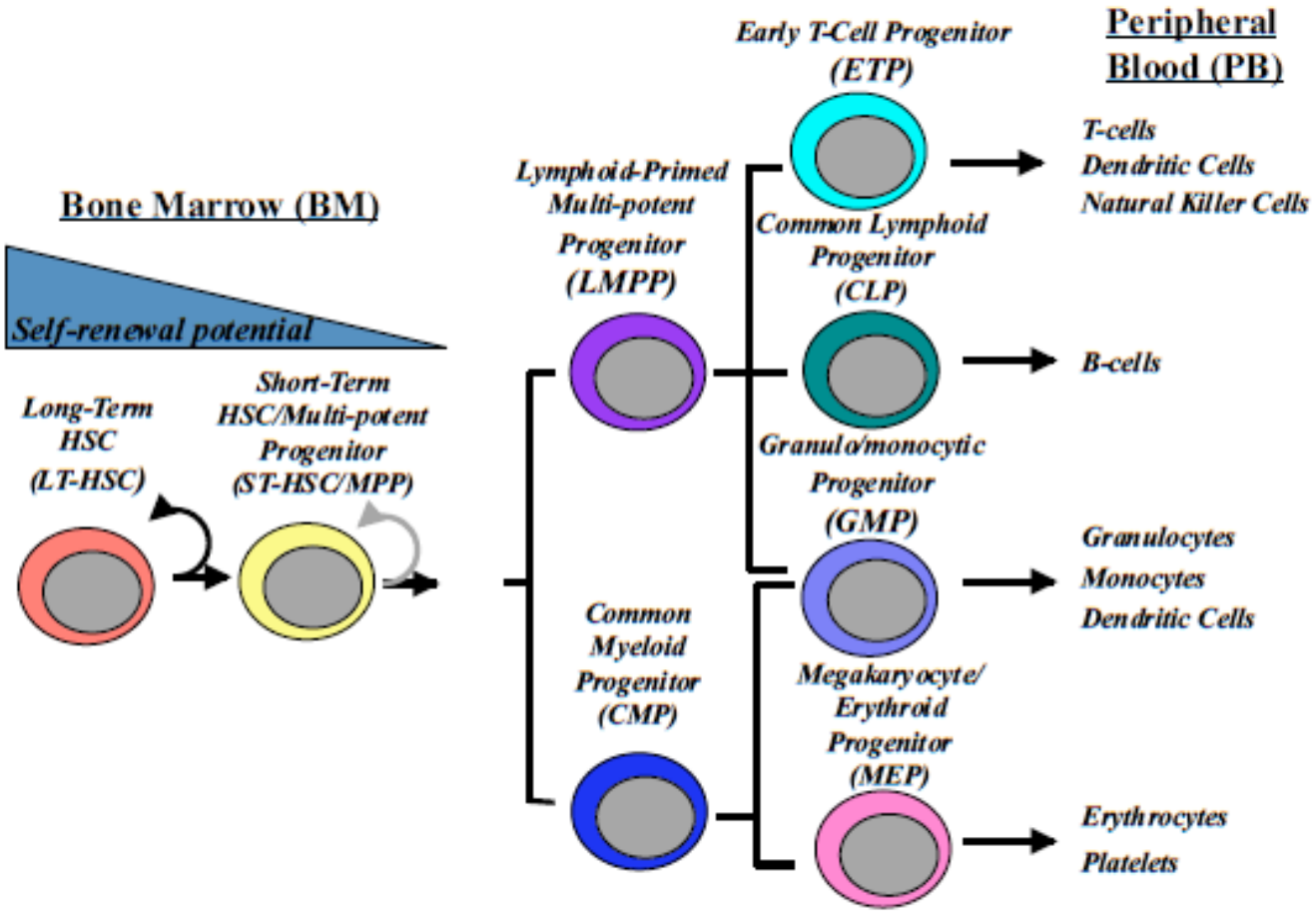
Bone Marrow (BM)
Self-renewal potential
Long-Term HSC (LT-HSC)
Short-Term HSC/Multi-potent Progenitor (ST-HSC/MPP)
Lymphoid-Primed Multi-potent Progenitor (LMPP)
Early T-Cell Progenitor (ETP)
Common Lymphoid Progenitor (CLP)
Granulo/monocytic Progenitor (GMP)
Common Myeloid Progenitor (CMP)
Megakaryocyte/ Erythroid Progenitor (MEP)
Peripheral Blood (PB)
T-cells
Dendritic Cells
Natural Killer Cells
B-cells
Granulocytes
Monocytes
Dendritic Cells
Erythrocytes
Platelets

Figure 5. Model of murine hematopoietic hierarchy. Hematopoiesis begins with the LT-HSC that has the self-renewal capacity as well as the ability to give rise to all of the mature hematopoietic cell types (multipotency). As the LT-HSC differentiates, it loses self-renewal potential and becomes more lineage restricted as it continues through each progenitor step until the cell is committed to a specific lineage.

gave rise to multipotent progenitor activity. This initial discovery paved the way for researchers in the hematopoietic field to build upon this concept of immunophenotyping HSC populations. Through the years, improvements on monoclonal antibody production to cell surface markers, as well as advancements in multi-color fluorescence activated cell sorting (FACS), have led to the continual refinement of the identification and purification of HSCs based on the unique cell surface expression found on these cells compared to the rest of the BM cells. Although multiple laboratories have defined numerous labeling schemes, the ultimate goal of each of them is to identify the most purified population of LT-HSC (Table 2).

Most of the HSC purification schemes are based off the Lineage$^-$ (typically negative for Gr-1, Mac-1, B220, CD3, and Ter-119) Sca-1$^+$, c-Kit$^+$ (LSK) cell surface phenotype [82-84]. However, this population contains a mixture of hematopoietic stem and progenitor cells (HSPC), with only 10% of this population functionally active as bona fide LT-HSCs [80]. Therefore, the LSK compartment should only be considered enriched for HSCs. Aside from the LSK population, detailed phenotypes have also delineated a number of different progenitor cell types, such as lymphoid and myeloid progenitors as well as the sequential progenitors for each of these populations (Table 2). The myeloid progenitors are defined as the Sca-1$^-$ portion of the LSK population, and can be further subdivided into common myeloid progenitors (CMP, CD34$^+$FcγR$^-$), granulo/monocytic progenitors (GMP, CD34$^+$FcγR$^+$) and megakaryocyte/erythroid progenitors (MEP, CD34$^-$FcγR$^-$) (Table 2). Replacing the traditional multipotent progenitor (MPP) model, a more recent lineage analysis has defined the LSK/Flt3^{hi}

Table 2. Cell surface phenotypes commonly used to distinguish various hematopoietic stem and progenitor cells

Marker Phenotype	Cell Type
LSK	Hematopoietic stem and progenitor cells (HSPCs)
SP^{LSK}	Long-term HSCs (LT-HSC)
$LSKCD48^{-}CD150^{+}$	LT-HSCs
$LSKFlt3^{-}CD34^{-}$	LT-HSCs
$LSKFlt3^{-}CD34^{+}$	Short-term HSCs (ST-HSC)
$LSKFlt3^{+}CD34^{+}$	Mutlipotent Progenitor (MPP)
$Lin^{-}IL7R\alpha^{+}c\text{-}Kit^{+}Sca\text{-}1^{+}$	Common Lymphoid Progenitors (CLP)
$c\text{-}Kit^{+}Sca\text{-}1^{-}$	Myeloid Progenitors
$c\text{-}Kit^{+}Sca\text{-}1^{-}CD34^{+}Fc\gamma R^{med}$	Common myeloid progenitor (CMP)
$c\text{-}Kit^{+}Sca\text{-}1^{-}CD34^{-}Fc\gamma R^{-}$	Megakaryocyte-erythrocyte progenitor (MEP)
$c\text{-}Kit^{+}Sca\text{-}1^{-}CD34^{+}Fc\gamma R^{hi}$	Granulocyte-macrophage progenitor (GMP)

population as a lymphoid-primed multipotent progenitor (LMPP), which tends to make more lymphoid cells, but is still capable of going down the myeloid path.

In the last few years, other cell surface markers have been identified that enrich for HSCs either in conjunction with the LSK scheme, or on their own [80]. Though there are many immunophenotyping schemes in use, the most widely accepted and validated are those that include analyzing the expression of CD34, Flk2 (Flt3), or the signaling lymphocytic activation molecule (SLAM) family of receptor molecules, CD48 and CD150 [85-87]. By using the differential expression of CD34 and Flt3, it is possible to separate out LT-HSC ($LSK/Flt3^-/CD34^-$) from the ST-HSC ($LSK/Flt3^-/CD34^+$) and multipotent progenitor (MPP) cells ($LSK/Flt3^+/CD34^+$) (Table 2). Moreover, 50% of LSK $CD48^-CD150^+$ cells were functionally active as LT-HSCs in bone marrow transplant (BMT) assays. More recently, a combination of all of these antibodies marked the most pure LT-HSC (LSK $Flt3^-CD34^-CD48^-CD150^+$). Another approach that has been used to identify and purify HSCs is based on the fact that HSCs express high levels of membrane transport pumps, compared to other BM cells. Thus, they are able to efflux particular dyes such as Hoechst 33342 or Rhodamine 123. This ability results in a small proportion of cells that contain low fluorescence staining from these dyes, which is referred to as the 'side population' (SP), and is highly enriched for HSCs [80]. As can be expected, the combination of the immunophenotyping markers for HSCs in conjunction with the SP has been used as another way to highly purify functional LT-HSCs. It should be noted that cell surface marker expression could change after deletion of a gene in the mouse, so special care is taken when analyzing a new knockout mouse model that the immunophenotyped population is still functional.

Hematopoietic HSPC functional assays

Although immunophenotyping has been extremely useful in the identification and purification of HSPC populations, the only way to truly test for effective HSCs is through functional assays. Numerous assays have been developed over the years to test for functional HSPCs, which has helped make the hematopoietic compartment one of the pioneering systems in the study of adult stem cell biology.

Although *in vitro* assays cannot replicate LT-HSC functions, *in vitro* and short-term *in vivo* assays have been developed to test progenitor cell function. These progenitor assays include the colony-forming cell (CFC) assay, cobblestone area-forming cells (CAFC)/long-term culture-initiating cell (LTC-IC) assays, and the colony-forming unit-spleen (CFU-S) assays [83, 84]. The CFC assays use low numbers of bone marrow cells plated in a semi-solid agar, usually methylcellulose-based culture media, in the presence of a particular cocktail of cytokines to determine the number and type of colonies that are formed. Based on the identification of colonies that are formed, information can be gleaned about the progenitor cell content of the starting population. In this regard, the CAFC and LTC-IC assays are co-culture systems that can be used to predict the frequency of HSCs. Although the reliability of these assays is controversial due to variable culture conditions and the use of different feeder layers, they are useful in limiting dilution format to quantify HSC numbers when homing ability or other functions required for *in vivo* engraftment may compromise the reliability of transplant assays. The CFU-S assay measures cells that home to the spleen, rapidly proliferate and form macroscopic colonies that provide short-term (1-3 weeks) *in vivo* reconstitution after injection into an irradiated recipient mouse. Once cells could be sorted and purified

based on their immunophenotype, specific populations could be injected into the recipients to determine what day after injection each population forms the macroscopic colonies. By doing this, it was discovered that the megakaryocyte erythroid progenitors (MEPs) formed the colonies on day 8 after injection (CFU-S_8), and that a combination of MEPs and ST-HSCs/MPPs formed the colonies on day 12 after injection (CFU-S_{12}) [88]. The CAFC, LTC-IC, and CFU-S assays all reflect progenitors more primitive than the CFCs, but more mature than HSCs.

Since the HSC is required for blood formation throughout the life of an animal, it must remain in a dormant state of the cell cycle, or quiescent, to protect itself over time. Given the importance of HSC quiescence for the maintenance of stem cell function, particularly stem cell self-renewal, analysis of the cell cycle status in stem cells is a key property to test for when assessing HSC functions [80, 83, 84]. Most HSCs are predominantly in the G_0 or G_1 phase of the cell cycle, with approximately 75% of LT-HSCs resting in G_0. Common methods for detecting cell cycle status are Ki-67 staining, Hoechst 33342 DNA staining (HO), Pyronin Y RNA stain (PY), or bromodeoxyuridine (BrdU) labeling. Ki-67 is a marker used to determine the growth fraction of a cell population as it is only expressed in the active phases of the cell cycle (G_1, S, G2/M) and not in resting cells (G_0). HO labels the DNA so the DNA content of the cell can be determined, while PY can distinguish between G_0 and G_1 based on the amount of RNA in the cell. G_0 cells have little to no RNA because they are quiescent, and G_1 cells contain a lot of RNA as they are preparing to enter the S phase. All three of these methods provide a snap-shot of the cell cycle status of a given cell population. BrdU is used to measure the proliferative history of a cell population, as it can be administered to the cells for a

given amount of time, after which it is incorporated into newly synthesized DNA during the S phase of the cell cycle. Therefore, BrdU can reveal what proportions of HSCs have entered or completed S phase over the time of the labeling period.

The gold standard that has been accepted for testing true LT-HSC function is the competitive repopulation assay (CRA) [80, 83, 84]. This assay assesses the ability of a test cell population (for example, knockout cells) to sustain long-term BM engraftment in the presence of a congenic control population of cells, which can be distinguished from each other by cell surface markers (test cells, typically $CD45.2^+$; control cells, typically $CD45.1^+$). It has been determined that the bone marrow cells should be able to reconstitute multiple lineages for at least 16 weeks post-transplant for this to be considered true long-term reconstitution. This assay can be further utilized to assess the number of HSCs by performing limiting dilution transplants and back-calculating the number of LT-HSCs using Poisson statistics. Moreover, serial transplantation can be used to determine the self-renewal capacity of the LT-HSC.

Lineage cell fate decisions

The intricately designed hierarchy of the hematopoietic system requires carefully orchestrated cellular pathways that direct lineage cell fate decisions. Lineage commitment is the step-wise process by which a multipotent HSPC becomes increasingly restricted in its cell fate choices until it is eventually a committed progenitor of one specific lineage. Due to the short half life of most blood cells, millions of mature BM cells in multiple lineages are replenished every second in humans [77], which demands high fidelity of the lineage allocation decisions.

Generally, lineage specification is governed by the expression of lineage-affiliated cytokines (Figure 6) and transcription factors (Figure 7) [89]. For example, two important lineage-specific cytokines are interleukin-7 (IL-7) and erythropoietin (EPO), which direct lymphoid and erythroid development, respectively. Two examples of lineage-affiliated transcription factors are GATA-1 and C/EBPα. GATA-1 is considered an 'erythroid factor' as it is highly expressed in MEPs, and C/EBPα is considered a 'myeloid factor' as it is present in GMPs. However, this simple concept that the expression of one transcription factor will produce a specific lineage is challenged by the fact that HSCs and earlier progenitors express 'lineage-restricting' transcription factors, albeit at generally low levels. This phenomenon is termed lineage priming, and suggests a process in which these early HSPCs are equipped for various lineages, and this selection is made when alternative possibilities are extinguished [89]. Thus, key lineage-specific factors must promote their own lineage differentiation, while simultaneously shutting off factors that favor other lineages. Accordingly, many examples corroborate this model of lineage cell fate specification. One example is the GATA-1 and PU.1 transcription factors that promote erythroid/megakaryocytic/ eosinophil and myeloid differentiation, respectively. These proteins interact and physically antagonize each other's actions. Morpholino knockdown of GATA-1 shifted progenitors to a myeloid fate in zebrafish, whereas the knockdown of PU.1 had the opposite effect and favored the erythroid lineage [89-91]. Therefore, valuable information can be gained by the selective deletion of one of the factors that are involved in lineage allocation choices to determine which lineages require that factor for their survival.

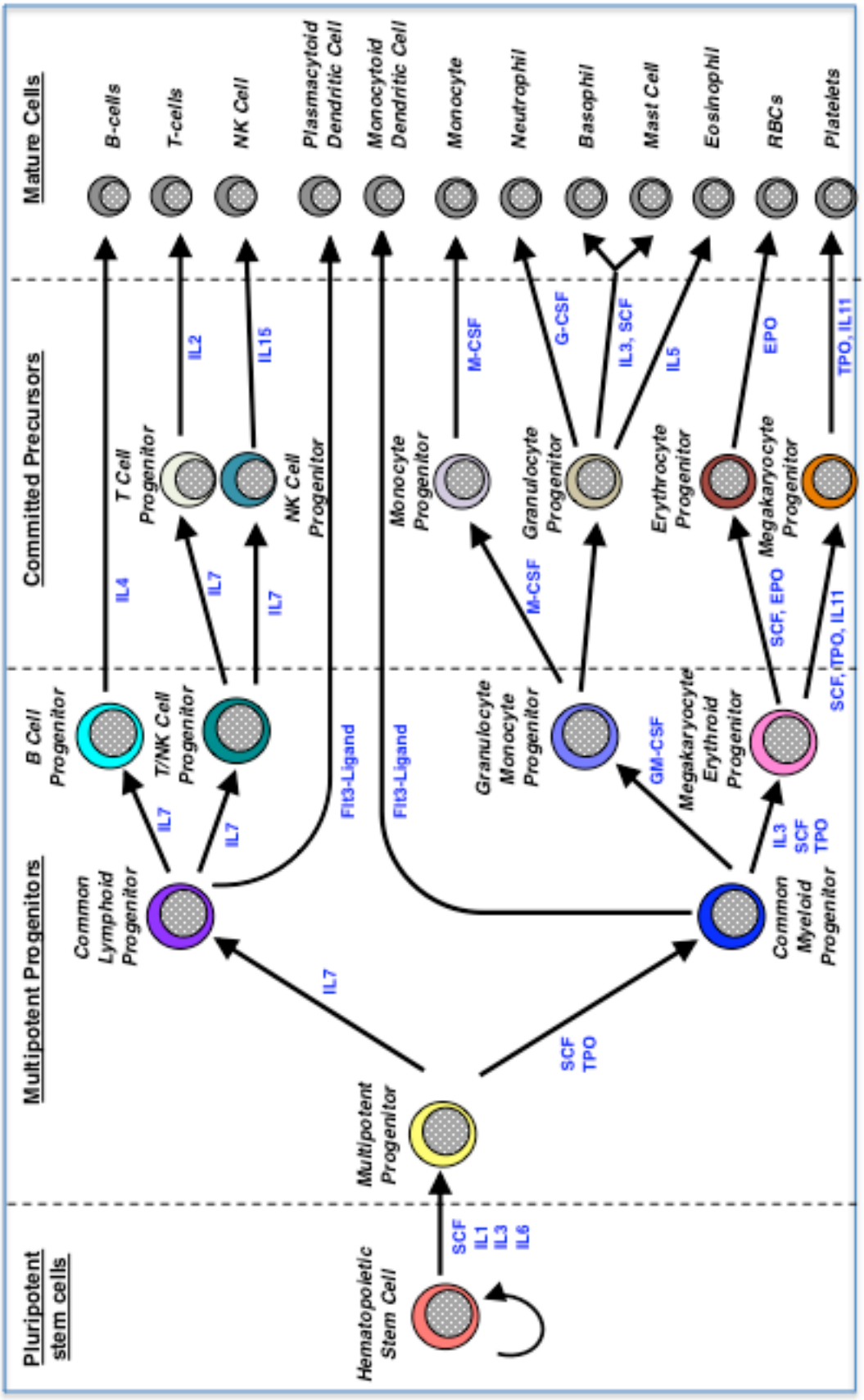
Pluripotent stem cells
Multipotent Progenitors
Committed Precursors
Mature Cells
Hematopoietic Stem Cell
SCF
IL1
IL3
IL6
Multipotent Progenitor
IL7
SCF
TPO
Common Lymphoid Progenitor
IL7
IL7
Common Myeloid Progenitor
IL3
SCF
TPO
B Cell Progenitor
T/NK Cell Progenitor
Flt3-Ligand
Flt3-Ligand
Granulocyte Monocyte Progenitor
GM-CSF
Megakaryocyte Erythroid Progenitor
SCF, TPO, IL11
SCF, EPO
IL4
IL7
IL7
T Cell Progenitor
NK Cell Progenitor
Monocyte Progenitor
M-CSF
M-CSF
Granulocyte Progenitor
Erythrocyte Progenitor
Megakaryocyte Progenitor
IL2
IL15
G-CSF
IL3, SCF
IL5
EPO
TPO, IL11
B-cells
T-cells
NK Cell
Plasmacytoid Dendritic Cell
Monocytoid Dendritic Cell
Monocyte
Neutrophil
Basophil
Mast Cell
Eosinophil
RBCs
Platelets

Figure 6. Critical cytokines required for blood development. Schematic of hematopoietic differentiation depicting the soluble factors that contribute to the differentiation process of various lineages in blue. IL, interleukin; SCF, stem cell factor; EPO, erythropoietin; TPO, thrombopoietin.

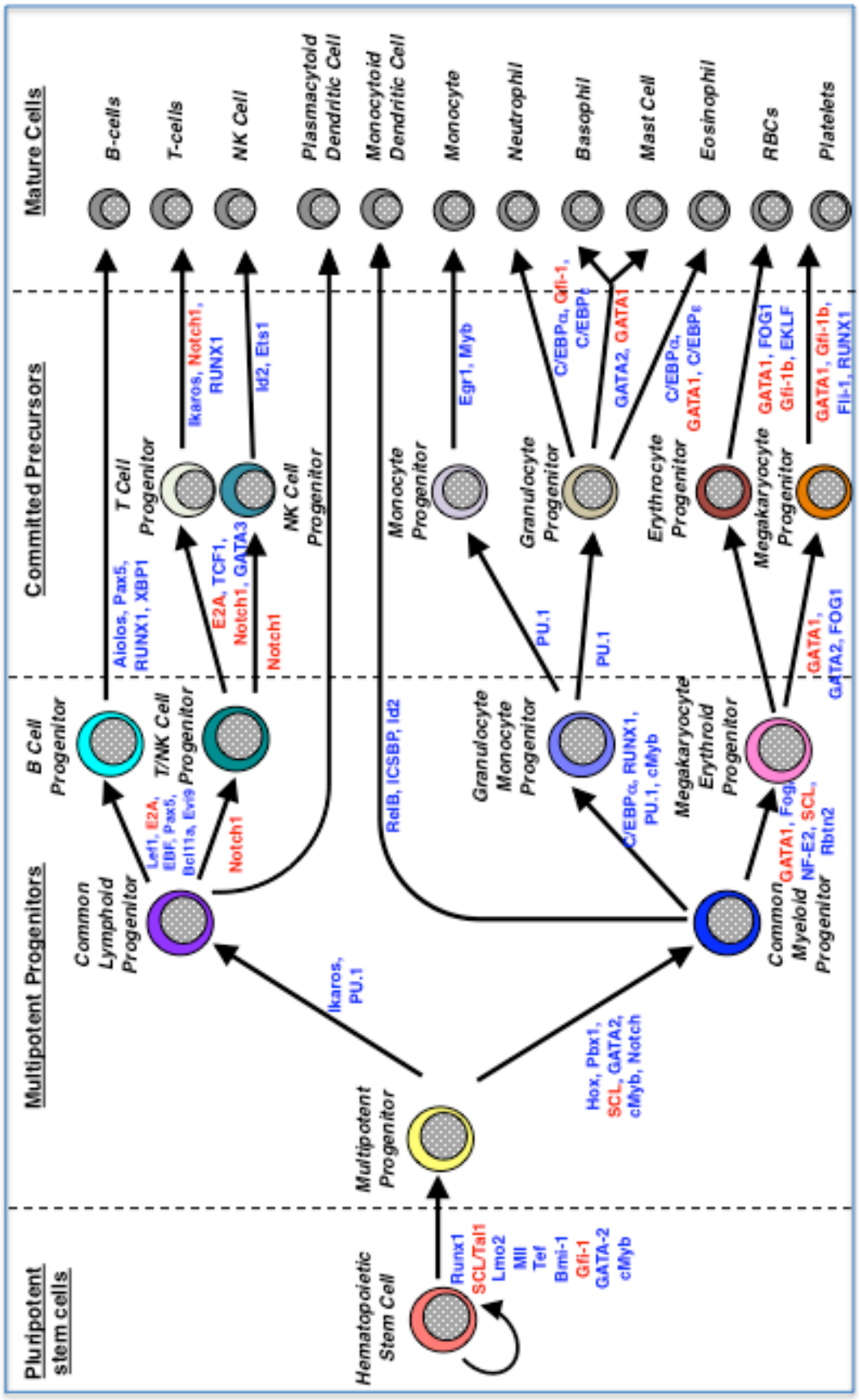
Pluripotent stem cells
Multipotent Progenitors
Committed Precursors
Mature Cells
Hematopoietic Stem Cell
Runx1
SCL/Tal1
Lmo2
Mll
Tel
Bmi-1
Gfi-1
GATA-2
cMyb
Multipotent Progenitor
Hox, Pbx1, SCL, GATA2, cMyb, Notch
Ikaros, PU.1
Common Lymphoid Progenitor
Lef1, E2A, EBF, Pax5, Bcl11a, Evi9
Notch1
B Cell Progenitor
Aiolos, Pax5, RUNX1, XBP1
T/NK Cell Progenitor
E2A, TCF1, Notch1, GATA3
Notch1
T Cell Progenitor
Ikaros, Notch1, RUNX1
NK Cell Progenitor
Id2, Ets1
RelB, ICSBP, Id2
Common Myeloid Progenitor
GATA1, Fog, NF-E2, SCL, Rbtn2
Granulocyte Monocyte Progenitor
PU.1
C/EBPα, RUNX1, PU.1, cMyb
Monocyte Progenitor
Egr1, Myb
Granulocyte Progenitor
C/EBPα, Gfi-1, C/EBPε
PU.1
GATA2, GATA1
Megakaryocyte Erythroid Progenitor
GATA1, C/EBPα
Erythrocyte Progenitor
C/EBPα, GATA1, C/EBPε
GATA1, FOG1
Megakaryocyte Progenitor
Gfi-1b, EKLF
GATA1, Gfi-1b, Fli-1, RUNX1
GATA1, GATA2, FOG1
B-cells
T-cells
NK Cell
Plasmacytoid Dendritic Cell
Monocytoid Dendritic Cell
Monocyte
Neutrophil
Basophil
Mast Cell
Eosinophil
RBCs
Platelets

Figure 7. Critical transcription factors required for lineage cell fate decisions in hematopoiesis. Schematic of hematopoietic differentiation depicting the transcription factors that have been shown to characterize particular cell transitions in blue (generally determined through conventional gene knockout studies). Transcription factors that specifically bind to Mtg16 are highlighted in red.

When alterations are made in the lineage allocation of HSPCs, this can result in the development of impaired hematopoiesis or even lead to a disease state. Therefore, identification of the cellular pathways that are involved in the process of lineage cell fates should enhance our understanding of how disease mutations may subvert this normal process to impact the development of the disease, and how targeting of such mutations can lead to better therapies.

Leukemia stem cells

Given the important roles of the HSC in self-renewal and multipotency, it is not surprising that deregulation of these processes have been associated with the development of hematopoietic malignancies. In fact, recurrent leukemia-associated genetic abnormalities have been detected in the HSCs of patients with acute myeloid leukemia (AML). There is ample evidence that a small subpopulation of slow-cycling leukemic cells is resistant to standard chemotherapeutic agents and lead to recurrence of the disease after treatment. In addition, leukemia cell populations contain a lot of heterogeneity, similar to that of normal hematopoiesis that stems from an HSC [82, 92]. Though these properties are reminiscent of HSCs, this was not proven until the early nineties when Dick and colleagues began studies to determine what cell type was propagating the disease [93]. To test this, they took human patient leukemic blasts and used FACS to sort them between immature fractions ($CD34^+CD38^-$) and more mature fractions ($CD34^+CD38^+$). Each fraction was then injected into immunocompromised non-obese diabetic-severe combined immunodeficiency (NOD-SCID) mice to perform xenotransplantation. Only the immature ($CD34^+CD38^-$) fraction was able to transfer the

leukemia to the mice, which suggested that the normal HSC was the likely target cell for transformation to form the leukemia. This led to the hypothesis of the leukemia-initiating cell (LIC), which are functionally defined by their ability to serially propagate the disease in transplanted mice, and gave way to the more commonly used term of the leukemia stem cell (LSC). Though the LSC possesses stem cell phenotypes, a number of studies have shown that not only can the LSC originate from an HSC, but it can also originate from a progenitor cell that has acquired mutations that allow it to self-renew and therefore propagate the disease (Figure 8 [94]) [82].

While current treatments for leukemia can eliminate the bulk of the tumor, there is increasing evidence that suggests the persistence of the LSC, due to its insensitivity to current therapies, can be responsible for recurrence of the disease after treatment is stopped. For example, *in vitro* assays have shown that chronic myeloid leukemia cells that express breakpoint cluster region-abelson (BCR-ABL) transcripts are extremely sensitive to the tyrosine kinase inhibitor, imatinib [95]. However, there was a small subset of quiescent leukemic cells, which resembled normal HSCs that exhibited resistance to imatinib-induced death. Moreover, patients who show a complete cytogenic response to imatinib treatment still harbor CFC and LTC-IC cells with the BCR-ABL transcript, and there is evidence that patients who initially achieved excellent response to imatinib treatment can later show recurrence of the disease. Therefore, it has become increasingly clear that more research is required to understand the molecular pathways that are involved in the transformation of LSCs so that therapies that specifically target the LSC can be designed to improve treatment outcomes in leukemia patients. Given that Mtg16 interacts with numerous transcription factors that are vitally

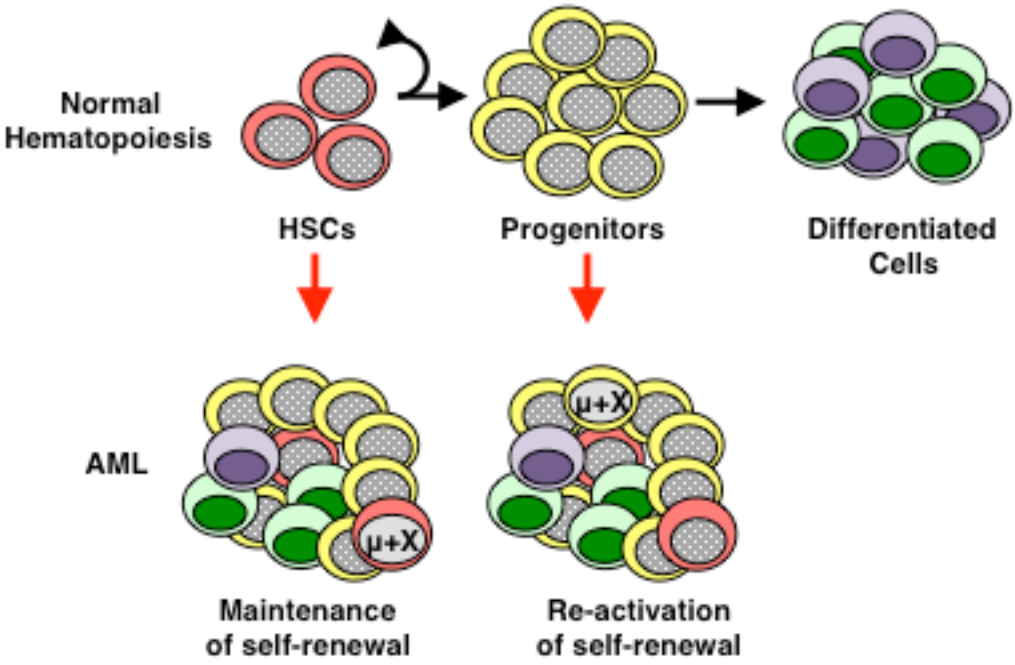

Figure 8. Leukemia fusion proteins can transform different hematopoietic pools into LSCs. Normal hematopoiesis proceeds from the HSC through committed progenitor cells to fully differentiated cells. Certain initial mutations (μ) may require the properties of the normal HSC, i.e., extended life span and self-renewal, such that cooperating mutations (X) can be subsequently acquired. However, other fusion proteins also possess the ability to induce sufficient self-renewal in committed progenitors and therefore subsequent mutations can be acquired. In AML that forms in the HSC, a reservoir of mutant HSCs would likely make eradication more difficult, since HSCs are more resistant to treatment. Conversely, in progenitor-derived AML, such a reservoir would not exist, and therefore treatment would be more successful.

important for proper blood development, this suggests that Mtg16 is a likely candidate for a master regulator of hematopoiesis. Therefore, knowledge about the normal role of Mtg16 in hematopoietic stem and progenitor cells can lead to insight into novel therapeutic targets for the treatment of acute myeloid leukemia.

CHAPTER II

MATERIALS AND METHODS

Plasmids

The murine *Eto2/Mtg16* cDNA was obtained from Dr. Shari Meyers (LSUHSC, Shreveport, LA). The pPNT vector used for making the targeting construct was provided by the Vanderbilt-Ingram Cancer Center Transgenic Mouse/ ES Cell Shared Resource [96]. *MSCV-c-Myc* and *MSCV-Bcl2* were obtained from Dr. James DeGregori, Univ. of Colorado *[97]*). The *Gfi1* cDNA was a gift from Dr. Tarik Moroy (Institut de recherches cliniques de Montréal) and the plasmids encoding PLZF and BCL6 were provided by Dr. Ari Melnick (Albert Einstein School of Medicine).

Mtg16-deficient mice

We obtained the genomic sequence of the *Mtg16* allele using the Celera Discovery System and NIH databases and found the genomic organization of this locus was similar to that of *Mtg8* and *Mtgr1*. We amplified 3 homology regions from TL1 genomic DNA. Homology region 1 (HR1) was generated with the following primers: 5'-**CTCGAG**TATGAGGGTTGCATGGTGTTTTGGTTGG-3' and 5'-**GGCGCGCCTTA ATTAA***ATAACTTCGTATAGCATACATTATACGAAGTTAT*CAGTTTCCCAACCCTGC CTAGTTC-3'. Homology region 2 (HR2) was generated with the following primers: 5'-G**ACGCGT***ATAACTTCGTATAATGTATGCTATACGAAGTTAT*CCACGGAGAATGAA CCATCCTGGATTA-3' and 5'-**ACGCGTCAATTG**ACAAAGATGTCCTACATCAC

TGGGGCT-3'. Homology region 3 (HR3) was generated with the following primers: 5'-**CAATTG***ATAACTTCGTATAATGTATGCTATACGAAGTTAT*CACCCCTACCATGCAT CCAAAGAAGAT-3' and 5' CTGGTTGATGACAGTCAGGGCATCCTC-3'. The restriction enzyme sites are shown in bold and the loxP sites are in italics. The HR2, which contains the genomic sequence of *Mtg16* exon 8 flanked by LoxP sites, was ligated to HR3, which includes 2 kb of *Mtg16* genomic sequence. The HR2-HR3 combination was ligated to HR1, which contains 6kb of *Mtg16* genomic sequence. A neomycin-resistance cassette was PCR amplified from the pPNT vector with the following primers: 5'-**TTAATTAA**CTAGAGTCGGCTTCTG-3' and 5'-**TTAATTAA**CTTTTCCCAAGG CAGTCTG-3'. The PAC1 restriction sites were used to add the neomycin cassette in between HR1 and HR2. A BamHI – HindIII fragment containing a thymidine Kinase cassette was isolated from the *pPNT* vector and ligated into the *KS bluescript* vector (*TK-KSBS*). The complete *HR1-LoxP1-Neomycin* Cassette-*LoxP2-HR2-LoxP3-HR3* fragment was ligated into the *TK-KSBP* vector. The completed targeting construct was electorporated into TL1 embryonic stem cells. DNA isolated from the resulting single cell clones were digested with *Xmn* I and analyzed by Southern Blot for homologous recombination. A clone containing the correctly targeted *Mtg16* locus was identified and injected into C57Bl/6 blastocytes. Male chimeric mice were mated with C57Bl/6 females and agouti pups were tested for the targeted allele. The following primers were used to detect the floxed Exon 8: 5'-CTGGGTCTCGACAAGAAGAAGTG-3' and 5'-GTCCATGATGCAGTTCAGAAG-3'. Thus, the wild-type allele yielded a 704 bp product and the floxed allele a 647 bp product.

Mice containing a single copy of the targeted *Mtg16* allele were mated with mice

transgenic for the Cre recombinase driven off the *EIIA* promoter. The resulting offspring were analyzed for recombination between LoxP1 and LoxP3. The recombination event was detected using the following primers: 5'- ATGCAAGAACTAGGCAGGGTT-3' and 5'- GTCCATGATGCAGTTCAGAAG-3'. The expected product sizes are 1,405 bp for the wild-type allele and 282 bp for the recombined allele. These mice were backcrossed to C57Bl/6J and subsequently analyzed to determine effect of loss of *Mtg16* expression. The data in Chapter III was generated using mice from N3 to N4 backcrossed into the C57Bl/6J strain, and the data in Chapter IV was generated using mice from N10.

Cell Culture and protein analysis

Embryonic stem cells were grown on irradiated murine embryonic fibroblast (MEFs) feeder layers in DMEM containing 15% fetal calf serum, 0.1mM non-essential amino acids, 2mM L-glutamine, 50µg/ml gentamicin, 10^3 U/ml LIF, and 55µM ß-mercaptoethanol (Gibco/Invitrogen). Bone marrow cells were co-cultured with MSCV producing BOSC23 cells in DMEM containing 10% fetal bovine serum supplemented with IL-6 (PeproTech), SCF (PeproTech), and LIF (Chemicon). Cos7 cells were cultured in DMEM supplemented with 10% fetal calf serum, 0.1mM non-essential amino acids, 2mM L-glutamine (Gibco/Invitrogen). Transfection and co-immunoprecipitations for protein association studies were performed as described [54]. Immunoblot analysis was performed using anti-Eto2 G-20 (Santa Cruz, Inc.) or monoclonal antibodies to the indicated epitope tags. Nuclear extracts were prepared from 5 X 10^6 splenocytes that were washed with PBS and the cells were then resuspended in buffer A (10mM HEPES (pH 7.9), 10mM KCl, 1.5mM $MgCl_2$, 0.34M sucrose, 10% glycerol, 1mM DTT and protease

inhibitors). Triton-X-100 (final concentration of 0.1%) was then added to the cells and incubated on ice for 8 min. The nuclei were collected by centrifugation and the nuclear pellet was resuspended in RIPA buffer containing protease inhibitors and subjected to 10% SDS-PAGE.

Histology and peripheral blood analysis

Peripheral blood smears or sections of spleen or bone marrow were fixed in buffered formalin overnight at room temperature prior to embedding in paraffin and sectioning. Sections were lightly counterstained with Mayer's Hematoxylin and Eosin (H&E) according to standard procedures. For the identification of reticulocytes, peripheral blood was isolated in heparinized tubes and mixed with Reticuloctye staining solution (Sigma). The cells were counterstained on slides and the reticulocytes were counted per 100 cells in a field. Further assessment of complete blood counts was performed on the HEMAVET HV950FS blood analyzer (Drew Scientific, Inc).

Flow Cytometry Analysis

Single cell suspensions were obtained by either flushing the tibia and femur, or mincing the spleen or the thymus. Following lysis of the red blood cells using the Erythrocyte lysis buffer, 1 X 10^6 to 4 X 10^6 cells were aliquoted into individual tubes. The cells were stained with antibodies against: CD3, CD4, CD8, IL-7Ra, Ter119, Gr-1, Mac-1, B220, CD41, ScaI, c-Kit, Flt3, CD34, FcgR, CD45.1, CD45.2, Flt3, CD150, or CD48. For the BrdU incorporation assays, mice were sacrificed two hours after intraperitoneal injection of 1 mg of BrdU. Cells were then harvested as previously

described and analyzed using the BrdU Flow Kit (BD Pharmingen). To assess the cell cycle status of the LSK cells, bone marrow cells were resuspended in RPMI with 10% FBS and incubated with 10 μg/mL of Hoechst 33342 (Invitrogen) for 45 minutes at 37°C, washed and incubated with the indicated antibodies. Finally, the cells were fixed overnight at 4°C in 5% paraformaldehyde in PBS and incubated with 0.5 μM Pyronin Y (Polysciences, Inc.) for 30 minutes on ice prior to analysis.

Microarray and real-time quantitative PCR

Bone marrow cells were harvested as described and the lineage negative fraction was separated using the Lineage Cell Depletion Kit and MACS columns (Miltenyi Biotec). Total RNA was extracted using the Versagene Total RNA Purification Kit (Gentra Systems) and microarray analysis was performed with the Applied Biosystem Inc. expression system. RNA was pooled from 5 mice and biological triplicates used to further avoid mouse-to-mouse variability. For the MEP and $CD34^{hi}/Fc\gamma R^{low}$ populations, cells were sorted by FACS, pooled from 10 mice, and analyzed as described above. For the quantitative PCR, 1 mg of total RNA was transcribed with the iScript cDNA Synthesis kit (Bio-Rad) and $1/10^{th}$ of the reaction was used for PCR using the iQ SYBER Green Supermix (Bio-Rad) on an iCycler (Bio-Rad) or using TaqMan on an automated ABI platform. PCR reactions were performed in triplicate. The expression of the gene of interest was calculated relative to the levels of *b-actin*, *Gapdh*, or *GusB*. Primers sequences were selected from the PrimerBank Database [98] [PrimerBank IDs: 6671756a2, 6753310a2, 31077096a3 and 16975506a2]. The networks were generated through the use of Ingenuity Pathways Analysis (Ingenuity® Systems,

www.ingenuity.com). The network Score is based on the hypergeometric distribution and is calculated with the right-tailed Fisher's Exact Test. The score is the negative log of this p-value.

Stem Cell and Progenitor Cell Assays

CFU-S

For evaluation of spleen colony-forming unit (CFU-S) abilities, 5 X 10^4 bone marrow cells derived from either *Mtg16*$^{+/+}$ or *Mtg16-null* mice were transplanted into lethally irradiated (900 rads) C57Bl/6 wild-type mice. For retroviral infection, the recombinant retroviruses were produced after transient transfection of BOSC23 cells and the bone marrow cells infected by co-culture for 48 hr in DMEM supplemented with 10% fetal bovine serum (FBS), IL-6, SCF, and LIF. This protocol yields 25-30% infection such that 200,000 cells were injected into the tail veins of recipient mice to match 50,000 wild type cells. However, to ensure that low infection rates were not an issue, as many as 1,000,000 cells were injected. The spleens were isolated 8 or 12 days post-transplant and fixed in Tellsniczky's fixative.

Methylcellulose CFC

Single cell suspensions were obtained either by flushing cells from the tibia and femur or mincing the spleen of mice. The red blood cells of the spleens were lysed with Erythrocyte lysis buffer (Sigma). The cells were mixed with methylcellulose media containing rmSCF, rmIL-3, rhIL-6, rhEpo (Stem Cell Technologies Methocult® GF M3434), methylcellulose containing rmSCF, rmIL-3, rhIL-6 (Stem Cell Technologies

Methocult® GF M3534), or a BFU-E-specific methylcellulose (Stem Cell Technologies Methocult® SF M3436), which contains a proprietary combination of cytokines including rhEpo, and plated on 35mm dishes in duplicate. Colonies were grown at 37C, 5% CO_2 for 8-14 days and colonies were counted. The numbers of cells plated for each condition tested is stated in the figure legend. For the analysis of megakaryocytes, 1 x 10^5 cells were mixed with Megacult®-C media (Stem Cell Technologies), collagen (1.1 mg/ml), and rmIL-3 (10 ng/ml), rhIL-6 (20ng/ml), rhIL-11 (50ng/ml), and rhThrombopoietin (TPO, 50ng/ml) and plated in 35mm plates in duplicate. Cultures were grown at 37^o C, 5% CO_2 for 6 days and were then transferred to a slide (Stem Cell Technologies, Catalog # 04863). The colonies were fixed and stained for acetylcholinesterase activity, and the number of colonies scored by manual counting (as described in the manual for Megacult®-C).

Methylcellulose Replating

To perform the methylcellulose serial replating assays, we harvested bone marrow and plated 2x10^4 total bone marrow cells in methylcellulose media (Methocult GF M3434, StemCell Technologies). Every 7 days for 4 weeks, the numbers of colonies were counted, the plates were harvested, and 2x10^4 cells were replated in methylcellulose media.

Phenylhydrazine Treatment

For Phenylhydrazine (PHZ) treatment, stock solutions of PHZ (10mg/ml; Acros Organics, CAS: 59-88-1, EC: 200-444-7) were prepared fresh in PBS and filter sterilized

on the day of injections (the solution changed color over time, which is why fresh stocks were always made for each injection). 40mg/kg were subcutaneously injected on days 0, 1, and 3, and peripheral blood (PB) was drawn at days 0, 3, and 5 for complete blood counts (CBC) counts to follow how the mice were responding to the PHZ. Since all of the *Mtg16*-null mice were dying by day 5, the experiment was terminated at day 5. In addition to collecting PB for CBC counts at the time point, the spleen and bone marrow were also harvest for H & E sections and to plate in methylcellulose (M3434 and M3436) to determine progenitor cell activity in response to PHZ.

5-Fluorouracil Treatment

For the 5-Fluorouracil (5-FU; Sigma, F6627-5G) treatment, a batch of stock solutions of 10mg/ml in PBS were prepared and frozen after sterile filterization (need to make a batch large enough for the entire experiment to ensure consistent treatment). On the days of injections, an aliquot would be thawed at 55^{o}C to dissolve the 5-FU and the solution was brought back to room temperature before being injected into the mice. 100mg/kg of 5-FU was injected I.P. every 7 days and the mice were monitored for survival.

LTC-IC

For the long-term culture initiating-cell (LTC-IC) assay, $3x10^3$ lineage-negative cells were cultured on OP9 stromal cells and weekly semi-replenishment of media was performed (using the StemCell Technologies procedure). At one-week intervals, a set of wells was harvested and the cells were plated in methylcellulose media (Methocult GF

M3434, StemCell Technologies) and cultured for 10 days to determine the percentage of positive wells.

Bone Marrow Transplantation

For bone marrow transplantation, a single cell suspension of bone marrow cells was obtained from the tibia and femur, and the red blood cells were lysed with erythrocyte lysis buffer (Buffer EL, Qiagen). Bone marrow cells were injected via the tail vein into lethally irradiated (900 rads) recipient wild-type C57Bl/6 mice.

Competitive Repopulaition Assay

For competitive reconstitution assays, lethally irradiated C57Bl/6 CD45.1 congenic mice were used as recipients. The *Mtg16*$^{+/+}$ or *Mtg16*-null donor cells were mixed with C57Bl/6 CD45.1 bone marrow cells at a ratio of 9:1, respectively. Reconstitution potential of the donor (CD45.2) cells was monitored by flow cytometry of the peripheral blood. For the secondary competitive repopulation transplants, the bone marrow was harvested as described 12 weeks after the primary competitive transplant, and 2 x 10^6 total bone marrow cells were injected into the tail vein of lethally irradiated recipients.

Homing

To assess total bone marrow cell homing, we used the vital dye carboxyfluorescein succinimidyl ester (CFSE; Molecular Probes, Inc.). Wild type or *Mtg16*-null bone marrow cells were allowed to take up CFSE *ex vivo*, injected into the

tail vein of irradiated recipient mice, and the bone marrow and spleens of recipient mice were analyzed by flow cytometry 6 hr later to determine the percentage of cells containing CFSE-dependent fluorescence. Analysis was performed on a Becton Dickinson FACSCalibur, LSRII, or FACSAria flow cytometer. To assess progenitor cell homing, donor bone marrow (Wild-type or *Mtg16*-null) was harvested and prepared as described for the bone marrow transplants. 1 x 10^7 cells were injected via the tail vein into lethally irradiated recipient wild-type C57Bl/6 mice and an aliquot was also plated in methylcellulose culture to quantify the input number of committed progenitor cells. Sixteen hours later, the recipient mice were euthanized and the cells from the femur and tibia were harvested. Single-cell suspensions of the marrow cells were cultured in triplicate to assess the donor output colony-forming units in the recipient animals. For estimating total bone marrow (BM) recovery, the femur/tibia content was assumed to represent 9% of total BM [99].

Chromatin Immunoprecipitation (ChIP) Assays

Chromatin Immunoprecipitation (ChIP) assays were performed using Murine Erythroleukmia (MEL) cells. 1 x 10^7 cells per condition were crosslinked with 1% Formaledhyde (Sigma) for 20 minutes and the crosslinking reaction was quenched by the addition of glycine to a final concentration of 125mM for 5 minutes. Cells were collected, washed, and resuspended in a low salt ChIP buffer (50mM HEPES KOH, ph7.5, 140mM NaCl, 1mM EDTA pH8.0, 1% Triton X-100, and 0.1% sodium deoxycholate). Samples were sonicated and cleared by centrifugation, then precleared with the addition of Protein G Sepharose 4B (Sigma). Samples were incubated over-

night with goat IgG (Santa Cruz), anti-Eto2 G20 (Santa Cruz), anti-E47 SC-763x (Santa Cruz), or Rabbit IgG control (Millipore). Immune complexes were collected by incubation with Protein G Sepharose 4B (Sigma) then washed with a low salt ChIP buffer, a high salt ChIP buffer (50mM HEPES KOH pH7.5, 500mM NaCL, 1mM EDTA pH8.0, 1% Triton X-100, and 0.1% sodium deoxycholate) and lithium chloride/NP40 buffer (10mM TrisCl, pH8.0, 250mM LiCl, 0.5% NP-40, 0.5% sodium deoxycholate). DNA-antibody complexes were eluted with elution buffer (1% SDS and 100mM sodium bicarbonate) and the crosslink was reversed with 200 μM NaCl at 65^{o}. DNA was precipitated with the addition of 100% EtOH, RNase treated, Proteinase K (Sigma) treated, and isolated using the Qiagen PCR Purification kit. RT-PCR was performed with 2 μl of each sample in duplicate using SybrGreen (BioRad) and the BioRad ICycler and normalized to input. Primer sequences are as follows:

E2F2 Intron 1: F- 5'-GGACTCTGGAGGGCTAATGTTG-3'

R-5'-GCAATGTCTTCACTCGGCTCGG-3';

E2F2 Intron 2: F-5'TCAGACAGATGAGCGGGGAGGTG-3'

R-5'-GCCTCTGCCAGCCGCTTGAAA-3';

E2F2 3' UTR: F-5'-TGGTTTCCCCTCCCTGTGAGGC-3'

R-5'-AGACCTGTAGCCACCACGGTCC-3';

CCND1 TCF: F-5'-CTGCCCGGCTTTGATCTCT-3'

R-5'-AGGACTTTGCAACTTCAACAAAACT-3';

CCND1 EBox/CSL: F-5'-CTGGTCTGGCATCTTCGG-3'

R-5'-GAGAATGGGTGCGTTTCCG-3';

N-Myc: F-5'-CCCGAATGCCTACATAATTCT-3'

R-5'CCTTGGAAGGGTGGCTCA-3';

Mtg16: F-5'-AATATTCACAGGGCCTGACCAA-3'

R-5'-AAATGCCTGCAAGCGGATTA-3'

Immunofluorescence staining

Bone marrow collected from both femurs was separated into lineage marker positive (CD5, CD45R (B220), CD11b, Anti-Gr-1 (Ly6G/C), 7-4, and Ter-119) and negative fractions using the MACS Magnetic Lineage Cell Depletion system (Miltenyi Biotech), or FACS purified for the LSK/Flt3^{-}, LSK/Flt3^{+}, and MP sorted populations. The cells were allowed to adhere to poly-L-Lysine coated coverslips, fixed in 2% paraformaldehyde for 15 minutes at room temperature, and permeabilized in 0.5% Triton X-100. DNA double-stranded breaks were detected using a 1:2000 dilution of anti-phosphoH2AX (γH2AX, Millipore) or 1:1000 anti-53BP1 and 1:2000 dilution of goat anti-mouse Cy3 (Jackson Laboratories) and the nuclei were counterstained with 4,6-diamidino-2-phenylindole (DAPI). Stained coverslips were mounted on glass slides and 0.5 μM optical slices were digitally captured using an Olympus FluoView1000 scanning confocal microscope. The number of foci per DAPI-positive nucleus was counted in >80-100 cells per lineage fraction per mouse. Statistical analysis was performed using a Student's t-test.

CHAPTER III

DELETION OF MTG16, A TARGET OF THE t(16;21), ALTERS HEMATOPOIETIC PROGENITOR CELL PROLIFERATION AND LINEAGE ALLOCATION

Background and Significance

Non-random, somatically acquired, chromosomal translocations are commonly associated with the development of acute leukemia and affect genes that control cell proliferation, differentiation, survival, and lineage decisions that affect stem cell self-renewal and progenitor cell differentiation [1]. While translocations can cause the over-expression of dominantly acting oncogenes such as *BCL2* or *c-MYC* [100, 101], the majority of the fusion proteins that are created in the myeloid lineage create weak oncogenes that do not have a single dominant phenotype. As such, the genes that are disrupted by these translocations have been extensively studied in order to understand the function of the translocation fusion proteins.

The Myeloid Translocation Gene on chromosome 16 (MTG16, also known as ETO-2 or *CBFA2T3*) and Myeloid Translocation Gene on chromosome 8 (MTG8, also known as Eight-Twenty-one or ETO) are disrupted by the t(16;21) and t(8;21), respectively. Both of these translocations create fusion proteins containing the DNA binding domain of RUNX1 (formerly called AML1) fused to nearly full-length of MTG8 or MTG16 [13, 15-17]. Gene disruption strategies have been valuable to dissect the regulatory pathways and identify the critical factors that mediate the decision of a stem

cell to self-renew and quiesce or to enter the rapidly expanding progenitor cell pool to populate the various hematopoietic cell lineages. Many of these key regulators are DNA binding transcription factors, which control gene expression programs to influence proliferation and differentiation. By contrast, only a limited number of the transcriptional regulators and chromatin remodeling factors that are recruited by DNA binding factors have been pinpointed as contributors to stem cell functions. This is especially true for transcriptional corepressors and gene silencing factors. Although a great deal of information has been gathered about the molecular interactions of the MTG family members through the analysis of the leukemia-related fusion proteins [102], less is known about the physiological functions of this gene family. Gene targeting studies of *Mtg8/Eto* and *Mtgr1* have indicated a role in intestinal development, but have yet to identify any defects in hematopoiesis [56, 103]. We have created mice lacking *Mtg16* to better understand the physiological action of this key regulator.

Results

Mtg16-null mice are viable with signs of mild anemia

To examine the role of *Mtg16/Eto2* in hematopoiesis, we deleted exon 8 of the gene, because splicing from exon 7 to exon 9 introduces a stop codon in the mRNA, thereby triggering nonsense mediated mRNA decay. Homologous recombination was used to insert LoxP sequences flanking exon 8 and the *G418 resistance gene* (*Neo*) containing a 5' LoxP site was inserted directly upstream of exon 8 (Fig. 9A). Embryonic stem (ES) cells with a correctly targeted allele were identified and injected into

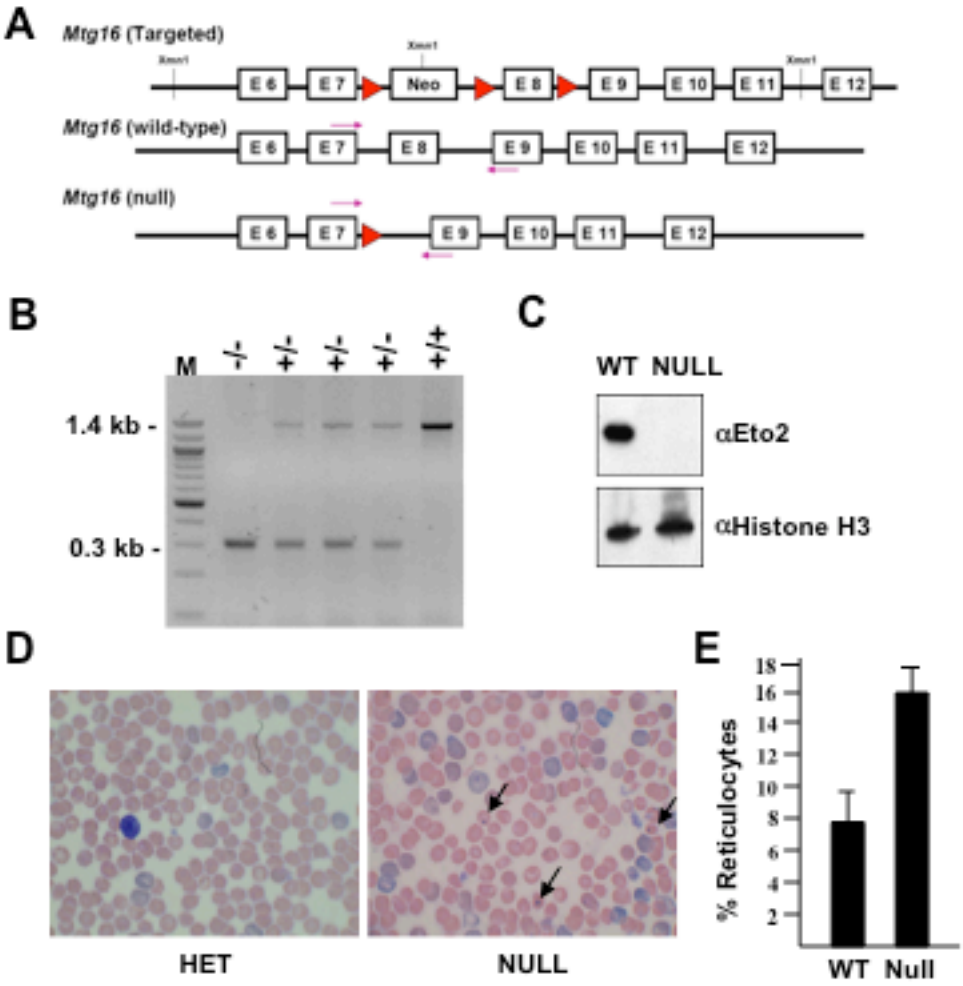

Figure 9. Generation of *Mtg16*-null mice. (A) Schematic diagram showing a portion of the wild type Mtg16 (*Cbfa2t3)* locus, targeting construct, and the resulting mutated locus after Cre-recombinase mediated deletion of Exon 8 and the *Neomycin-resistance* cassette and the probes used. (B) PCR of genomic DNA demonstrates that Exon 8 has been deleted (0.3 kb band). M, 100 bp ladder. (C) Western blot of nuclear extract from wild type or *Mtg16*-null splenocytes shows the absence of Mtg16 protein. Histone H3 was used as a loading control (lower panel). (D and E) Peripheral blood smears from heterozygous or null mice were stained with Reticulocyte stain (D) and the numbers of reticulocytes quantified by visual inspection after counting at least 200 hundred cells and the mean of several measurements shown as a bar graph (E); the error bars are standard errors of the mean (E). The arrows in (D) indicate Howell-Jolly bodies.

blastocysts. Examination of the progeny by genomic PCR or Southern blot analysis confirmed germline transmission of the "floxed" allele. The mice carrying the targeted allele were crossed with transgenic *E2A-Cre-recombinase* mice and offspring lacking exon 8 and *Neo* were identified. Genomic PCR (Fig. 9B), Southern blot analysis (data not shown), and Western blot analysis of splenocytes (Fig. 9C) confirmed that *Mtg16/Eto2* was inactivated.

On a mixed 129SvEv x C57BL/6 genetic background, mice lacking *Mtg16* were obtained at the expected frequency, were fertile, and appeared anatomically normal. Although one allele of *Mtg16* is deleted in up to 40% of ductal breast carcinoma [4], there was no overt defect in breast development observed by whole mount preparation and H&E sectioning (data not shown). Given the targeting of *Mtg16* by the t(16;21) in AML, we examined the peripheral blood for any defects. Complete blood counts revealed a mild anemia in some mice and a compensatory reticulocytosis at 4 weeks of age. Both Wright staining and reticulin staining of peripheral blood smears from 4 week old mice indicated that *Mtg16*-null mice have on average twice as many circulating reticulocytes (Fig. 9D and 9E, and data not shown). Consistent with this finding, we observed an increased number of Howell-Jolly bodies, which are nuclear remnants found in circulating, young red blood cells in response to anemia or splenic dysfunction (Fig. 9D, arrows).

Mtg16-null mice display disruptions in allocation to bone marrow progenitor cells

The peripheral blood phenotypes prompted us to examine the bone marrow, spleen and thymus of *Mtg16*-null mice. Upon gross examination of the spleens of 4-week

old *Mtg16*-null mice, we noted splenomegaly with an average spleen weight 2-fold greater than the littermate controls. Histological examination of the spleens of these mice indicated that there was a disruption in the architecture (Fig. 10A) with the red pulp of the *Mtg16*-null spleens containing excess lymphoid, myeloid, erythroid, and megakaryocytic elements consistent with extramedullary hematopoiesis. The presence of excess myeloid progenitor cells was confirmed using methylcellulose colony formation assays (Fig. 10B). However, this was a transient effect as the spleens were of similar size as the littermate controls at 8 and 12 weeks, which is coincident with the mice reaching full size. Therefore, the extramedullary hematopoiesis in the spleen correlates with the need for more red cells during rapid neonatal growth.

Flow cytometry using lineage specific antibodies confirmed that all of the hematopoietic lineages were present in the bone marrow of these mice, but that there were disruptions in lineage allocation (Fig. 11A). There were somewhat fewer total B220 positive B-cells, as well as $B220^{hi}$ cells. In addition, it appeared that there were fewer maturing erythroid progenitor cells, as fewer cells were $Ter119^{+}$. There were also fewer $CD41^{+}$ cells, suggesting reduced numbers of megakaryocytes (Fig. 12A). Conversely, more cells were $Gr1^{+}/Mac1^{+}$, suggesting that the inactivation of *Mtg16* allowed more cells to enter the granulocyte/macrophage pathway. As for erythropoiesis, while fewer cells were Ter119 positive, once committed to this lineage, the cells continued to differentiate, as the subpopulations distinguished by staining with anti-CD71 and anti-Ter119 were all present and in similar proportion to the control mice (Fig. 11B). Methylcellulose colony formation assays confirmed these flow cytometry results, as there

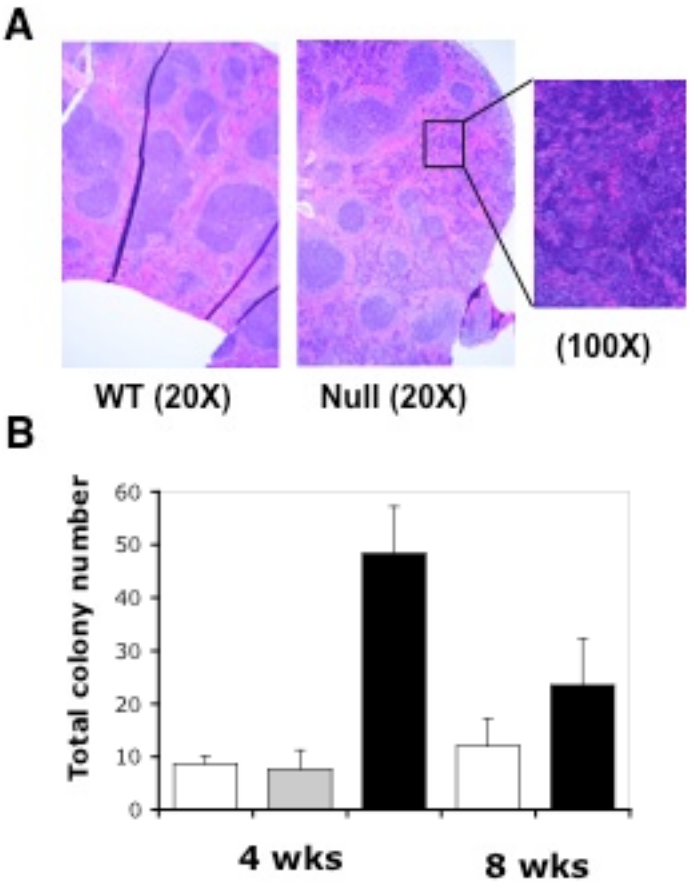

Figure 10. *Mtg16*-null mice display extramedullary hematopoiesis in the spleen. (A) Sections of wild type and *Mtg16*-null spleens were stained with H&E and photographed. High magnification inset shows the presence of myeloid cells. (B) Methylcellulose colony formation assays using IL-6, IL-3, SCF and Epo with splenocytes from wild type (empty bars), *Mtg16*-heterozygous (gray bar) and *Mtg16*-null (full bar) mice that were 4 or 8 weeks of age. Colonies were counted and the average and standard error displayed as bar graphs.

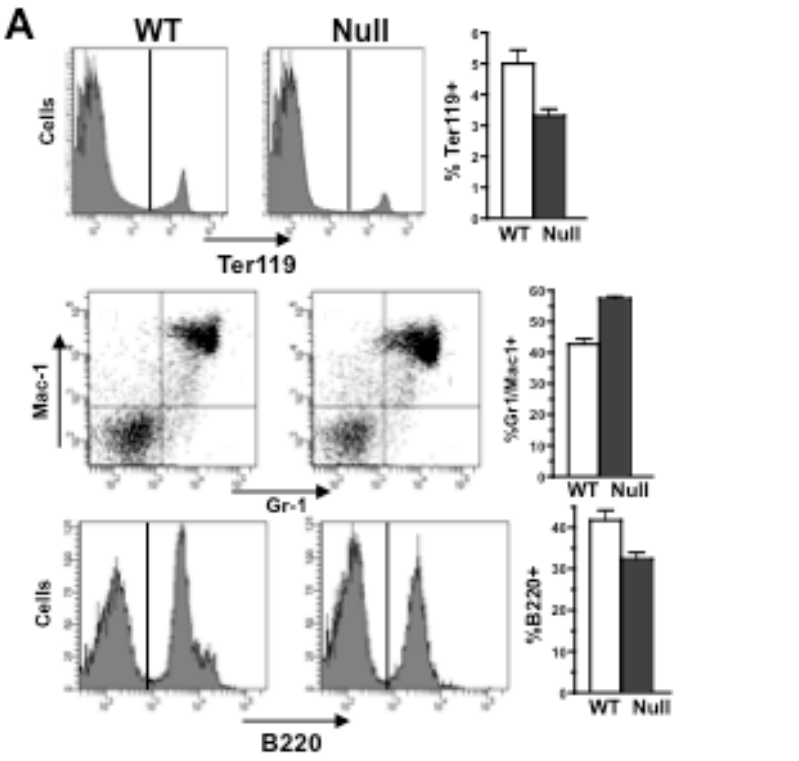

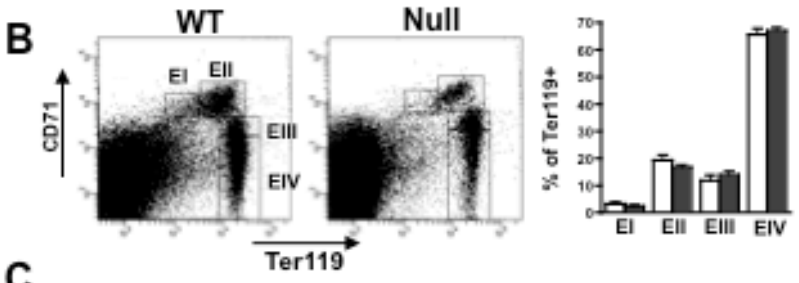

C

	Bone Marrow		Spleen	
	WT	*Mtg16-Null*	WT	*Mtg16-Null*
BFU-E	7.5 ± 2.5	0.0 ± 0.0	29.5 ± 2.5	4.0 ± 1.0*
CFU-M	100.0 ± 4.0	97.0 ± 2.0	14.0 ± 3.0	20.5 ± 2.5
CFU-G	22.0 ± 8.0	62.0 ± 7.0	4.0 ± 1.0	40.5 ± 1.5**
CFU-GM	61.5 ± 10.5	97.5 ± 5.5	6.0 ± 0.05	16.5 ± 0.5**
CFU-GEMM	4.5 ± 0.5	1.0 ± 0.05*	2.0 ± 0.05	1.5 ± 0.5

D

	Bone Marrow		Spleen	
	WT	*Mtg16-Null*	WT	*Mtg16-Null*
CFU-M	48.5 ± 1.5	36.5 ± 6.5	22.0 ± 1.0	27.0 ± 2.0
CFU-G	43.5 ± 7.5	123.0 ± 13.0*	1.5 ± 0.5	27.5 ± 2.5**
CFU-GM	85.0 ± 2.0	83.5 ± 11.5	1.5 ± 0.5	13.0 ± 0.05**

E

	Bone Marrow		Spleen	
	WT	*Mtg16-Null*	WT	*Mtg16-Null*
BFU-E	49.13 ± 1.817	0.0 ± 0.0***	23.5 ± 6.5	0.0 ± 0.0

Figure 11. Hematopoietic defects in *Mtg16*-null mice. (A) Flow cytometry analysis of bone marrow from wild type and *Mtg16*-null mice using the lineage specific antibodies indicated. An example of the cell plot histograms is shown. An unpaired two-tailed t-test indicated that the changes observed in the number of cells were significant (Ter119, $p = 0.0086$; Gr1/Mac1, $p = 0.0001$; B220, $p = 0.011$). (B) Flow cytometry analysis of erythropoiesis using anti-Cd71 versus anti-Ter119. The boxes mark the 4 stages of differentiation. An unpaired two-tailed t-test indicated that there were no statistical differences ($n = 5$ for each population observed). (C) Bone marrow (2.5×10^4 cells) or spleen (2.0×10^5) cells were plated in methylcellulose containing IL-3, IL-6, Epo, and SCF and colonies were quantified after 8-10 days in culture. (D) Bone marrow (2.5×10^4) or spleen (2.0×10^5) cells were plated in granulocyte and monocyte-specific methylcellulose containing IL-3, IL-6, and SCF and colonies were quantified after 8-10 days in culture. (E) Bone marrow (5×10^4) or spleen (5×10^5) cells were plated in BFU-E-specific methylcellulose and colonies were quantified after 14 days in culture. An unpaired two-tailed t-test indicated that some of the differences in the colony numbers were significant (*, $p = 0.01$-0.05; **, $p = 0.001$-0.01; ***, $p < 0.001$). Shown are representative results from an experiment done in duplicate that are consistent with other biological replicates.

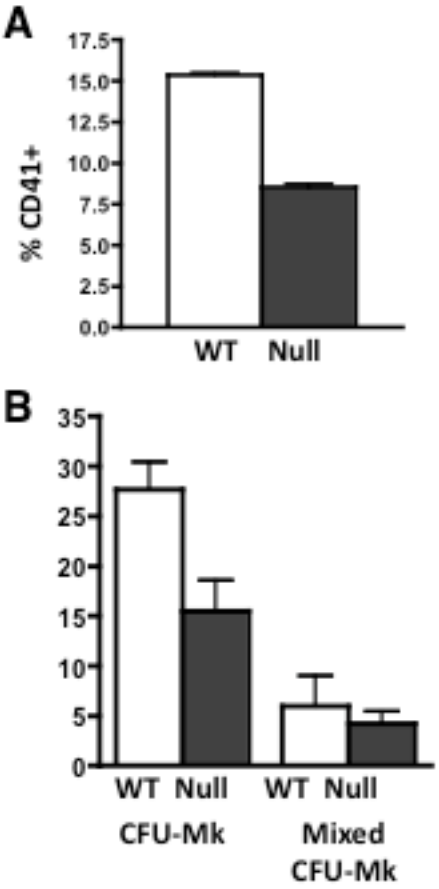

Figure 12. *Mtg16-null* mice have decreased numbers of CD41+ Megakaryocyte Progenitors. (A) A histogram of the flow cytometry analysis of bone marrow from wild type and *Mtg16-null* mice using anti-CD41. Open bars are from control mice and dark bars represent *Mtg16-null* mice. An unpaired two-tailed t-test indicated that the decrease was significant ($p < 0.001$, $n=3$). (B) A histogram showing the quantification of the number of megakaryocyte progenitors formed from bone marrow (1×10^5) cells plated in collagen-containing (megacult®-C) media with IL-3, IL-6, IL-11 and TPO. Shown are representative results from an experiment done in duplicate that are consistent with other biological replicates. An unpaired two-tailed t-test indicated that the decrease in CFU-MK was significant ($p = 0.036$, $n =2$).

were consistently more CFU-G colonies formed from both the bone marrow and the spleen (Fig. 11C, 11D). This increase in the granulocytic lineage appeared to be at the expense of the erythroid lineage, as there were only a few BFU-E formed (Fig. 11C, 11E). Although megakaryocytes and erythroid cells share a common progenitor cell (MEP), colonies containing mature megakaryocytes were produced in vitro (Fig. 12B). Thus, while there were no complete blocks in hematopoietic differentiation in the absence of *Mtg16*, there was altered production of cells within lineages and a dramatic reduction in BFU-E activity *in vitro*.

Loss of *Mtg16* sensitizes mice to the effects of phenylhydrazine

The reduction in the number of $Ter119^+$ cells, the impairment in BFU-E, and the association of Mtg16 with TAL1/Scl and Gfi1b in hematopoietic cell lines [46, 47] led us to test the response of *Mtg16*-null mice to erythropoietic stress. Phenylhydrazine is a hemolytic agent used in the past to treat patients with polycythemia vera and is used experimentally in provoking stress erythropoiesis [104]. Cohorts of control and *Mtg16*-null mice were injected with 40 mg/kg phenylhydrazine, which is a regimen that this well tolerated in wild type mice (Fig. 13A). However, the *Mtg16*-null mice quickly became moribund and the experiment was terminated at day 5 (Fig. 13A). Erythropoietic stress stimulates a dramatic proliferative response in the bone marrow and spleen. In the spleen, myeloid progenitor cells rapidly expand to regenerate the erythropoietic system. At the gross level, spleens of control mice increased in size by over 4-fold to meet the phenylhydrazine challenge (Fig. 13B) and the total red blood cell counts and hematocrits were reduced by only about 50%, as expected. By contrast, the spleens

A

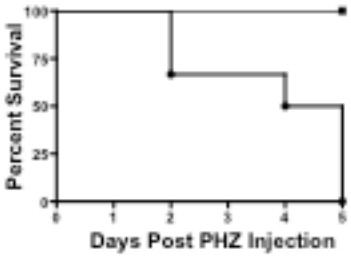

B

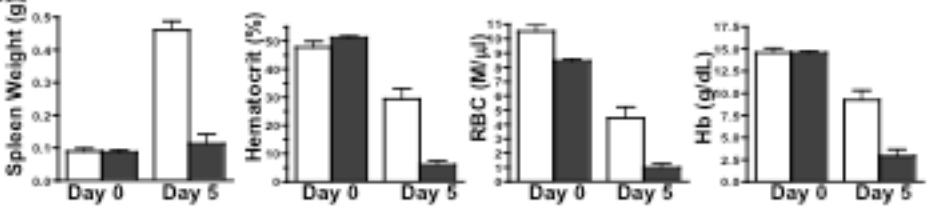

C

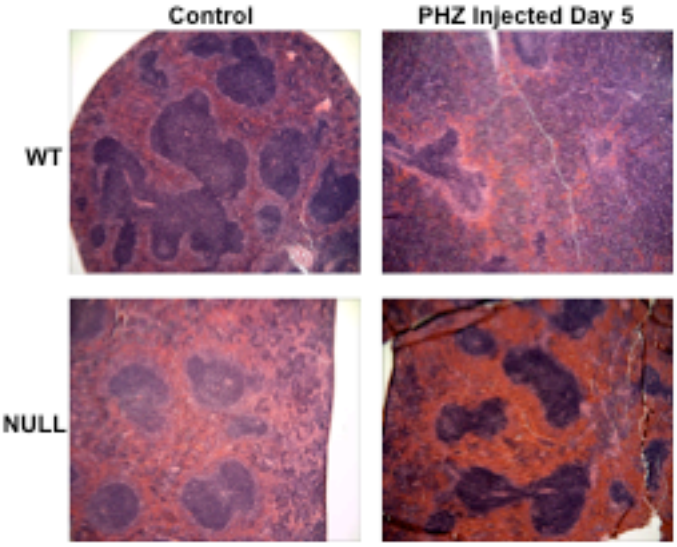

D

	PHZ Day 3 Bone Marrow		PHZ Day 3 Spleen		PHZ Day 5 Bone Marrow		PHZ Day 5 Spleen	
	WT	*Mtg16-Null*	WT	*Mtg16-Null*	WT	*Mtg16-Null*	WT	*Mtg16-Null*
BFU-E	10.0 ± 1.0**	0.0 ± 0.0	19.0 ± 3.0	0.0 ± 0.0 *	5.5 ± 0.5	1.0 ± 1.0	50.5 ± 2.5	0.0 ± 0.0 **
CFU-M	58.0 ± 10.0	31.5 ± 4.5	26.5 ± 3.5	40.5 ± 0.5	44.5 ± 2.5	58.0 ± 1.0*	51.5 ± 6.5	101.0 ± 1.0*
CFU-G	36.5 ± 2.5	48.5 ± 4.5	7.5 ± 1.5	65.5 ± 3.5**	32.0 ± 6.0	99.5 ± 2.0*	22.0 ± 4.0	183.0 ± 3.0***
CFU-GM	11.5 ± 1.5	16.0 ± 0.05	8.5 ± 2.5	17.5 ± 1.5	19.0 ± 2.0	22.5 ± 2.5	15.5 ± 4.5	82.0 ± 2.0**
CFU-GEMM	6.0 ± 2.0	2.0 ± 1.0	4.0 ± 1.0	0.0 ± 0.0	10.5 ± 9.5	0.5 ± 0.5	1.5 ± 0.5	0.0 ± 0.0

E

	PHZ Day 3 Bone Marrow		PHZ Day 3 Spleen		PHZ Day 5 Bone Marrow		PHZ Day 5 Spleen	
	WT	*Mtg16-Null*	WT	*Mtg16-Null*	WT	*Mtg16-Null*	WT	*Mtg16-Null*
BFU-E	44.17 ± 2.81	0.0 ± 0.0***	41.5 ± 2.5	0.0 ± 0.0**	57.5 ± 3.5	0.0 ± 0.0	69.5 ± 2.5	0.0 ± 0.0

Figure 13. Mtg16 is required during hematopoietic stress. (A) Survival curves of mice injected with phenylhydrazine. (B) Characterization of the hematopoietic response to phenylhydrazine shown schematically as graphs. Open bars are from control mice and dark bars represent *Mtg16*-null mice. An unpaired two-tailed t-test indicated that the decrease in red blood cells (RBC) at day 3 is significant ($p = 0.0009$, $n=6$) and all of the changes observed at day 5 were significant (Spleen weight, $p = 0.001$; Hematocrit, $p = 0.0044$; RBC, $p = 0.001$; Hemoglobin (Hb), $p = 0.0083$; $n = 3$). (C) Histological analysis of wild type and *Mtg16*-null spleens before and 5 days after administration of phenylhydrazine. (D) Colony results from bone marrow (2.0×10^4) or spleen (1×10^5) cells plated methylcellulose containing SCF, IL-3, IL-6 and Epo at day 3 or day 5 after PHZ injection. Shown are representative results from an experiment done in duplicate that are consistent with other biological replicates. (E) Colony results from bone marrow (5×10^4) or spleen (1×10^5) cells plated in erythroid-specific methylcellulose at day 3 or day 5 after PHZ injection. An unpaired two-tailed t-test indicated that some of the differences in the colony numbers were significant (*, $p = 0.01$-0.05; **, $p = 0.001$-0.01; ***, $p < 0.001$). Shown are representative results from an experiment done in duplicate that are consistent with other biological replicates.

of *Mtg16*-null mice did not increase in size and the red cell count plummeted along with the hematocrit (Fig. 13B). Histological analysis of the spleens of these mice indicated that the control mice were able to expand their progenitor populations to meet the hematopoietic challenge, but the *Mtg16*-null progenitor population failed to expand 5 days after the first injection of phenylhydrazine (Fig. 13C). Methylcellulose colony formation assays confirmed these results, as there was either a dramatic reduction or no BFU-E colonies formed using either a combination of Epo, IL-6, IL-3, and SCF (Fig. 13D) or Epo alone (Fig. 13E), but with a concomitant increase in CFU-M, CFU-G, and CFU-GM colonies from the spleens of the *Mtg16*-null phenylhydrazine-treated mice (Fig. 13D).

Inactivation of *Mtg16* disrupts progenitor cell gene expression networks

Mtg16 is the most highly expressed MTG family member in the early progenitor and stem cell populations [60]. Thus, loss of *Mtg16* is expected to alter transcriptional networks to affect erythroid progenitor cell proliferation. To begin to define the changes in gene expression underlying these phenotypes, we performed cDNA microarray analysis of immature bone marrow progenitor cells to further define the mechanistic basis of these defects. The bone marrow from young adult, sex matched, wild type and *Mtg16*-null mice was pooled and lineage positive cells were removed using the lineage panel of antibodies coupled to magnetic beads. Total RNA from the lineage negative cells was prepared and used for cDNA microarray analysis (Fig. 14A). The mis-regulation of numerous genes associated with stem cell and progenitor cell function was observed, including *Socs2*, *Gfi1*, *HoxB2*, *PU.1*, and members of the *C/EBP* family (Fig. 14A). The

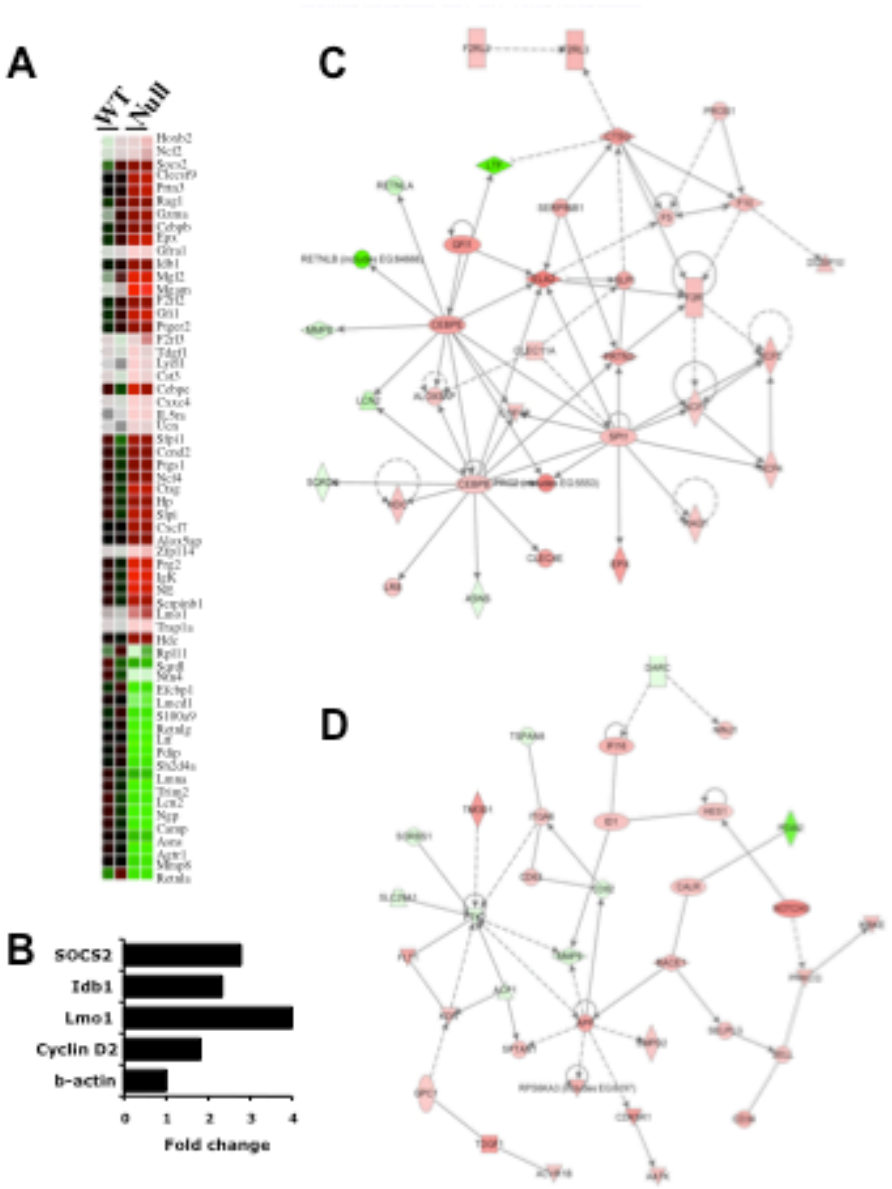

Figure 14. *Mtg16*-null progenitor cells have alterations in gene expression. (A) Heat map showing some of the changes in gene expression that occur in lineage negative bone marrow progenitor cells as determined by cDNA microarray analysis. The heat map shows genes whose expression is higher in the *Mtg16*-null cells as red and those genes that are lower in green. (B) Quantitative RT-PCR of selected genes to validate the microarray studies. An additional 15-20 cell cycle related genes were also analyzed without significant changes. (C and D) The two most significant networks from Ingenuity Pathway analysis showing genes whose expression changes in the absence of *Mtg16*. "Hematopoietic system development and function" is shown in C (score = 47) and "immune response, cell-to-cell signaling" is shown in D (score also = 47). Red, up-regulated; Green, down-regulated.

changes in expression of selected target genes were confirmed by quantitative RT-PCR (Fig. 14B, and data not shown). In addition, quantitative RT-PCR was used to examine the expression of numerous cell cycle regulators whose induction could contribute to the observed phenotypes including the retinoblastoma family members and cyclin dependent kinase inhibitors. However, we did not detect statistically significant changes in the expression of these genes either by microarray or by quantitative RT-PCR (data not shown).

When the mRNAs that showed a greater than 2-fold change were analyzed using Ingenuity Pathway Analysis software, two networks of transcription factors and their regulated genes were found to be altered (Fig. 14C, 14D; red is up, green is down, network score 47 for each shown). Within these networks we noted that several genes that are regulated by Gfi1, which recruits MTG8, were de-repressed. These included *Gfi1* itself, *Neutrophil Elastase* (*Ela2*) and *C/EBPε* (Fig. 14C) [105, 106]. We then performed a visual inspection of the array data to examine the expression of genes that are regulated by these and other DNA binding factors that recruit MTG family members. By expanding the expression array criteria to as low as 1.7 fold, we noted that 2 additional Gfi1-regulated genes, the *IL6 receptor* and *C/EBPα,* were induced as was *Socs3*, which is regulated by Gfi1b [105, 107]. In addition, we found that the BCL6-regulated genes *Stat1*, *Id2*, *CD69*, *Cyclin D2*, and *Cxcr4* were up-regulated in the null mice [108] and that *PLCγ*, *Gadd45β*, and *Hes1*, which are regulated by "E-proteins" (e.g., HEB and E47 [45, 109]) were similarly activated. These results prompted us to extend this analysis to demonstrate that these factors can also associate with Mtg16. Immunoprecipitation

followed by Western blot analysis indicated that Mtg16 bound to both Gfi1 and PLZF, and modestly associated with the PLZF-related factor BCL6 (Fig. 15).

The gene expression analysis identified transcriptional networks that are disrupted when *Mtg16* is inactivated and also identified multiple genes whose activation might alter cell cycle progression, including *Socs2* and *Socs3*, which dampen cytokine receptor signals [110, 111] and the C/EBP family members that can bind to and impair the action of E2Fs [112-114]. In addition, we found that the levels of mRNA encoding the cyclin dependent kinase inhibitor p27 was induced an average of 1.7-fold in the *Mtg16*-null cells, but that the levels of *p21* were not significantly altered either in the microarray analysis or in quantitative RT-PCR assays (data not shown). Cumulatively, these small changes in gene expression may have a significant impact on progenitor cell proliferation. In contrast, few genes associated with the induction of apoptosis were identified. Finally, we noted that *Cd34*, which is expressed in common myeloid progenitor and granulocyte/macrophage progenitor cells, was up-regulated in the *Mtg16*-null mice.

Inactivation of *Mtg16* yields a c-Kit^{+}/Cd34^{hi}/FcgR^{low} myeloid progenitor population

The stimulation of *Cd34* and genes that control myelopoiesis (e.g., C/EBP family members) could be due to altered transcription of these genes in the absence of Mtg16, or it could be due to a skewing of lineage allocation toward myeloid progenitor cells. Therefore, we examined the early progenitor bone marrow compartment using flow cytometry to define the ratios of early progenitor cells in the bone marrow of *Mtg16*-null mice. For this analysis, we first depleted maturing cells (lineage positive) and then

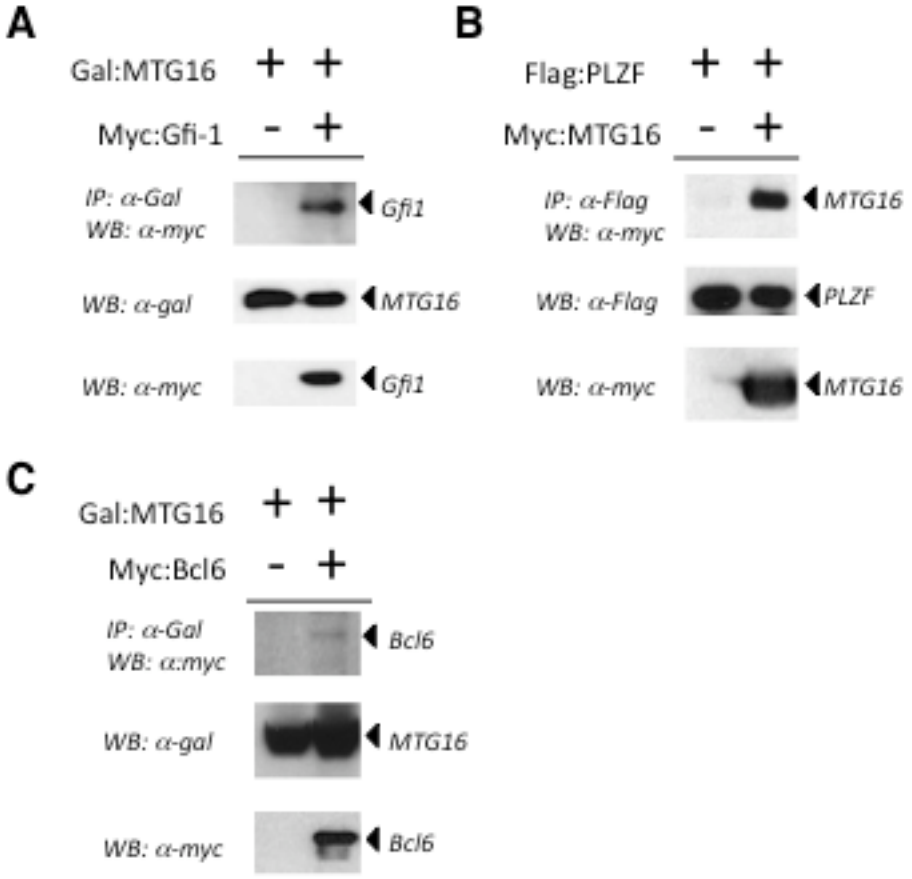

Figure 15. Mtg16 associates with Gfi1, PLZF, and BCL6. The proteins indicated containing either a GAL4 DNA binding domain, a Flag or a c-Myc epitope tag were co-expressed and the association between these proteins determined by immunoprecipitation (IP) followed by western blot (WB) analysis with the indicated antibodies.

identified cells expressing combinations of c-Kit, but not Sca1, and used the FcγR and Cd34 to distinguish myeloid progenitor populations by flow cytometry [115, 116]. As compared to wild type control mice, the *Mtg16*-deficient mice contained slightly fewer lineage$^-$/c-Kit$^+$/Sca1$^+$ cells (LSK, Fig. 16A). Within the myeloid progenitor cells (lineage$^-$/c-Kit$^+$/Sca1$^-$), there were fewer megakaryocyte-erythroid progenitor cells (MEPs, Fig. 16A, $p < 0.05$), but more common myeloid progenitor cells (CMPs, Fig. 16A and 16B) and more granulocyte/macrophage progenitor cells (GMPs, Fig. 16A and 16B) [88, 115]. In addition, the *Mtg16*-null mice contained a cell population that highly expressed *Cd34*, but poorly reacted with anti-FcγR (Fig. 16A, 16B).

To determine what lineage of cells the Cd34^{hi}/FcγR^{low} cells represented, we used FACS to isolate these cells along with CMPs, GMPs, and MEPs from wild type and null mice and cultured these cells in methylcellulose supporting myeloid progenitor cell growth. Consistent with the FACS data that indicates that deleting *Mtg16* in the bone marrow creates more granulocytic-lineage precursors, in both CMP and GMP populations, there were consistently more CFU-G colonies formed with a dramatic loss of BFU-E (Fig. 16C, 16D; see Fig. 17 for photographic examples of the colonies formed). The *Mtg16*-null Cd34^{hi}/FcγR^{low} cells formed similar numbers of CFU-M, CFU-G, and CFU-GM colonies under these conditions as wild type CMP cells, but had little or no potential to yield BFU-E (Fig. 16C, 16D, 16E).

Next, we sorted the Cd34^{hi}/FcγR^{low} cells from the null mice and compared gene expression in these cells to MEPs from wild type or null bone marrow to further test whether these are MEPs that had de-regulated Cd34 expression. Comparison of the Cd34^{hi}/FcγR^{low} cells to MEPs from the null mice indicated that this was a distinct cell

A

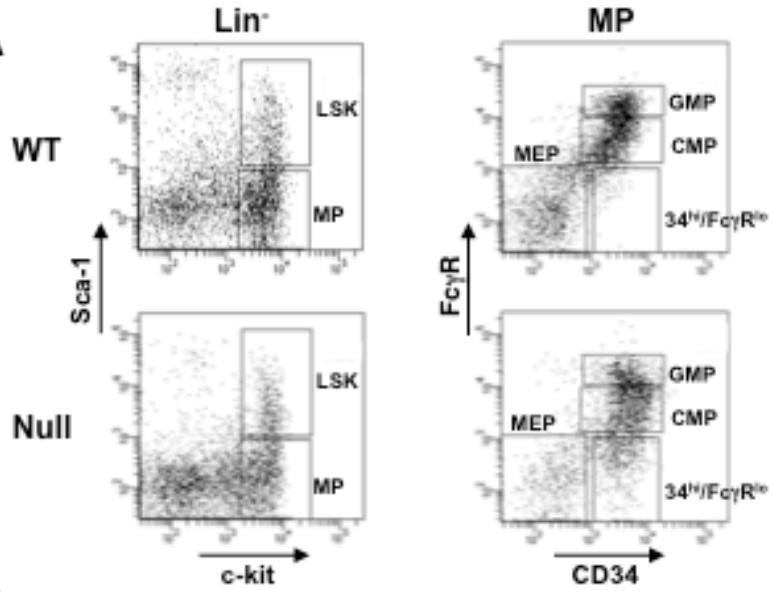

B

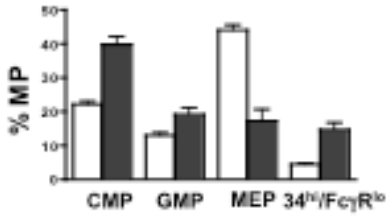

C

	CMP		GMP		MEP		CD34^{hi}/FcγR^{low}
	WT	*Mtg16-Null*	WT	*Mtg16-Null*	WT	*Mtg16-Null*	*Mtg16-Null*
BFU-E	32.5 ± 12.16	2.5 ± 1.19*	0.0 ± 0.0	0.0 ± 0.0	4.0 ± 1.0	0.0 ± 0.0	1.0 ± 0.5774
CFU-M	58.25 ± 6.836	47.75 ± 9.096	79.0 ± 17.10	47.0 ± 6.819	0.0 ± 0.0	0.5 ± 0.5	46.5 ± 12.17
CFU-G	21.5 ± 6.09	96.5 ± 9.115***	104.0 ± 11.07	132.5 ± 22.53	0.0 ± 0.0	0.0 ± 0.0	23.5 ± 1.5
CFU-GM	21.25 ± 5.633	30.75 ± 3.146	13.25 ± 4.785	5.25 ± 2.78	0.0 ± 0.0	1.05 ± 0.05**	15.0 ± 1.732
CFU-GEMM	1.0 ± .7071	1.0 ± .7071	0.0 ± 0.0	0.0 ± 0.0	0.0 ± 0.0	0.0 ± 0.0	0.25 ± 0.25

D

	CMP		GMP		CD34^{hi}/FcγR^{low}
	WT	*Mtg16-Null*	WT	*Mtg16-Null*	*Mtg16-Null*
CFU-M	83.75 ± 13.89	64.0 ± 4.708	79.0 ± 6.892	48.5 ± 4.735*	50.25 ± 1.652
CFU-G	25.75 ± 8.509	105.5 ± 7.73***	121.3 ± 21.58	176.0 ± 10.45	32.5 ± 3.069
CFU-GM	22.0 ± 3.83	25.25 ± 4.715	24.75 ± 4.956	12.25 ± 3.065	17.75 ± 5.513

E

	CMP		GMP		MEP		CD34^{hi}/FcγR^{low}
	WT	*Mtg16-Null*	WT	*Mtg16-Null*	WT	*Mtg16-Null*	*Mtg16-Null*
BFU-E	16.5 ± 3.5	0.0 ± 0.0*	0.0 ± 0.0	0.0 ± 0.0	3.0 ± 2.0	0.0 ± 0.0	0.0 ± 0.0

Figure 16. *Mtg16*-null bone marrow contains a c-Kit^{+}/Cd34^{hi}/FcgR^{lo} population. (A) Flow cytometry using lineage depleted bone marrow and anti-c-Kit, -ScaI, -FcgR, and -Cd34. From the graphs on the left, the c-Kit^{+}/Sca1^{lo} (MP) cells were gated and further analyzed using anti-FcgR and anti-Cd34 (graphs on the right). (B) Quantification of the gates shown in the right hand panels in (A). Open bars are from control mice and dark bars represent *Mtg16*-null mice. An unpaired two-tailed t-test indicated that the changes observed in the number of cells were significant (CMP, $p = 0.001$; GMP, $p = 0.019$; MEP, $p = 0.0001$; Cd34^{hi}/FcgR^{lo}, $p = 0.0012$; $n = 5$). (C) The indicated populations from the graphs in (A) were sorted by FACS and 500 cells were plated in methylcellulose containing SCF, IL-3, IL-6, and EPO and colonies were quantified after 8-10 days in culture. (D) The indicated populations from the graphs in (A) were sorted by FACS and 500 cells were plated in methylcellulose containing SCF, IL-3, and IL-6 and colonies were quantified after 8-10 days in culture. (E) The indicated populations from the graphs in (A) were sorted by FACS and 2000 cells were plated in erythroid-specific methylcellulose and colonies were quantified after 14 days in culture. An unpaired two-tailed t-test indicated that some of the differences in the colony numbers were significant (*, $p = 0.01$-0.05; **, $p = 0.001$-0.01; ***, $p < 0.001$. Shown are representative results from an experiment done in duplicate that are consistent with other biological replicates.

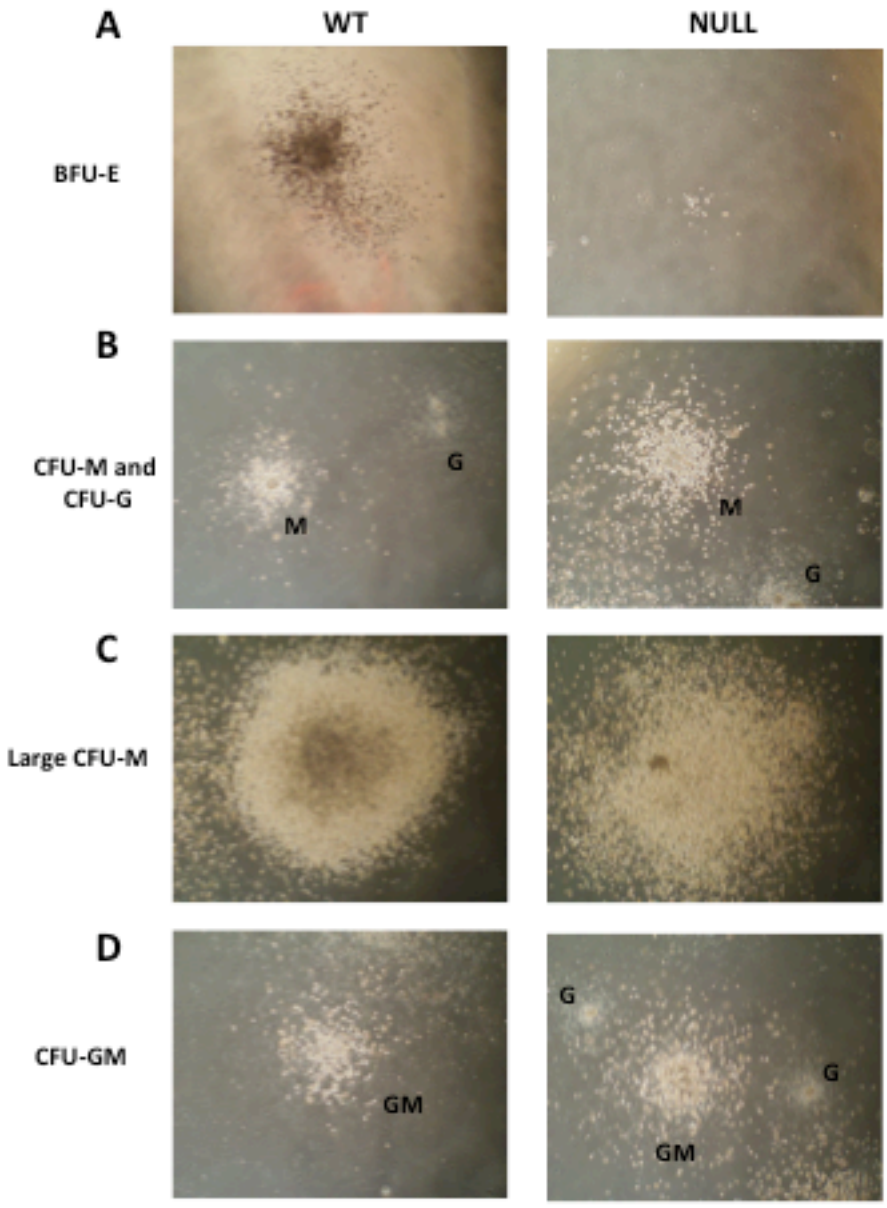

Figure 17. Identification of the methylcellulose colonies formed from wild type and *Mtg16*-null bone marrow populations. Digital photographs showing examples of the colonies that were quantified in Figure 5 C-E. (A) BFU-E (from MEP) (B) CFU-M and CFU-G (from CMP): (C) large CFU-M (from CMP); (D) CFU-GM (from CMP).

population, rather than an aberrant MEP population, as there were dramatic changes in gene expression profiles (Fig. 18A). These included the expression of granulocytic-specific genes such as Myeloperoxidase, Neutrophil Elastase 2, CD52, Cathespsin G, as well as transcriptional regulators such as Gfi1, C/EBPα, C/EBPδ and C/EBPε, which contribute to granulocyte differentiation [63, 112, 113, 117-120]. In addition, the Erythropoietin Receptor (EpoR) was dramatically under-represented in the $Cd34^{hi}/Fc\gamma R^{low}$ population. Overall, the gene expression profiles and growth characteristics of this population (Fig. 16) were most consistent with an abnormal granulocytic/macrophage progenitor that fails to express the FcγR, but maintained expression of c-Kit and Cd34.

This analysis also allowed us to directly compare wild type and null MEP gene expression (Fig. 18B). Even in these committed progenitor cells, there were dramatic differences in gene expression. Some of the key genes that were up-regulated include the regulators of differentiation *Id1*, *Id2*, *Fli1, Pu.1, Hes5*, and regulators of cytokine signaling and cell proliferation such as Socs2, Cdc25b, p18ink4, and p21 (Fig. 18C). Whereas the microarrays did not detect changes in *Gata3*, Q-RT-PCR found that it was up-regulated relative to *Gata1* (Fig. 18C). Conversely, genes that were under expressed included the transcription factors Mef2c, Klf5, and Pax2. Ingenuity Pathway analysis uncovered 4 highly significant networks that were dis-regulated in *Mtg16*-null MEPs versus wild type MEPs (Fig. 19). One of these networks (Fig. 19C, Cancer and Cellular Growth) contains many key regulators of the cell cycle, proliferation, and cellular differentiation including *p21*, *cyclin D*, *Id1*, *Id2*, *Notch1*, *Hes5*, and *Fli1*.

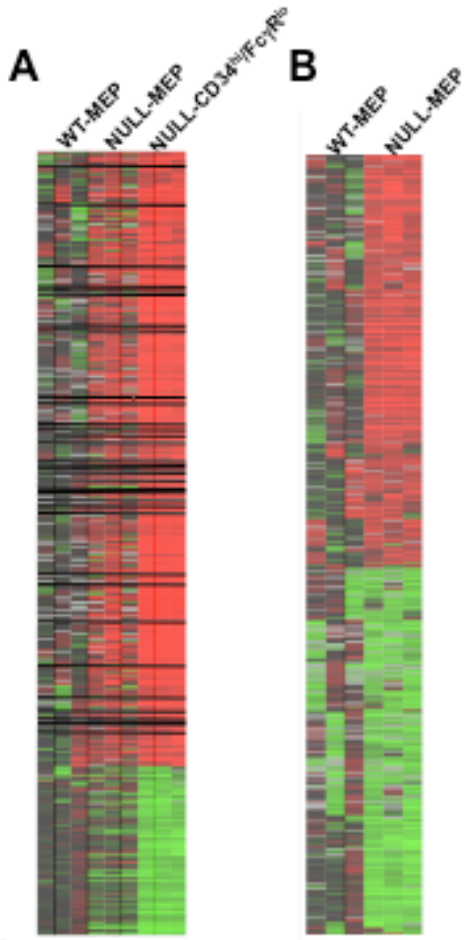

C

	Null-MEP vs. WT-MEP		Null-CD34^{hi}/FcγR^{low} vs. WT-MEP		Null- CD34^{hi}/FcγR^{low} vs. Null-MEP	
	Microarray	RT-PCR	Microarray	RT-PCR	Microarray	RT-PCR
CcnD1	-2.132 ± 0.4258	-1.308 ± 0.2778	4.091 ± 0.4901	5.040 ± 0.09285	9.444 ± 1.131	6.324 ± .1167
CcnE1	NC	-0.4557 ± 0.7702	-8.997 ± 1.818	-7.403 ± 2.179	-6.885 ± 1.391	-6.646 ± 1.957
p21	5.532 ± 1.422	5.322 ± 1.245	35.93 ± 5.887	23.59 ± 1.636	5.503 ± 0.9018	4.789 ± 0.3265
GATA1	NC	1.075 ± 0.01650	-5.328 ± 0.9201	-4.069 ± 0.5870	-6.194 ± 1.070	-4.372 ± 0.4157
GATA3	NC	4.812 ± 1.625	12.89 ± 2.359	15.11 ± 6.946	2.773 ± 0.5415	3.492 ± 1.605
Gfi1	NC	3.710 ± 1.265	34.12 ± 10.88	173.6 ± 27.78	15.49 ± 4.937	55.29 ± 9.005
Id1	3.163 ± 0.8507	10.28 ± 0.5809	11.25 ± 2.387	34.52 ± 12.04	3.605 ± 0.7649	6.458 ± 1.903
Id2	5.940 ± 2.141	3.348 ± 0.7118	21.32 ± 2.878	20.64 ± 6.081	4.301 ± 0.5806	9.253 ± 0.9002
N-myc	6.656 ± 2.133	35.41 ± 7.831	43.98 ± 10.10	313.3 ± 30.48	7.716 ± 1.773	3.396 ± 1.184
EpoR	NC	-0.4063 ± 0.8129	-11.03 ± 0.3229	-5.384 ± 0.7716	-10.13 ± 0.2986	-5.065 ± 0.7260

Figure 18. Gene expression analysis defines the *Mtg16*-null c-Kit^{+}/ Cd34^{+}/FcgR^{lo} population. (A) and (B) Heat map comparisons of the indicated FACS sorted populations showing some of the changes in gene expression that occur in lineage negative bone marrow progenitor cells as determined by cDNA microarray analysis. The heat map shows genes whose expression is higher in red and those genes that are lower in green. (C) Quantitative RT-PCR of selected genes to validate the microarray studies.

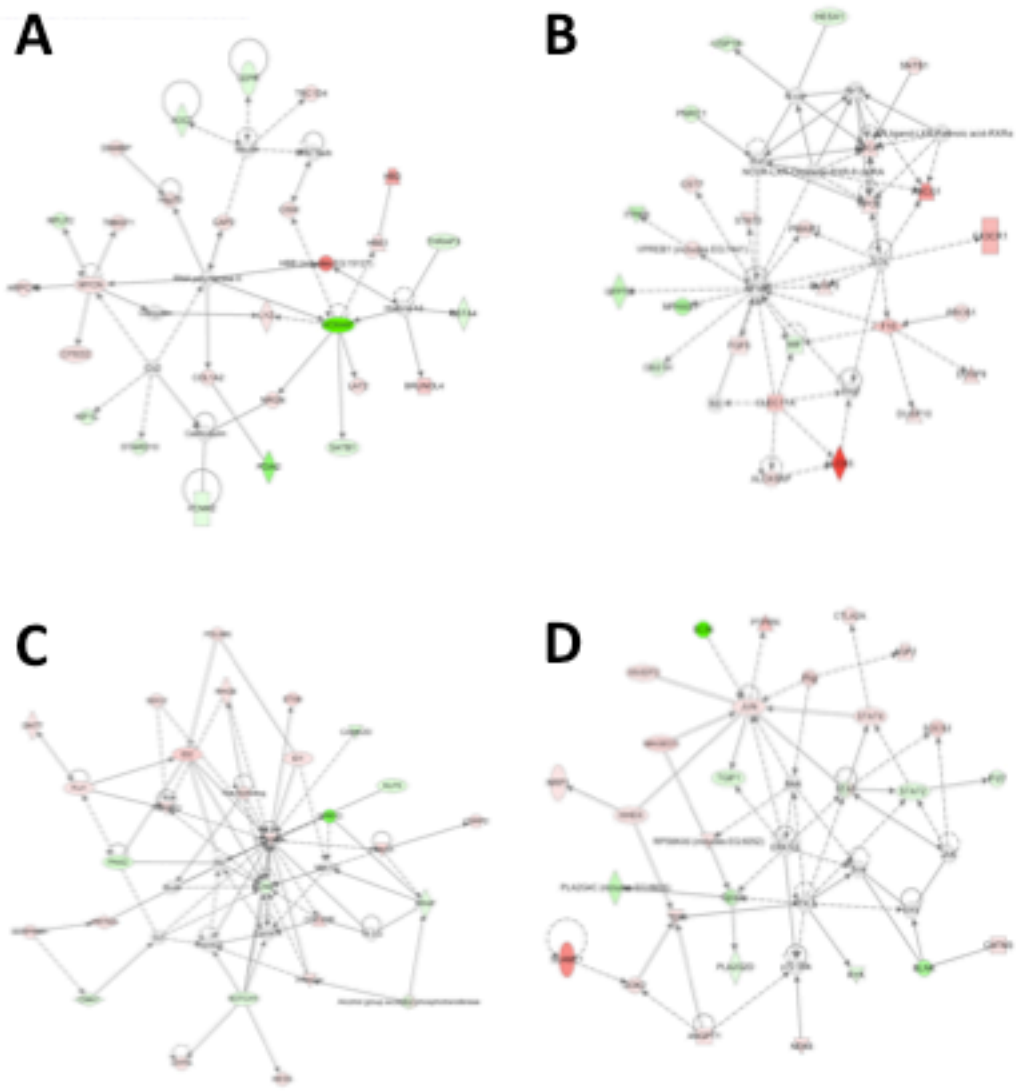

Figure 19. Ingenuity Pathway Networks from the MEP Gene Expression Data. (A) Network 1: Immune & lymphatic system development & function, organ morphology, cancer (score = 40). (B) Network 2: Lipid metabolism, molecular transport, small molecule biochemistry (score = 38). (C) Network 3: Cancer, cellular growth & proliferation, tumor morphology (score = 38). (D) Network 4: Cell signaling, cardiovascular development & function, cell-to-cell signaling & interaction (score = 36).

Mtg16 is required for short-term stem cell, multi-potent progenitor, and MEP proliferation

Short-term stem cell and progenitor cell functions can be further examined using a spleen colony-forming assay. MEPs form colonies on the spleen 8 days after bone marrow transplantation (CFU-S_8), and short-term stem cells and multi-potent progenitor cells and MEPs form splenic colonies in roughly equal numbers 12 days after transplantation (CFU-S_{12}) [88, 115]. As expected, wild type bone marrow from littermate control mice yielded copious numbers of colonies at both 8 and 12 days post transplantation (Fig. 20A). In contrast, *Mtg16*-null bone marrow failed to form colonies and only produced "white patches" of cells at either 8 or 12 days after transplantation (Fig. 20A). The presence of the patches of cells in the spleens transplanted with null marrow, suggested that the *Mtg16*-null progenitor cells found their way to the spleen, but failed to expand to form colonies. When bone marrow cells were labeled *ex-vivo* with the tracking dye CFSE, they homed to the spleen in similar numbers as the wild type donor control cells (Fig. 20B). Thus, while the bone marrow of *Mtg16*-deficient mice sustains the mice in the naïve animal, these cells are completely defective in the CFU-spleen assay (Fig. 20A) and fail to undergo the rapid expansion necessary after challenge with phenylhydazine (Fig. 13). The defect in CFU-S could be due to either a failure of the cells to rapidly expand and form large colonies or could be due to increased cell death. Given that the endogenous splenocytes had received a lethal dose of radiation and would not synthesize DNA, we were able to use BrdU incorporation to measure the cycling status among the injected cells in the spleens 8 days after bone marrow transplantation. In mice transplanted with wild type bone marrow, roughly 40% of the cells were cycling. In

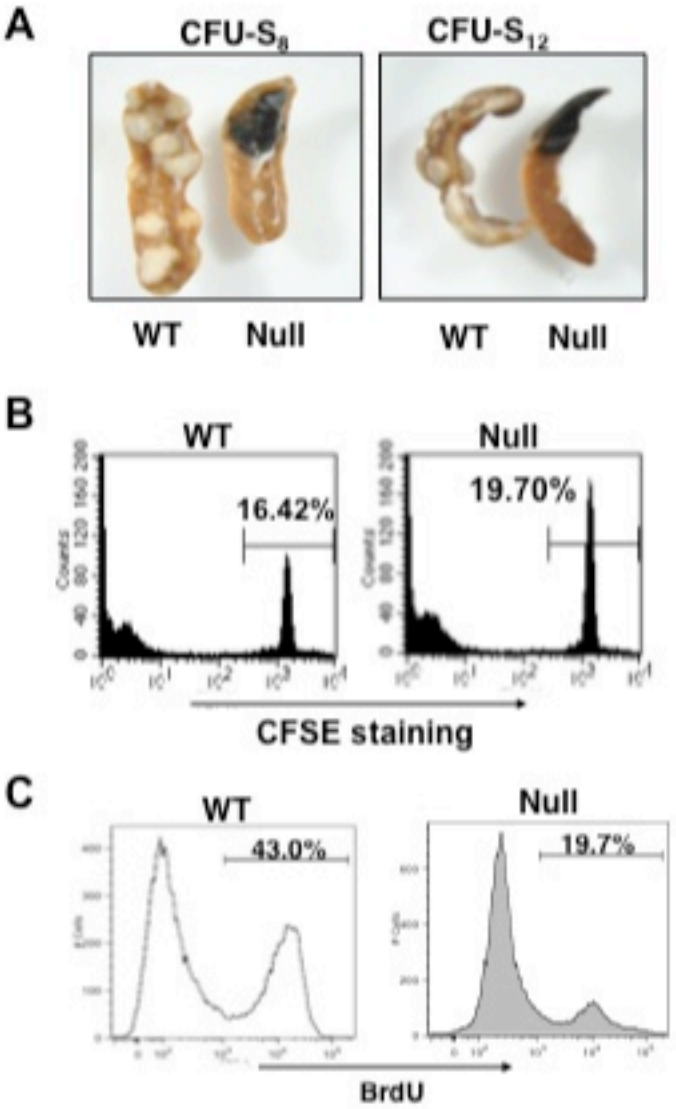

Figure 20. Inactivation of *Mtg16* impairs hematopoietic progenitor cell proliferation. (A) CFU-S_8 and CFU-S_{12} were obtained for wild type and *Mtg16*-null bone marrow. (B) CFSE labeling indicates that *Mtg16*-null bone marrow cells home to the spleen. Bone marrow cells were labeled *ex vivo* and injected into the tail vein of lethally irradiated mice and the CFSE labeled cells that home to the spleen determined by FACS 6 hr after injection. (C) Cell cycle analysis of transplanted splenocytes. Eight days after bone marrow transplantation the mice were injected with BrdU 2 hours before sacrificing, the splenocytes were harvested, and the percentage of total BrdU positive cells in the spleens determined using flow cytometry. The histograms show a representative example.

contrast, the *Mtg16*-null bone marrow produced half the number of BrdU positive cells in the spleen 8 days post transplant (Fig. 20C). While the irradiation of the recipient mice did not allow a determination of the level of apoptosis, the BrdU incorporation data suggests that the mechanistic basis of the *Mtg16*-null progenitor cells is a defect in proliferation.

The *Mtg16* defect in CFU-S can be overcome by expression of *c-Myc*

To further define the mechanism underlying the *Mtg16*-null defect, we attempted to genetically complement the proliferation defect. Our gene expression studies identified a host of genes that are de-regulated upon inactivation of Mtg16, making siRNA or cross breeding with mice lacking these genes impractical. Therefore, we asked whether expression of genes that can block apoptosis or stimulate proliferation might bypass the *Mtg16*-null proliferation defect. *Bcl2* expression was used to impair apoptosis and *c-Myc* was expressed to promote proliferation, due to its ability to bypass cyclin-dependent kinase inhibitors such as p27 and p21 [121, 122], which were up-regulated in the mull mice. Expression of *c-Myc* also leads to the activation of E2F family members and cell cycle progression [123], which might overcome the action of C/EBP family members and bypass any impaired signaling caused by expression of Socs family members (Fig. 14). Our culture conditions for MSCV infection favored the expansion and transduction of stem cells and multi-potent progenitor cells, which required us to focus on CFU-S_{12}. The *in vitro* selection for rapidly growing cells led to the formation of somewhat larger micro-colonies on the spleens in the vector control, but no fully formed colonies were observed (MSCV, Fig. 21A, 21B). This further confirms that these cells

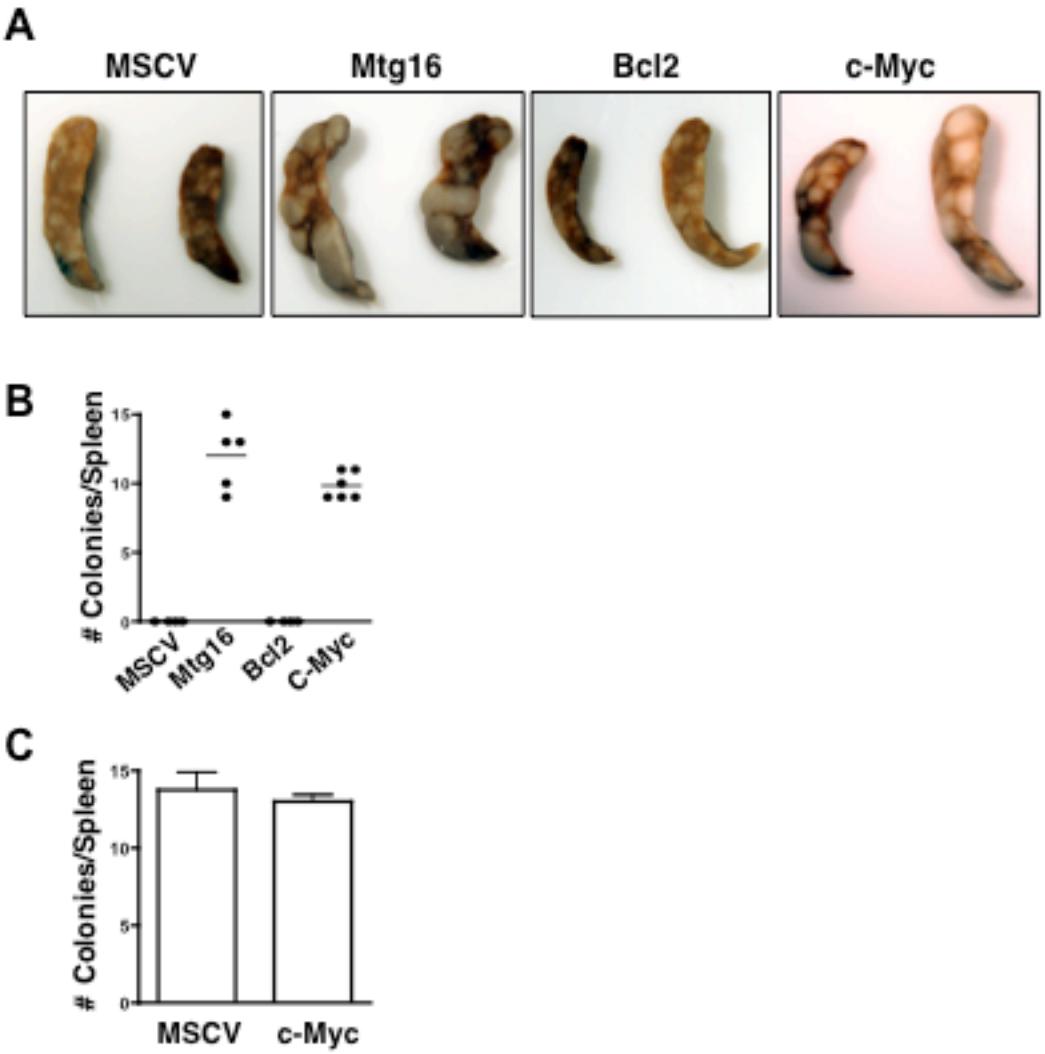

Figure 21. Overexpression of *c-Myc* in Mtg16-null bone marrow cells reconstitutes the number of CFU-S_{12} colonies. (A) Expression of *c-Myc*, but not *Bcl2*, complements the *Mtg16*-null defect in CFU-S_{12} assays. *Mtg16*-null bone marrow cells were infected with recombinant murine stem cell viruses expressing the indicated cDNAs and injected into irradiated recipient mice for CFU-S_{12} assays. (C) Quantification of the number of colonies formed in the CFU-S_{12} assay in (A). An unpaired two-tailed t-test indicated that the changes observed in the number of colonies were significant when compared to the number of colonies from MSCV (*Mtg16*, $p < 0.0001$, n=5; *c-Myc*, $p < 0.0001$, n = 6). (C) Wild-type bone marrow cells were infected with recombinant murine stem cell viruses expressing the indicated cDNAs and injected into irradiated recipient mice for CFU-S_{12} assays. Histogram showing the quantification of the number of colonies formed in the CFU-S_{12} assay.

correctly home to the spleen, but fail to expand into colonies. Re-expression of *Mtg16* complemented the proliferation defect leading to the formation of robust colonies, which confirms that these defects are specific to *Mtg16* (Fig. 21A). While expression of *Bcl2* had no effect on colony formation, expression of *c-Myc* complemented the *Mtg16*-null defect *in vivo*. Expression of *c-Myc* in wild type bone marrow did not affect CFU-S number (Fig. 21C). Thus, inactivation of *Mtg16* causes a profound defect in progenitor cell expansion.

Discussion

The chromosomal translocations that are associated with acute leukemia target master regulators of cell fate decisions, apoptosis, and cellular proliferation [124]. Gene targeting of *Mtg16* demonstrates that this gene is largely dispensable for normal development and viability in an unstressed environment and that the neonatal extrameduallary hematopoiesis in the spleen occurs in response to the rapid growth during early development. However, there were fewer MEPs, and the formation of an abnormal $Cd34^{hi}/Fc\gamma R^{low}$ progenitor cell population that had the growth properties and gene expression pattern characteristic of a myeloid progenitor cell. Hematopoietic stress disrupted the homeostasis that is achieved in the bone marrow of these mice and magnified the role of *Mtg16* progenitor cell proliferation (Fig. 13). The *Mtg16*-null mice succumbed to acutely induced anemia, which appeared to be due to a failure to expand erythropoiesis in the spleen. Spleen colony formation assays emphasized the proliferation defect. This assay also assesses the function of multi-potent progenitor cells and short-term stem cells [88, 115], and the total lack of colonies at day 12 after bone

marrow transplantation indicates that these immature cells are also functionally defective in the *Mtg16*-null bone marrow.

The disruption in the allocation of cells to the different myeloid progenitor populations in the *Mtg16*-null mice is reminiscent of the defects in the small intestine of *Mtgr1*-deficient mice [56]. *Mtgr1*-null mice also survive into adulthood, but these mice fail to maintain the secretory lineage cells in the small intestine [56]. This phenotype is somewhat similar to deletion of *Gfi1* in the gut [125] and Gfi1 can recruit Mtgr1 [43, 56]. In addition to the small intestinal phenotype, the colons of the *Mtgr1*-null mice were hypersensitive to the ulcerative agent dextran sodium sulfate (DSS). After treatment with DSS, the *Mtgr1*-null colonic epithelium failed to correctly regenerate, suggesting altered stem cell functions [57]. Targeted gene disruption of *Mtg8* indicated that it is required for development of the gut [103], but without defects in lineage contributions. While there are no obvious phenotypes in the intestines of *Mtg16*-null mice (data not shown), the gut phenotypes observed in the *Mtg8*- and *Mtgr1*-deficient mice coupled with the identification of mutations in *MTG8* in colorectal carcinoma and *MTG16* in breast cancer, suggests that further analysis of these mice, perhaps after cellular stress, is warranted.

Mechanistically, the altered progenitor cell functions can be traced to changes in gene expression patterns that can be linked to impaired repression by the DNA binding factors that recruit Mtg16. These include PLZF, BCL6, TAL1/SCL, Gfi1, Gfi1b, and Heb [42-47]. Gene expression profiling identified the de-repression of genes that are regulated by many of these factors, which not only confirms the veracity of the arrays, but also provides a molecular mechanism for how loss of *Mtg16* affects cell lineage decisions. For example, Gfi1 auto-regulates its own expression and

represses both *C/EBPε*, and *Neutrophil Elastase*, while PLZF regulates *HoxB2*. Indeed, the entire gene network that includes *Gfi1*, *C/EBPε*, and *PU.1* was dis-regulated in the *Mtg16*-null bone marrow (Fig. 14C). Within this network it is possible that the removal of *Mtg16* impaired *Gfi1*-mediated repression of *C/EBPε*, which in turn affects the expression of *PU.1* (Spi1) and *C/EBPβ* to alter the cell fate decisions in favor of granulocytes and monocytes. However, it is also noteworthy that C/EBPβ can associate with MTG8, and that PU.1 associates with RUNX1-MTG8 [26, 126]. Thus, this network analysis points toward a more direct involvement of Mtg16 with multiple key regulators of hematopoiesis.

It is also notable that two of the DNA binding factors that recruit MTG family members, Gfi1b and TAL1/Scl, contribute to erythropoiesis [72, 127, 128]. While TAL1/Scl can both activate and repress transcription, Gfi1b is commonly viewed as a dedicated repressor such that loss of a corepressor could partially impair Gfi1b actions [67, 129]. Mice lacking Gfi1b died during embryogenesis, apparently due to defective erythropoiesis, such that its contribution to adult hematopoiesis has yet to be defined [67]. Nevertheless, removal of one of the corepressors that is recruited by Gfi1b is likely to contribute to the defective proliferation, especially given that Gfi1b can control cellular proliferation via repression of the p21 cyclin-dependent kinase inhibitor. Indeed, p21 was up-regulated in *Mtg16*-null MEPs, but other CDK inhibitors were also turned on as were drivers of the cell cycle such as *N-Myc*. Like Gfi1b, TAL1/Scl is also required for embryonic hematopoiesis, but when deleted in adult mice, these mice were mildly anemic. While the bone marrow was defective in CFU-S assays, these mice had increased numbers of MEPs and normal percentages of CMPs and GMPs [72, 127, 128,

130], whereas the *Mtg16*-null mice have fewer MEPs and an abnormal $Cd34^{hi}/Fc\gamma R^{low}$ myeloid progenitor cell population (Fig. 16 and 18). Therefore, it is difficult to pinpoint single genes or pathways that would mediate the *Mtg16*-null phenotypes observed.

Loss of function of *Mtg16* may be associated with the formation of acute leukemia, as the t(8;21) fusion protein can associate with Mtg16 and impair its function in granulopoiesis [131]. The t(8;21) is associated with an increase in early myeloid progenitor cells and deletion of *Mtg16* function caused an accumulation of these populations (Fig. 16). Moreover, when expressed during embryogenesis, the t(8;21) fusion protein also impaired erythropoiesis [28, 132]. Though counterintuitive, the fusion protein impaired proliferation *in vitro,* and *in vitro* inactivation of Mtg16/ETO2 impaired the proliferation of erythroid cells [47, 54, 133, 134]. Our *in vivo* study of CFU-S_{12} indicated that this proliferation defect is also found in multipotent progenitor cells and short-term stem cells (Fig. 20). Thus, loss of *Mtg16* functions could contribute to some of the phenotypes associated with the t(8;21), perhaps by favoring lineage allocation towards the CMP/GMP populations and away from erythropoiesis.

Chapter IV

MTG16/ETO2 IS REQUIRED FOR MAINTENANCE OF HEMATOPOIETIC STEM CELL QUIESCENCE

Background and Significance

The balance between hematopoietic stem cell (HSC) differentiation and self-renewal must be maintained to ensure homeostasis, long-term stem cell viability, and suppress cancer formation [135]. Thus, the discovery of factors that control these processes in HSCs is important in terms of tumorigenesis and for their use in clinical applications such as hematopoietic cell transplantation. In addition, understanding the role of regulatory factors in hematopoietic stem cell function can be applied to other organ systems [136].

Interestingly, the engineered inactivation of many transcription factors that recruit MTG family members identified them as key regulators of stem cell functions and lineage allocation in mice. In several instances, these phenotypes were related to inappropriate cycling of the lineage negative, $Sca1^+$, c-Kit^+ (LSK) stem/progenitor cells (e.g., Gfi1, E2A), which caused depletion of stem cell pools or noncompetitive long-term stem cells [64, 65, 76]. In addition, *Mtg16* is the dominant MTG family member expressed in hematopoietic stem and early progenitor cells and microarray profiling of normal and leukemic stem cells suggests that *Mtg16* is expressed in these cells [60, 62]. These data suggest that MTG family members might contribute to stem cell functions.

Results

Defects in *Mtg16*-null hematopoietic stem cells

Mtg16$^{-/-}$ mice show only modest hematopoietic defects, but when challenged they lacked the ability to respond to erythropoietic stress [137]. These results, along with the linkage of MTG family members to Wnt and Notch signaling, prompted us to carefully examine the hematopoietic stem and progenitor cell compartments in *Mtg16*$^{-/-}$ mice. We used flow cytometry to identify lineage negative, Sca1^{+}, c-Kit^{+} (LSK) cells, which represents stem and early progenitor cells. These cells were reduced by roughly 2-fold in *Mtg16*$^{-/-}$ mice and when these cells were further divided based on Flt3 expression to focus in on the stem cell population, the LSK/Flt3^{-} cells were also reduced by nearly 2-fold (Fig. 22A, B, C). To confirm the reduction in the stem cell population, we further fractionated the LSK/Flt3^{-} cells with the signaling lymphocyte attractant molecule (SLAM) markers CD150 and CD48, which greatly enriches for long-term repopulating hematopoietic stem cells (LT-HSC) [85]. The LSK/Flt3^{-}/CD150^{+}/CD48^{-} fraction of cells (LT-HSC) was also reduced by slightly more than 2-fold in the *Mtg16*$^{-/-}$ mice (Fig. 22D).

Next, we used bone marrow transplantation assays to assess stem cell functions. While injection of only 200,000 wild type cells were sufficient to provide radioprotection and yielded 100% survival, injection of 200,000 *Mtg16*-deficient cells failed to reconstitute the marrow with all mice succumbing within 30 days. Injection of one million cells only extended the survival to a maximum of 52 days, suggesting that the stem cells were defective in repopulating the marrow (Fig. 23A). To bypass the lethality in the bone marrow transplant, we performed competitive bone marrow transplants using

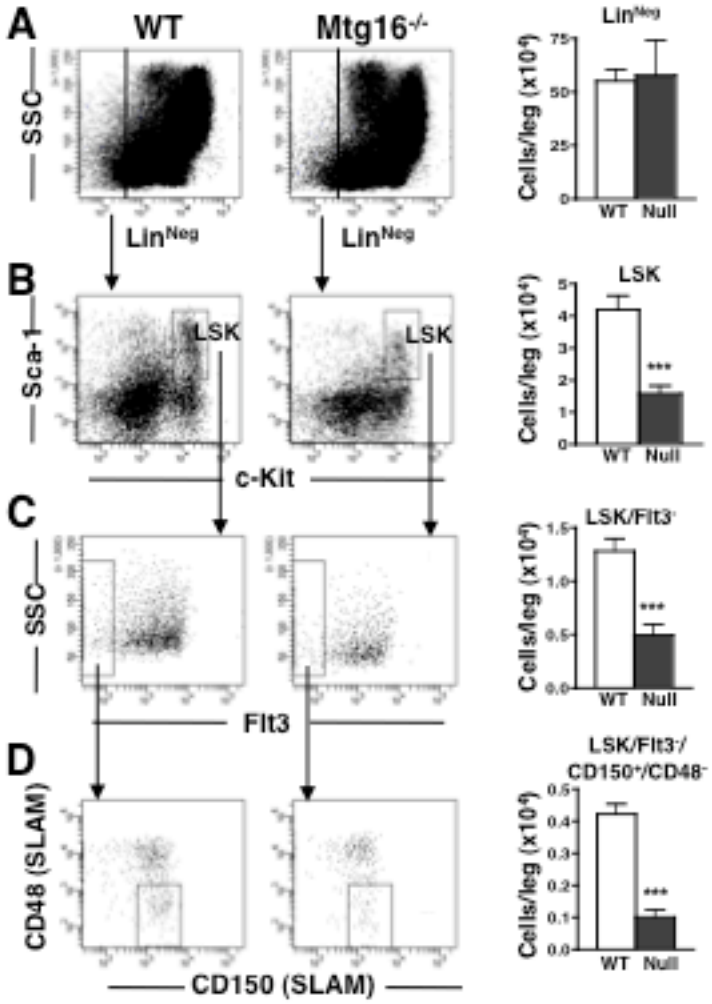

Figure 22. Loss of *Mtg16* decreases HSC numbers. Quantification of flow cytometry of whole bone marrow cells. Lineage negative cells were gated (A) and further analyzed using anti-Sca-1 and anti-c-Kit (B; LSK). The LSK cells were further fractionated using anti-Flt3 (C), which was further divided using anti-CD150/anti-CD48 (D) to obtain the LSK/Flt3$^-$ and LSK/FLt3$^-$/CD150$^+$/CD48$^-$ populations. Quantification of each of these populations is calculated for the number of cells per leg (femur + tibia) and is shown to the right of each flow cytometry panel (wild type (n = 5), empty bars; *Mtg16*-null (n = 5), full bars). Data are expressed as mean ± the standard error of the mean (SEM). An unpaired two-tailed *t* test indicated that the changes observed in the number of cells were significant (***p ≤ 0.0001).

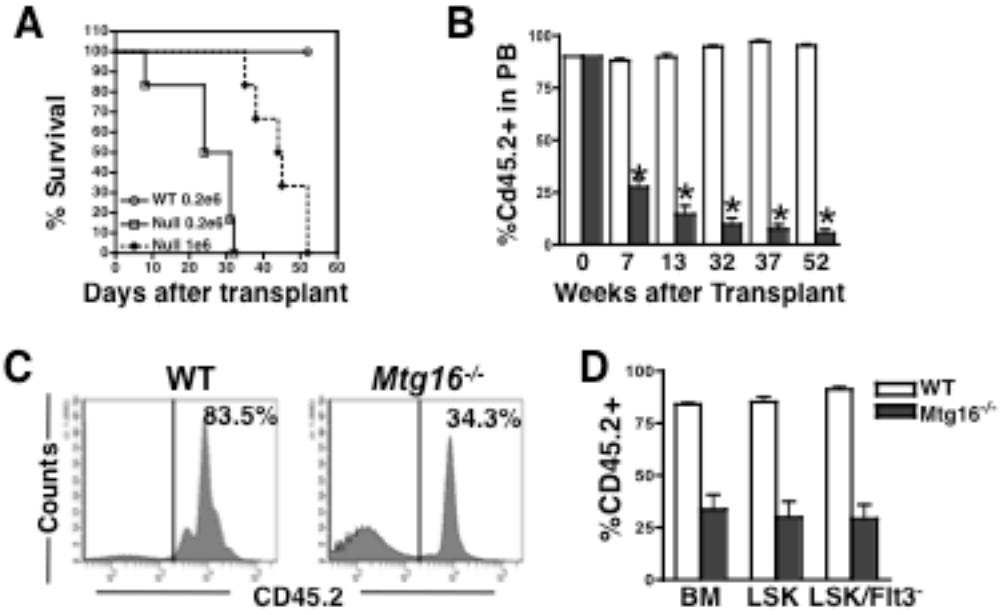

Figure 23. Inactivation of *Mtg16* disrupts HSC functions. (A) Survival curves of a representative transplant experiment using 200,000 wild type bone marrow cells (open circles), 200,000 *Mtg16*-null bone marrow cells (open boxes), or 1,000,000 *Mtg16*-null bone marrow cells (filled diamonds). (B) Competitive repopulation assay where 90% control (empty bars) or *Mtg16*-null (filled bars) $CD45.2^+$ bone marrow cells were co-injected with 10% wild type $CD45.1^+$ cells. The contribution of each population to long-term reconstitution of the bone marrow was assessed by flow cytometry using anti-CD45.1 and anti-CD45.2 to enumerate cells in the peripheral blood. Data are expressed as mean ± SEM at different times after transplantation. An unpaired two-tailed *t* test indicated these differences (marked by an *) were statistically significant at all time points after transplantation ($P<0.0001$; $n = 5$). (C) Flow cytometry analysis of whole bone marrow to determine the percentage of CD45.2 that had repopulated the bone marrow 12 weeks after a competitive repopulation assay. Shown is a representative plot from an experiment performed in triplicate that is consistent with other biological replicates. (D) Graphical representation of the quantification of CD45.2 cells residing in the bone marrow (BM) and LSK or $LSK/Flt3^-$ compartments 12 weeks after competitive bone marrow transplantation.

10% wild-type ($CD45.1^+$) cells to provide radioprotection along with 90% *Mtg16*$^{-/-}$ ($CD45.2^+$) bone marrow cells. Within 7 weeks of transplant there were already substantial reductions in the number of *Mtg16*$^{-/-}$ cells in the peripheral blood, with only 25-30% $CD45.2^+$ cells present (Fig. 23B). By 13 weeks post-transplant, when the peripheral blood cells are derived from the long-term stem cells, the percentage of $CD45.2^+$ cells had dropped to below 20%. These percentages continued to erode over time, falling to nearly 10% after 1 year while control $CD45.2^+$ cells maintained a level of at least 90% (Fig. 23B).

Although the analysis of peripheral blood suggested dramatic defects in *Mtg16*$^{-/-}$ stem cells, excluding erythrocytes, the peripheral blood is mostly composed of B and T cells. Given that *Mtg16*$^{-/-}$ mice have decreased numbers of B cells under homeostasis [137] and *Mtg16* is required for the differentiation of T cells [61], we used flow cytometry analysis to examine the bone marrow 12 weeks after competitive transplantation. We found a 2- to 3-fold reduction in $CD45.2^+$ cells in the total bone marrow (Fig. 23C, 23D), whereas only half this number of cells (about 20%) made it into the peripheral blood (Fig. 23B). A further breakdown of the contribution of $CD45.2^+$ cells in the bone marrow showed an exaggerated skewing of the *Mtg16*$^{-/-}$ cells towards the myeloid lineage with nearly 90% of the *Mtg16*$^{-/-}$ cells being $Gr1^+$ and/or $Mac1^+$ (Fig. 24), which is an exaggeration of the phenotype observed at homeostasis [137].

We also examined the LSK and LSK/$Flt3^-$ cells in the bone marrow to determine the number of $CD45.2^+$ cells that remained at 12 weeks post-transplant (Fig. 23D and 25). There was a 2.8-fold reduction in $CD45.2^+$ LSK cells, and a 3-fold reduction in $CD45.2^+$ LSK/$Flt3^-$ stem cells that derived from the *Mtg16*$^{-/-}$ mice (Fig. 23, and Fig. 25

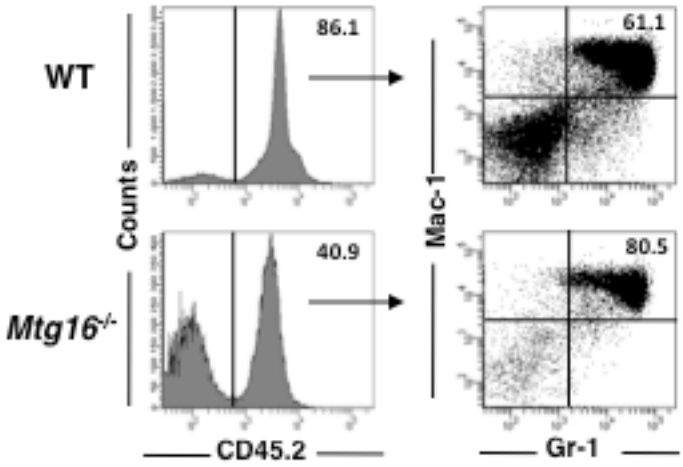

Figure 24. Inactivation of Mtg16 leads to enhanced Gr1⁺/Mac1⁺ production after competitive bone marrow transplantation. Flow cytometry analysis of CD45.2 cells that were Gr1⁺/Mac1⁺ 12 weeks after a competitive repopulation assay. Shown is a representative plot from an experiment performed in triplicate that is consistent with other biological replicates.

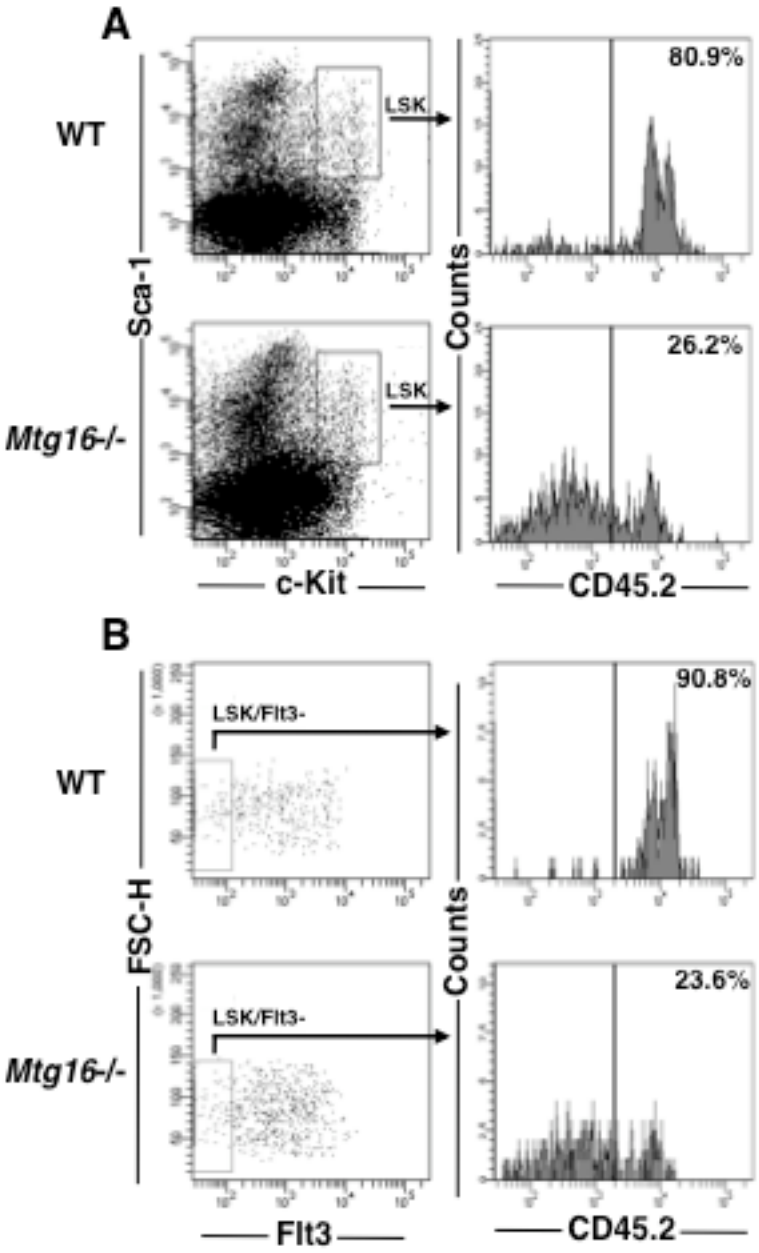

Figure 25. Flow cytometry analysis of LSK (A) or LSK/Flt3$^-$ (B) cells to determine the percentage of CD45.2 that had repopulated the bone marrow 12 weeks after a competitive repopulation assay. Shown is a representative plot from an experiment performed in triplicate that is consistent with other biological replicates. Graphical representation of quantified data is shown in Fig. 23.

for FACS plots). Although the *Mtg16*$^{-/-}$ bone marrow contains roughly half the normal number of LSK cells, these results suggested that the *Mtg16*$^{-/-}$ stem cells displayed a further defect after transplantation. Therefore, we performed a secondary transplant to further examine *Mtg16*$^{-/-}$ stem cell functions. Six weeks after transplanting irradiated recipient mice with bone marrow that contained from 25% to 45% CD45.2^{+} bone marrow (*Mtg16*$^{-/-}$), there was a dramatic loss of *Mtg16*$^{-/-}$ cells in the peripheral blood and flow cytometry analysis of the bone marrow of these mice indicated a near complete loss of *Mtg16*$^{-/-}$ LSK and LSK/Flt3^{-} cells (Fig. 26, see Fig. 27 for FACS plots for B). By contrast, control mice contained 80-90% CD45.2^{+} cells in the bone marrow (Fig. 26). Thus, *Mtg16* is required to maintain stem cells, even when normal progenitor cells are present, suggesting a stem cell-intrinsic defect.

Mtg16$^{-/-}$ cells home to the bone marrow

To ensure that this defect was not simply due to a failure of the stem cells to home to the marrow, we labeled bone marrow cells *ex vivo* with the vital dye carboxyfluorescein succinimidyl ester (CFSE) before injecting these cells into the tail vein of mice. Sixteen hours later, the bone marrow of these mice was analyzed by flow cytometry and the number of cells positive for CFSE was quantified (Fig. 28A). A similar number of null cells as compared to wild type controls were found in the bone marrow. Given that the CFSE experiment assessed whole bone marrow, we further examined the homing of stem and progenitor cells by performing methylcellulose colony formation assays 16 hours after bone marrow transplantation and calculating the percentage of stem/progenitor cells that correctly homed to the bone marrow (Fig. 28B).

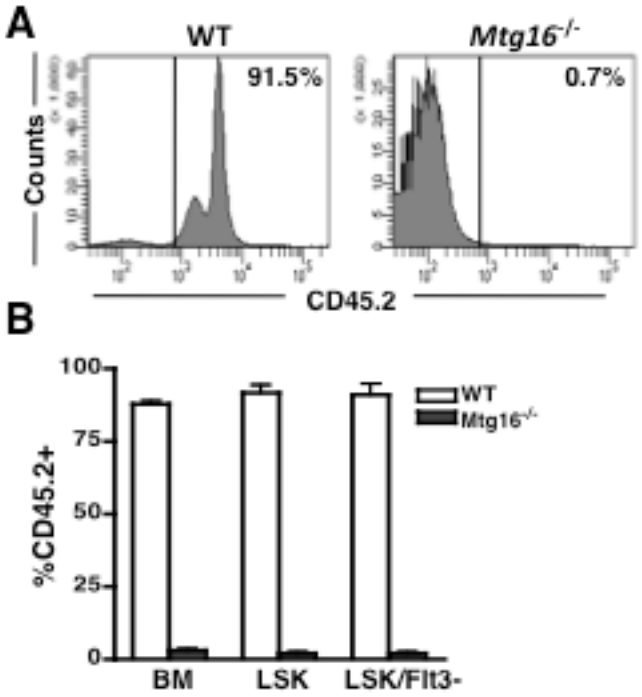

Figure 26. Serial transplantation reveals requirements for *Mtg16* in the maintenance of stem cells. (A) Flow cytometry analysis of whole bone marrow to determine the percentage of CD45.2 that had repopulated the bone marrow 6 weeks after secondary bone marrow transplantation from an initial competitive repopulation assay. Shown is a representative plot from an experiment performed in triplicate that is consistent with other biological replicates. (B) Graphical representation of the quantification of CD45.2 cells residing in the bone marrow (BM) and LSK or LSK/Flt3$^-$ compartments 6 weeks after secondary bone marrow transplantation.

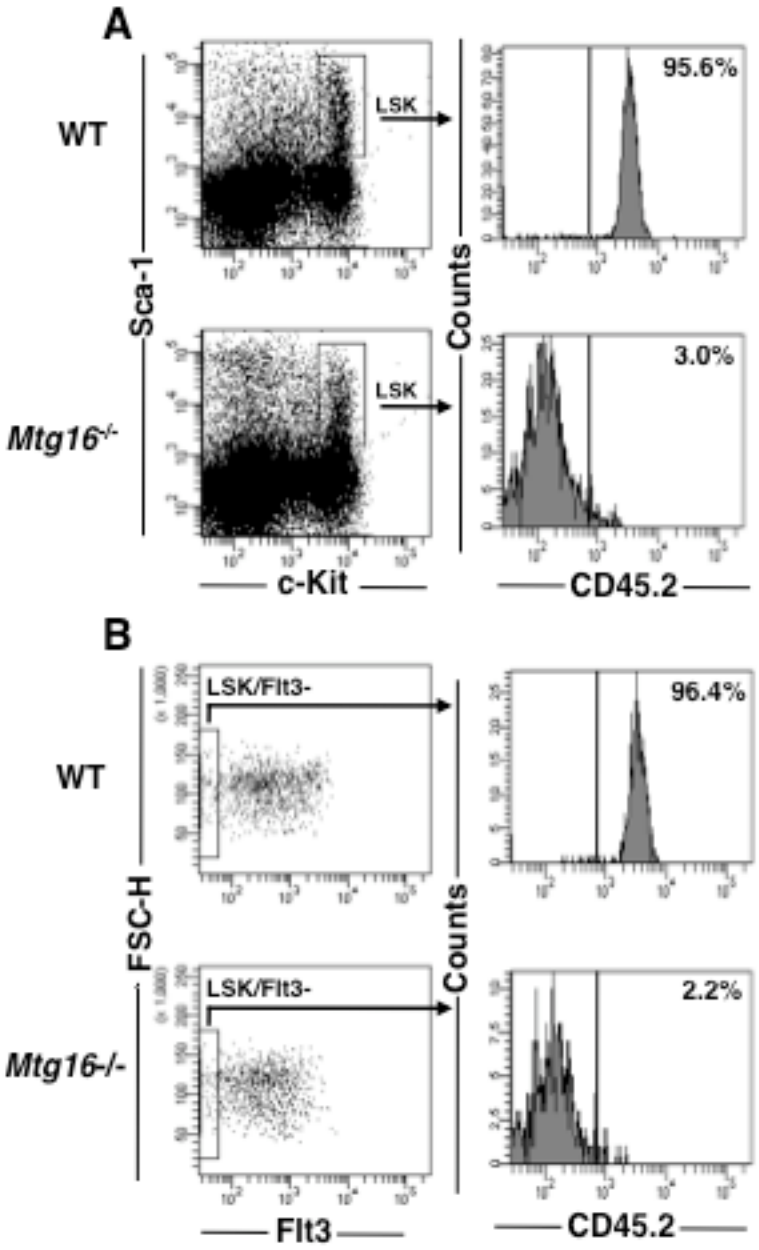

Figure 27. Flow cytometry analysis of LSK (A) or LSK/Flt3$^-$ (B) cells to determine the percentage of CD45.2 that had repopulated the bone marrow 6 weeks after a secondary competitive bone marrow transplant. Shown is a representative plot from an experiment performed in triplicate that is consistent with other biological replicates. Graphical representation of quantified data is shown in Fig. 26.

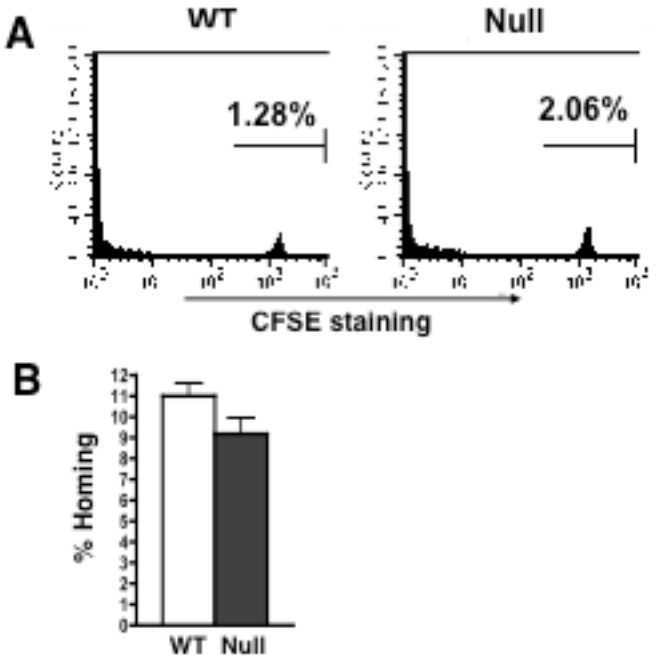

Figure 28. *Mtg16*$^{-/-}$ cells home to the bone marrow. (A) Bone marrow from control wild type and *Mtg16*$^{-/-}$ mice were stained with CFSE and injected into lethally irradiated recipient mice. The bone marrow was analyzed by flow cytometry to identify CFSE labeled cells. (B) Representative graph of the number of colony-forming cells that homed to the bone marrow 16 hours after injection into lethally irradiated recipient mice.

The small changes observed were within the statistical error, indicating that immature *Mtg16*$^{-/-}$ cells homed correctly to the marrow.

Mtg16 deficiency affects stem cell self renewal

The hematopoietic defects found in the LSK/Flt3^{-} and LSK/CD48^{-}/CD150^{+} stem cell compartments (Fig. 22) and identified in bone marrow transplantation assays, suggested that Mtg16 was required for stem cell self-renewal (Fig. 26). To further define the defect, we used *in vitro* analyses of stem cell functions. First, we serially cultured bone marrow cells in methylcellulose. Stem cells from control mice were able to form colonies through 3 consecutive rounds of culture in methylcellulose containing IL6, SCF, erythropoietin, and IL3, but yielded only about 15% of the number of colonies after the 4th culture (Fig. 29A). By contrast, *Mtg16*-null cells displayed a 4-fold reduction in replating ability after the second round of culture (Fig. 29A) and were essentially exhausted by the 4th culture. We extended these results by testing the function of *Mtg16*-null stem cells in a long-term culture-initiating cell (LTC-IC) assay, which tests long-term stem cell function in a controlled *in vitro* environment [138]. The initial cultures of 3,000 *Mtg16*-null lineage negative cells contained the same number of CFC-producing cells as 3,000 wild-type lineage negative cells. The same was true after one week in culture (Fig. 29B). However, by the second week of culture, the number of CFC-producing cells present in the *Mtg16*-null cultures was drastically reduced compared to the wild-type cultures, and almost completely absent after just three weeks in culture (Fig. 29B), indicating a loss of self-renewal.

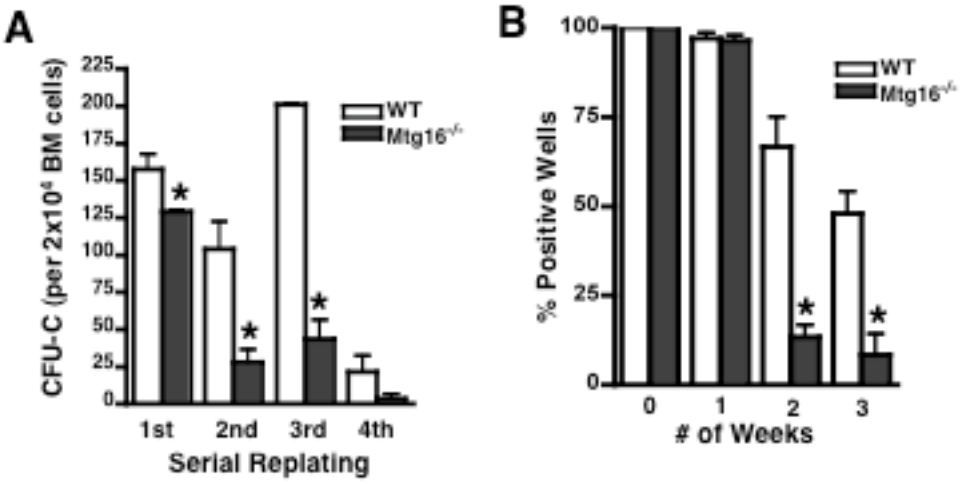

Figure 29. Inactivation of *Mtg16* leads to a loss of stem cell self-renewal. (A) Graphical representation of the numbers of methylcellulose colonies formed during serial replating assays where $2x10^4$ cells were plated every 7 days for 4 weeks (wild type, empty bars; *Mtg16*-null, full bars). Data are expressed as mean ± SEM. An unpaired two-tailed *t* test indicated these differences were statistically significant (marked by an *; 1st, P = 0.03; 2nd, P = 0.01; 3rd, P<0.001; n=4). Shown are representative results from an experiment done in duplicate that are consistent with other biological replicates. (B) Graphical representation of the numbers of methylcellulose colonies formed at the indicated times from LTC-IC cultures of wild type (open bars) and *Mtg16*-null (full bars) bone marrow cells. Data are expressed as mean ± SEM. An unpaired two-tailed *t* test indicated the difference at week 2 and week 3 after culture (marked with an *) was statistically significant (P<0.05; n=4). Shown are representative results from three separate experiments.

The inactivation of *Mtg16* alters the expression of cell cycle control genes

Given that Mtg16 appears to act as a transcriptional corepressor, we compared gene expression in control and *Mtg16*-null lineage negative, Sca1$^+$, c-Kit$^+$ cells using cDNA microarray analysis. Because these cells are rare, LSK cells were sorted and pooled from 10 wild type and 10 *Mtg16*-null mice and the experiment was performed using biological triplicates. The genes showing changes were categorized based on biological pathways or biological processes using the Panther classification system (representative cell cycle control genes are shown in Fig. 30A, see GEO for the full gene expression profiles) [139]. We consistently observed changes in genes that function in hematopoietic differentiation, including 4-6 fold higher levels of *Id1* and *Id2*, whose over-expression caused skewing of lineage allocation towards myelopoiesis and away from lymphopoiesis [140]. In addition, we noted that several genes that are associated with cell cycle control, or the transition out of quiescence, were up-regulated including *Fos*, *E2F2*, *Raf, Cyclin D1*, *Cdk2*, and *N-Myc*. The microarray data were confirmed using selected genes whose expression was altered in the arrays, including *Id1, Id2,* and *E2F2* that were up-regulated and the *Erythropoietin receptor* (*EpoR*), which was dramatically down-regulated (Fig. 30B). The low level of *EpoR* is important given the defects previously observed in "stress" erythropoiesis in the absence of *Mtg16* [137].

The levels of several key cell cycle control genes were consistently 2-4 fold higher than in control cells in either microarray data or by QRT-PCR (Fig. 30A, B). Therefore, we used chromatin immunoprecipitation (ChIP) assays to determine whether any of these genes are direct targets for regulation by Mtg16/Eto2. We focused the ChIP assays towards regions of these genes that are bound by factors that recruit MTG family

A

Gene Name	Gene Symbol	Fold Change
FBJ osteosarcoma oncogene	Fos	6.10
Glycogen synthase kinase 3 beta	Gsk3b	5.23
Sporulation protein, meiosis-specific, SPO11 homolog (S. cerevisiae)	Spo11	4.69
Cyclin-dependent kinase 2	Cdk2	4.10
Cyclin G2	Ccng2	3.80
Janus kinase 2	Jak2	3.41
V-raf-leukemia viral oncogene 1	Raf1	2.94
E2F transcription factor 2	E2F2	2.73
Cyclin D1	Ccnd1	2.70
Reticuloendotheliosis oncogene	Rel	2.68
CDC14 cell division cycle 14 homolog B (S. cerevisiae)	Cdc14b	2.50
CDC14 cell division cycle 14 homolog A (S. cerevisiae)	Cdc14a	2.11
Polo-like kinase 4 (Drosophila)	Plk4	1.71
Cell division cycle 25 homolog B (S. cerevisiae)	Cdc25b	1.60

Gene Name	Gene Symbol	Fold Change
Retinoid X receptor alpha	Rxra	0.63
Polymerase (DNA directed), delta 1, catalytic subunit	Pold1	0.59
Polymerase (DNA directed), gamma	Polg	0.53
Lethal(3)malignant brain tumor-like 2 (Drosophila)	L3mbtl2	0.50
Cell division cycle 34 homolog (S. cerevisiae)	Cdc34	0.50
Checkpoint kinase 1 homolog (S. pombe)	Chek1	0.47
CDC23 (cell division cycle 23, yeast, homolog)	Cdc23	0.41
X-ray repair complementing defective repair in Chinese hamster cells 2	Xrcc2	0.38
Minichromosome maintenance deficient 2 mitotin (S. cerevisiae)	Mcm2	0.38
Cyclin E1	Ccne1	0.37

B

	Mtg16-null vs. WT	
	Microarray	RT-PCR
CcnD1	2.71 ± 0.23	2.25 ± 0.25
E2F2	2.39 ± 0.49	2.7 ± 0.1
GATA3	1.85 ± 0.03	2.0 ± 0.40
Gfi1	NC	0.125 ± 1.38
Id1	5.6 ± 2.54	4.85 ± 1.25
Id2	6.61 ± 0.65	5.15 ± 0.85
N-myc	2.6 ± 0.06	3.55 ± 0.45
EpoR	-5.04 ± 3.27	-16.65 ± 6.65

Figure 30. *Mtg16*-null LSK cells have altered gene expression patterns. (A) Gene expression profiling of mRNA from LSK cells isolated from wild type and *Mtg16*-null mice were analyzed using cDNA microarrays. Panther ontology analysis was used to group genes into specific biological processes and representative genes associated with cell cycle control with their relative expression levels when *Mtg16* is deleted are shown. (B) Quantitative RT-PCR of selected genes was used to validate the microarray studies.

members including TCF4, E proteins, and CSL. While we were unable to detect Mtg16 at the TCF4, E protein, or CSL binding sites in the *Cyclin D1* or *N-Myc* promoters in murine erythroleukemia cells that express high levels of Mtg16 (Fig. 31B), we detected Mtg16 near an E2A binding motif in the first intron of *E2F2* [141], which we confirmed using anti-E47 (Fig. 31A). Mtg16/Eto2 localized to this site in *E2F2* using two different sets of primers to the first intron of *E2F2* (Fig. 31A; set 1 and set 2) and 2 additional anti-Mtg16/ETO2 antibodies (Hunt, Engel and Hiebert, unpublished data). While negative data with ChIP does not rule out the possibility that Mtg16 is required to suppress *Cyclin D1* or *N-Myc* or other regulators of the cell cycle, Mtg16 associates with *E2F2*, whose over expression is sufficient to drive quiescent cells into the S phase [142]. To determine if this interaction with E2F2 through E proteins contributes to the loss of stem cell self-renewal in the absence of *Mtg16*, we utilized a point mutation in *Mtg16* that is homologous to a mutation in *MTG8* that abrogated the binding of the MTG8 NHR1 domain to HEB AD1, which was sufficient to disrupt repression of E-protein mediated transcriptional activation [143, 144]. The Mtg16-F210A mutant mimics the MTG8-F154A mutant to eliminate E-protein AD1 binding, whereas a control Mtg16-R220A mutant mimics the MTG8-R164A mutant that retained the ability to bind to HEB AD1 [143]. The Mtg16-F210A and Mtg16-R220A mutants were reintroduced into *Mtg16*-null lineage-negative cells using *MSCV-IRES-GFP*, and both Mtg16 and the Mtg16-R220A mutant were capable of rescuing the loss of stem cell self-renewal in the LTC-IC assay (Fig. 31C). However, the F210A point mutant failed to rescue this loss of self-renewal (Fig. 31C). Therefore, appropriate regulation of E-protein activity is a necessary function of *Mtg16* in the maintenance of stem cell self-renewal through repressing cell cycle

genes, such as E2F2.

Mtg16 is required for maintaining stem cell quiescence

The up-regulation of cell cycle control genes suggested that the exhaustion of stem cells after serial competitive transplant of *Mtg16*$^{-/-}$ bone marrow was due to inappropriate entry of the stem cell population into the cell cycle. To test this hypothesis, BrdU was injected into control and *Mtg16*$^{-/-}$ mice to assess the number of LSK cells in the S phase of the cell cycle. Two hours after injecting BrdU, flow cytometric analysis revealed that a higher portion of LSK cells from *Mtg16*$^{-/-}$ mice incorporated BrdU, as compared with wild-type cells, indicating that more *Mtg16*-null stem and early progenitor cells had entered the cell cycle (Fig. 32A, see Fig. 33A for further quantification). Further analysis of the cell cycle was performed by flow cytometry analysis of the incorporation of the DNA dye Hoechst 33342 (HO) and RNA dye Pyronin Y (PY), which identifies quiescent cells based on their lower output of RNA. The lower percentage of *Mtg16*$^{-/-}$ LSK cells that were Hoechst and Pyronin low (G_0 cells) compared with wild-type mice indicated a loss of quiescent cells (Fig. 32B, see Fig. 33B for further quantification). Finally, we examined the LSK/Flt3^{-} long-term hematopoietic cell compartment and found that in the absence of *Mtg16*, nearly two thirds more LSK/Flt3^{-} cells were in the cell cycle (Fig. 32C, see Fig. 33C for FACS plots). These data suggest that loss of *Mtg16* allowed stem cell entry into the cell cycle.

Both the methylcellulose serial-replating and LTC-IC assays indicate that the *Mtg16*-null stem/progenitor cells have decreased self-renewal potential and, together with the competitive bone marrow transplants, suggest that Mtg16 may have intrinsic functions in the HSC. Therefore, we performed BrdU incorporation analysis on mice

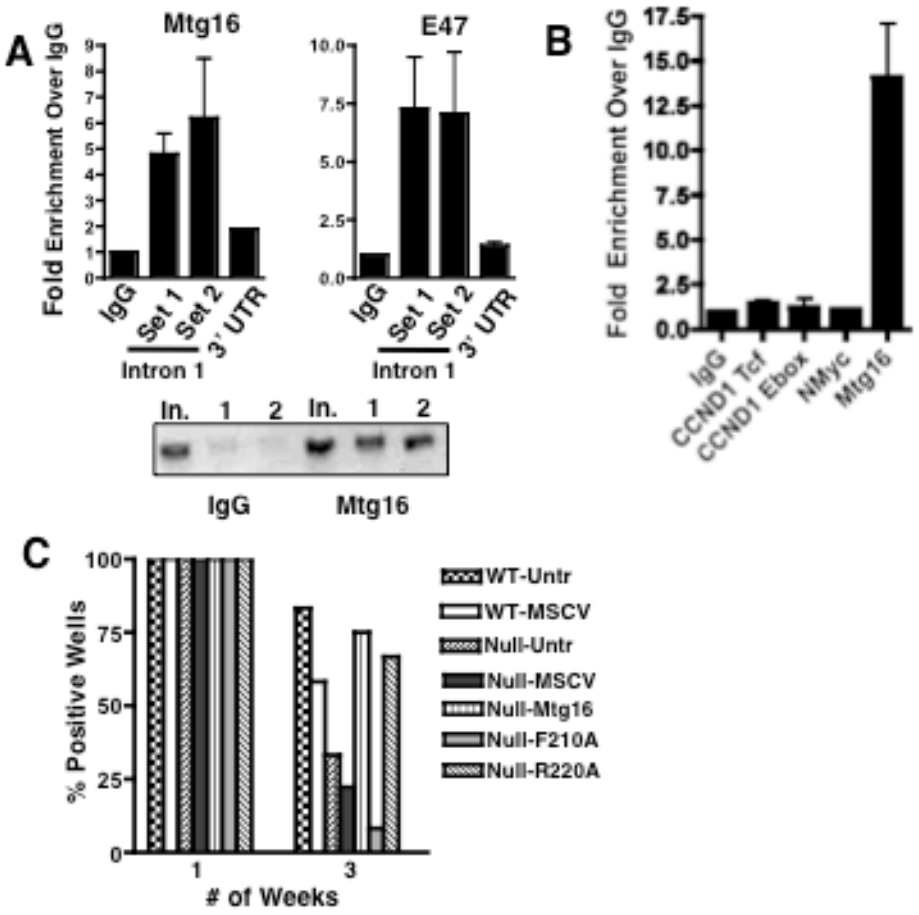

Figure 31. Mtg16 associates with the first intron of *E2F2* and this interaction is required to maintain *in vitro* self-renewal. (A) Chromatin immunoprecipitated with the either control IgG or anti-Mtg16/Eto2 from lysates of MEL cells was amplified with primers specific to two regions encompassing an E2A binding site in the first intron of *E2F2*, or as a control, the 3' untranslated region (UTR) of *E2F2* using quantitative PCR. Graph shows the level of signal relative to IgG set to "1". The panel at the right shows ChIP using anti-E47 with the same *E2F2* 1st intron primers. The ethidium bromide stained agarose gel shows a representative PCR reaction stopped after 30 cycles; In., input; 1 and 2 designate the duplicate PCR samples from the ChIP reaction using primer set #2 flanking the E2A binding site. (B) Immunopurified DNA was amplified with primers flanking a TCF4 binding site or both an E box and a CSL binding site in the *Cyclin D1* gene (*Ccnd1*) or regions encompassing a TCF4 binding site in *N-Myc*. ChIP of an E box site in *Mtg16* was used as a positive control. Graph shows the level of quantitative PCR signal relative to IgG set to "1". (C) Graphical representation of the numbers of methylcellulose colonies formed at the indicated times from LTC-IC cultures of wild type and *Mtg16*-null bone marrow cells that were untreated (untr) or infected with MSCV-virus expressing various constructs (empty vector, MSCV; Mtg16 full-length, Mtg16; Mtg16-F210A, F210A; or Mtg16-R220A, R220A). Data are expressed as mean ± SEM.

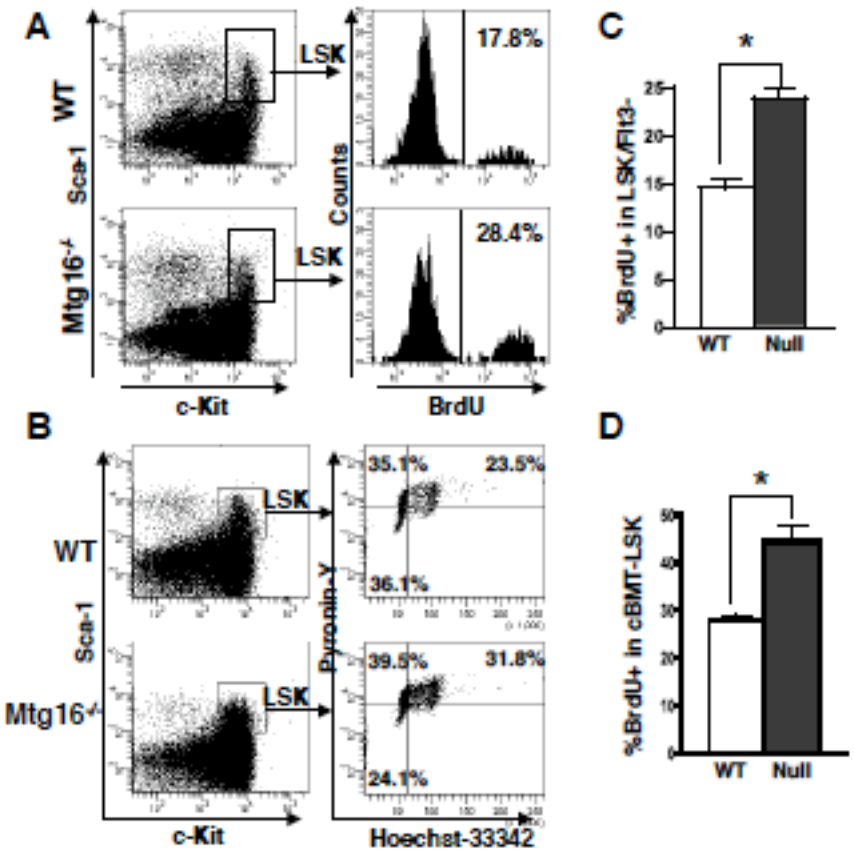

Figure 32. Inactivation of *Mtg16* leads to a decrease in the number of quiescent LSK cells. (A) Cell cycle status of LSK cells was analyzed using BrdU. Shown is a representative FACS plot from an experiment performed with 5 mice that is consistent with other biological replicates. Data are expressed as mean ± the standard error of the mean (SEM). An unpaired two-tailed *t* test yielded values for LSK BrdU+, P = 0.0002; n = 5. (B) Cell cycle status of LSK cells was analyzed with the DNA dye Hoechst 33342 (HO) and the RNA dye Pyronin Y (PY). Shown is a representative plot from an experiment performed in triplicate that is consistent with other biological replicates. Data are expressed as mean ± the standard error of the mean (SEM). An unpaired two-tailed *t* test yielded significance values for LSK $\%G_0$, P = 0.0324; n = 3. (C) Quantification of the percentage of LSK/Flt3$^-$ cells in S phase using BrdU incorporation as described in A, but incorporating anti-Flt3. Data are expressed as mean ± the standard error of the mean (SEM) and are consistent with other biological replicates. An unpaired two-tailed *t* test yielded P < 0.0001; n = 6. (D) Quantification of the number of LSK cells in the S phase 5-6 weeks after competitive repopulation was analyzed using BrdU as described in (A). Data are expressed as mean ± the standard error of the mean (SEM) and are from biological replicates. An unpaired two-tailed *t* test yielded CD45.2+, LSK BrdU+, P = 0.0069; wild type, n = 4; *Mtg16*–null, n = 8.

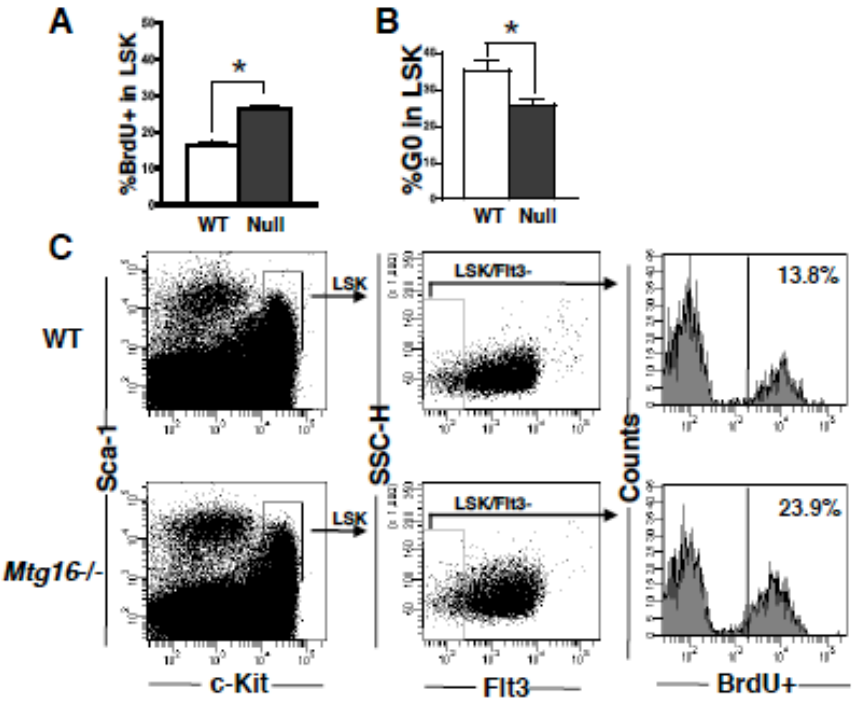

Figure 33. Quantification of cycling stem and progenitor cells. (A) Graph shows the quantification of the number of LSK BrdU⁺ cells from biological replicates in Fig. 32A. (B) Quantification of the percentage of G_0 LSK cells from biological replicates from Fig. 32B is shown graphically at the right (wild type, empty bars; *Mtg16*-null, full bars). (C) Cell cycle status of LSK/Flt3⁻ cells was analyzed using BrdU. Mice were injected with 1 mg of BrdU, and 2 hours later the bone marrow was harvested and lineage depleted. The lineage negative cells were then stained using anti-c-Kit, anti-Scal, anti-Flt3 and anti-BrdU. Shown is a representative FACS plot from an experiment performed with 6 mice that is consistent with other biological replicates. Graphical representation of quantified data is shown in Fig. 32C.

after competitive bone marrow transplantation using 90% null cells and 10% wild type. Because the yield of *Mtg16*$^{-/-}$ cells is low after transplant (Fig. 23), we were only able to examine LSK cells (rather than LSK/Flt3^{-}). Nevertheless, even in the presence of wild type progenitor cells that negate any *Mtg16*$^{-/-}$ progenitor cell defects, the *Mtg16*$^{-/-}$ LSK population showed an increase in the percentage of cycling cells, as compared to the control mice containing wild type CD45.2 LSK cells (Fig. 32D). These results suggest that the increased cycling observed in the LSK compartment was not due to downstream defects in progenitor cells, but that *Mtg16/Eto2* is required to suppress stem cell entry into the cell cycle.

Discussion

In this study, we examined the role of *Mtg16*, a transcriptional corepressor, in hematopoietic stem cell functions. Inactivation of *Mtg16* reduced hematopoietic stem cell numbers, and more importantly, resulted in a loss of self-renewal both *in vivo* and *in vitro*. This loss of self-renewal and eventual stem cell exhaustion appeared to be due to inappropriate entry of stem cells into the cell cycle. One function of Mtg16 is to link DNA binding transcription factors that control hematopoiesis to chromatin modifying enzymes such as histone deacetylases. We found that *E2F2*, a transcription factor that when over-expressed was sufficient to drive quiescent cells into the cell cycle, was up-regulated in *Mtg16*$^{-/-}$ LSK cells. In addition, Mtg16 robustly associated with an enhancer-like sequence in the first intron of *E2F2*, suggesting that *E2F2* is a direct target for Mtg16-mediated repression. However, this does not preclude Mtg16-dependent regulation of other key regulators of the cell cycle. Notably, *N-Myc* is consistently over-

expressed in gene expression analysis of *Mtg16*$^{-/-}$ cells [137]. Thus, Mtg16/Eto2 is likely required to maintain control of a cell cycle regulatory circuit that when mis-regulated can drive quiescent stem cells into DNA synthesis or prevent cycling stem cells from entering G_0 [142].

The site in the *E2F2* gene that was selected for ChIP was based on ChIP-seq data linking E2A to this region [141] and we confirmed that E2A does associate with this sequence (Fig. 31), suggesting that E2A or other E-proteins recruit Mtg16 to *E2F2* to control entry of cells into the cell cycle. The E-proteins (e.g., E2A, E2-2, and HEB) belong to a family of helix-loop-helix transcription factors that activate transcription by binding to the "E-box". These factors contain two activation domains, and the most N-terminal activation domain is also a key contact point for MTG/ETO family members [143-145]. The ability of E-proteins to activate transcription is modulated by the Id proteins as well as TAL1/SCL and related proteins. In proteomic analyses, MTG/ETO family members have been found in complexes containing E-proteins, TAL1/SCL, Lmo2, Gfi1, GATA factors, other transcriptional corepressors, and Tif1γ, which is required for transcriptional elongation [43, 46, 146-149]. While it is still unclear whether these proteomic studies are detecting one large complex or several smaller complexes, our results are consistent with *Mtg16* acting as a corepressor, perhaps by binding to E2A, such that the inactivation of *Mtg16* caused increased expression of *E2F2*, as well as other cell cycle control factors. It is notable that the phenotypes that arise in mice engineered to delete *E2A* [76] are similar to those seen in the absence of *Mtg16* in regards to loss of HSC numbers and functions.

The defects we observed in *Mtg16*-null mice also closely resembled the

phenotype associated with the deletion of *Lyl1*, a basic helix-loop-helix (bHLH) transcription factor that is closely related to TAL1/SCL and that may also associate with MTG/ETO family members [149, 150]. Although the *Lyl1*$^{-/-}$ mice displayed normal blood cell counts with only a slight reduction in the number of B cells, they too contain decreased numbers of LSK cells and LT-HSC frequencies, which resulted in decreased function in CFU-S_{12} and LTC-IC assays. In accordance, *Lyl-1*-null bone marrow was severely impaired in its competitive repopulation abilities, especially in the ability to reconstitute the B and T cell lineages [150]. However, the *Lyl1*-null bone marrow did not recapitulate the increased propensity toward myeloid development that we observed in the absence of *Mtg16*. Given that Mtg16 is a corepressor that interacts with multiple transcription factors and proteins, it is not surprising that its deletion would lead to more pleiotropic effects than the deletion of a single transcription factor. Taken together, these results highlight the importance of Mtg16 as a master regulator of hematopoiesis as it orchestrates the action of multiple transcription factors that are important for HSC functions in long-term self-renewal and in lineage cell fate decisions.

In addition to the involvement of Mtg16 in hematopoietic stem/progenitor cells, MTG family members may contribute to the function of other types of stem and progenitor cells. Mice with a deletion of *Mtgr1* failed to maintain secretory lineage cells in the small intestine [56]. After treatment with the ulcerative agent dextran sodium sulfate, which denudes the colonic epithelium, the *Mtgr1*-null colons displayed bifid glands and loss of glands, suggesting a defect in stem cell functions. These phenotypes were also associated with inappropriate cycling of the stem/progenitor cells in the crypts of the small intestine [57]. Gene targeting studies of *Mtg8* indicated that it is required for

the development of the murine gut, as some pups died due to deletion of the mid-gut [103]. In mice that retained the mid-gut, there was a dramatic loss of architecture, which could be due to defective stem cells. Thus, it is possible that all three MTG/ETO family members function in adult stem cells, perhaps to prevent entry into the cell cycle.

Our work may also hint of a role for MTG/ETO factors in leukemogenesis. Although little has been done with the t(16;21), the t(8;21) is viewed as a relatively weak oncogene, as patients can carry this translocation for several years before developing AML and patients with this translocation are considered to be in a good-risk category [151]. However, in mouse models of t(8;21) AML, the oligomerization domain, which also binds to endogenous Mtg16/Eto2 and Mtgr1, is essential to the transforming ability of the fusion protein [40, 41]. Therefore, it is possible that binding of the t(8;21) fusion protein to Mtg16 impairs the action of Mtg16 and causes the HSC to enter the cell cycle. In addition, the fusion protein can directly repress the expression of tumor suppressors such as $p14^{ARF}$, *Neurofibromatosis-1*, *PU.1* and *C/EBPa* [24-26, 152]. These data suggest that the t(8;21) could promote immortalization of hematopoietic stem and progenitor cells by repressing tumor suppressor genes, while triggering proliferation by activating genes such as *E2F2*.

CHAPTER V

MTG16 SUPPRESSES DNA DAMAGE IN HEMATOPOIETIC PROGENITOR CELLS

Background and Significance

Gene disruption of *Mtg16* in mice demonstrated that Mtg16 is not essential for viability or fertility, but it is required for hematopoietic progenitor cell proliferation [137]. In addition, like many of the transcription factors that recruit Mtg16, inactivation of *Mtg16* caused a reduction in stem cell pools and inappropriate cycling of stem and progenitor cells, which led to a loss of stem cell self-renewal. Thus, *Mtg16* is an important regulator of HSC self-renewal and multipotency, however; the mechanism by which this occurs needs to be further defined in order to better understand how *Mtg16* regulates HSC functions. Strikingly, mutations in DNA repair factors or other proteins that regulate genomic stability display similar phenotypes, which lead to premature hematopoietic failure [153, 154]. Therefore, it is important to determine if an increase in genomic instability also contributes to the hematopoietic defects found in the absence of *Mtg16*.

Results

Defects in *Mtg16*-null hematopoietic stem and progenitor cell proliferation

In many engineered mouse models, a reduction in hematopoietic stem cell (HSC) numbers is due to impaired progenitor cell function, which alters homeostasis between the HSC and hematopoietic progenitor cell (HPC) pools causing more stem cells to enter the cell cycle and differentiate rather than self-renew [153, 155, 156]. Because these phenotypes are difficult to separate *in vivo* where homeostasis is maintained, we assessed the proliferation of stem and progenitor cells *in vitro*. LSK/Flt3$^-$ cells were purified by FACS and cultured in the presence of IL6, SCF, and LIF on OP9 stromal cells to support stem/early progenitor cell growth. Under these conditions, the 2,500 LSK/Flt3$^-$ cells initially plated proliferated for 6-8 days and then gradually lost their proliferative capacity over the next 10-12 days in culture. In several experiments, *Mtg16*-null stem/hematopoietic progenitor cells showed less of an initial proliferative burst during the first 6-7 days in culture, but in other cultures this was less apparent (data not shown). However, when 400,000 cells were re-plated on days 7 and 14 and the total number of cells was determined, the *Mtg16*$^{-/-}$ cells showed a consistent and dramatic loss of proliferative capacity throughout the remaining time course (Fig. 34A). In addition, there was a substantial increase in the numbers of lineage marker positive cells with a concomitant loss in the numbers of lineage-negative cells in the absence of *Mtg16*, even after only 7 days in culture (Fig. 34B), with the vast majority of these cells becoming Gr1 and/or Mac1 positive (Fig. 35). This loss of lineage-negative

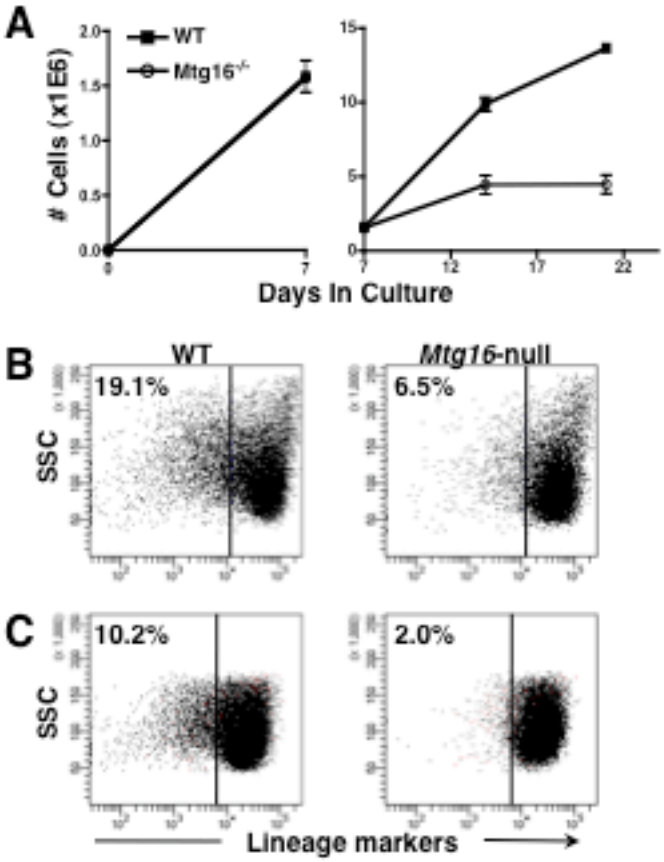

Figure 34. Inactivation of *Mtg16* affects progenitor cell proliferation. (A) 2,500 sorted LSK Flt3- bone marrow cells were cultured on an OP9-GFP stromal layer in IL6, SCF, and LIF and the proliferation in liquid culture was monitored by counting the total number of cells 7 to 21 days after harvesting the bone marrow cells. Data are expressed as mean ± SEM. An unpaired two-tailed *t* test indicated these differences were statistically significant (day 14, P = 0.0021; day 21, P = 0.0001). Shown are representative results from an experiment done in triplicate that are consistent with other biological replicates. (B-C) Flow cytometry analysis of day 7 (B) or day 14 (C) cultures using a combination of anti-CD3, anti-B220, anti-Gr1, anti-Mac1, and anti-Ter119 to distinguish mature cells from immature progenitor cells. Shown is a representative plot from an experiment performed in triplicate that is consistent with other biological replicates.

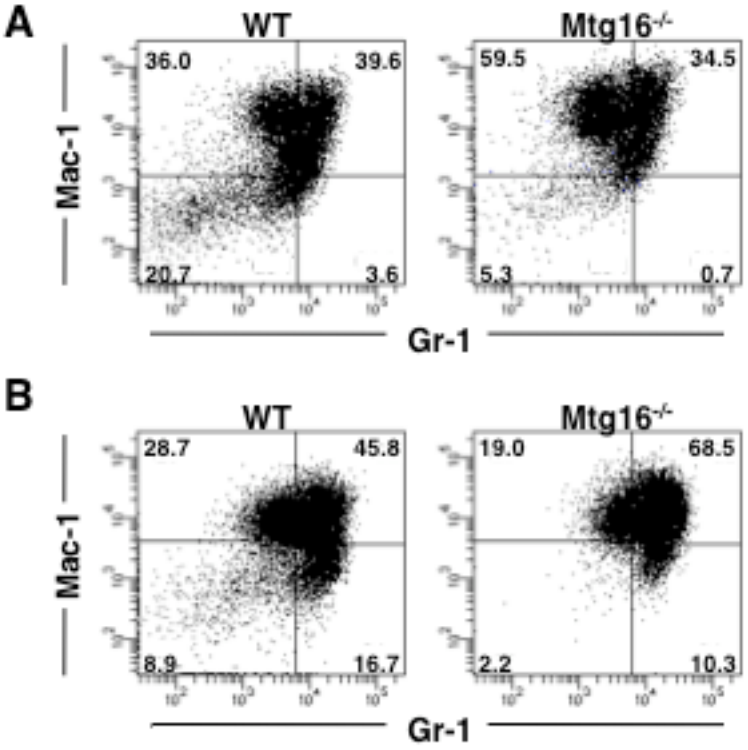

Figure 35. Inactivation of *Mtg16* leads to an increase in myeloid differentiation *in vitro*. (A) Flow cytometry analysis of day 7 LSK Flt3- cultures using a combination of anti-Gr1 and anti-Mac1 to quantify myeloid cell differentiation. Note that the double negative cells did not express any other lineage markers (data not shown). (B) Flow cytometry analysis of day 14 LSK Flt3- cultures using a combination of anti-Gr1 and anti-Mac1 to quantify myeloid cell differentiation. Note that the double negative cells did not express any other lineage markers (data not shown). Shown are representative plots from an experiment performed in triplicate that are consistent with other biological replicates.

cells from the *Mtg16*-null cells continued throughout the course of the culture as seen after 14 days in culture (Fig. 34C and Fig 35).

The precocious differentiation of LSK/Flt3$^-$ cells into myeloid progenitor cells provides a possible mechanism to explain the reduction of stem cell numbers in *Mtg16*$^{-/-}$ mice (Figure 22), as the progenitor cell population must be continually replenished. These data suggest that the increased differentiation (Fig. 34B, C) of stem/progenitor cells from *Mtg16*$^{-/-}$ mice caused greater numbers of stem cells to enter the cell cycle or more early progenitor cells to continue to cycle to maintain homeostasis.

Mtg16 is required to suppress DNA damage in cycling cells

In addition to the changes observed in transcriptional regulators and cytokine receptors that control hematopoiesis, or modulators of the cell cycle (Fig. 30), we also noted that a large number of genes that function in DNA metabolism were mis-regulated. Therefore, we tested whether the loss of *Mtg16* caused genotoxic stress, which is closely associated with hematopoietic failure syndromes [154, 157]. Immunofluorescence using anti-γH2AX, which is found at the sites of DNA double strand breaks and forms nuclear "foci" at the sites of the break, was used to assess DNA damage [158]. Preliminary assays suggested that there were numerous γH2AX foci in *Mtg16*-null blast-like cells, but not in mature bone marrow cells (data not shown). Therefore, we lineage-selected bone marrow from control and *Mtg16*-null mice using antibodies linked to magnetic beads prior to immunofluorescence. The mature, lineage positive cells from either genotype contained few γH2AX foci (Fig. 36A and B) with over 97% of the cells containing fewer than 5 foci. However, in lineage negative

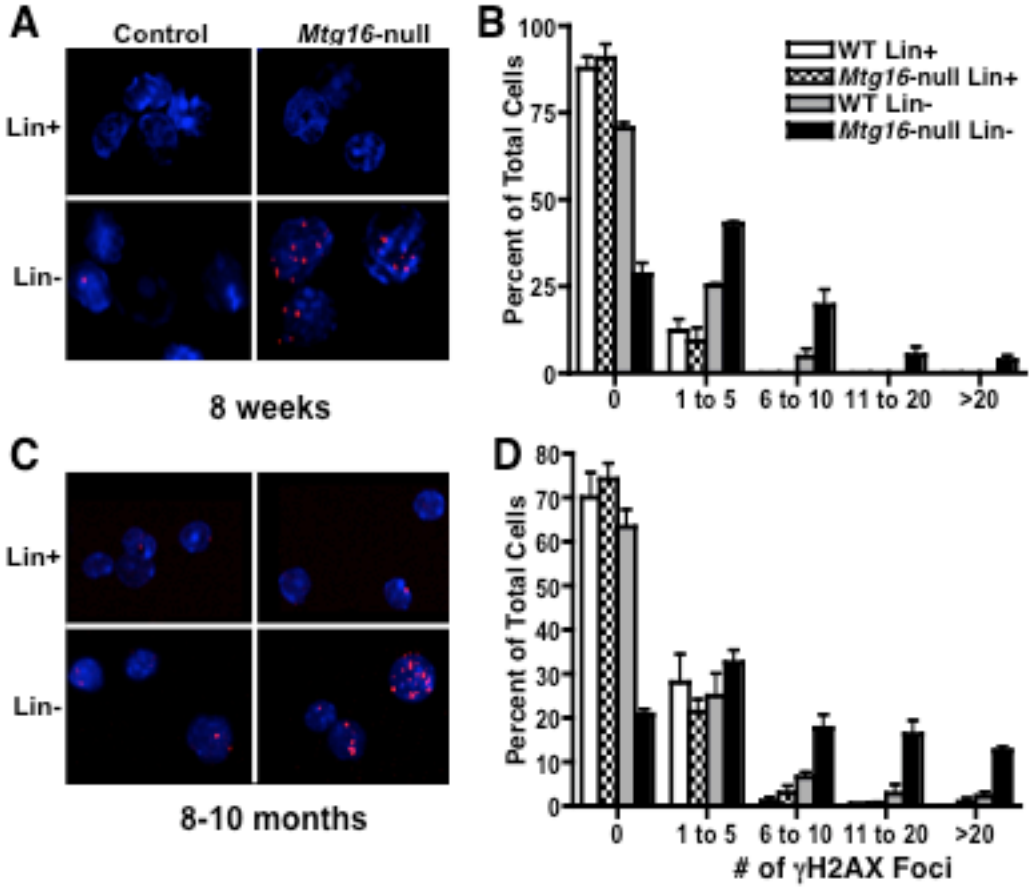

Figure 36. Lineage negative *Mtg16*-null progenitor cells contain hallmarks of DNA double strand breaks. (A) Immunofluorescence analysis using anti-gH2AX (red) to detect DNA double strand breaks. DNA was counterstained with DAPI (blue) to display the nuclei. Top panels show cells that were selected for the expression of Cd5, CD45R (B220), Gr1, Mac1, 7-4, and Ter119 (Lin^+) using antibodies linked to magnetic beads, whereas the bottom panels show Lin- progenitor cells. (B) Graphical representation of quantification of the percentage of cells containing the indicated number of gH2AX foci. (C) and (D), 8-10 month old mice were used in the same analysis as shown in A and B. These experiments were performed in triplicate and the data is expressed as the mean ± SEM.

cells 5-7% of the control cells contained signs of DNA damage, which is common in cells undergoing DNA replication. In contrast, nearly 30% of the *Mtg16*-null progenitor cells contained six or more γH2AX foci, with many containing a level of genotoxic stress that is sufficient to trigger cell cycle checkpoints [159, 160]. Similar results were obtained using a second marker of DNA double strand breaks, anti-53BP1 (data not shown). These data are consistent with the defects observed in *Mtg16*-null progenitor cell proliferation (Fig. 23A, 34A).

Given that *Mtg16*-null stem/progenitor cells displayed increased genotoxic stress in young mice (Fig. 36A, B), cohorts of wild type and *Mtg16*-null mice were aged to determine if DNA damage accumulated in older mice (Fig. 36C, D). We again segregated mature cells from the immature progenitor cells using lineage antibodies and enumerated γH2AX-containing foci. As expected, there was a small increase in the amount of DNA damage detected in wild type stem and progenitor cells from older mice, with 2-4% of the lineage negative cells containing more than 10 foci (Fig. 36C, D) [154, 157]. In the *Mtg16*-null cohort, there was an even more dramatic accumulation of anti-γH2AX foci in aged mice, with nearly a quarter of the stem/progenitor cells containing 11 or more foci (Fig. 36C, D).

Altered gene expression contributes to DNA damage

Genome wide siRNA and cDNA over expression screens have identified genes whose mis-regulation can trigger DNA double strand breaks [161, 162]. By comparing our gene expression changes to these databases, we identified 2 genes that were up regulated in the absence of *Mtg16* and that when over

A

Gene Symbol	Gene Name	Average FC
Hes1	hairy and enhancer of split 1 (Drosophila)	8.93
Maff	v-maf musculoaponeurotic fibrosarcoma oncogene family, protein F (avian)	2.43
Copz1	coatomer protein complex, subunit zeta 1	-1.76
Pold1	polymerase (DNA directed), delta 1, catalytic subunit	-1.67
Xrcc2	X-ray repair complementing defective repair in Chinese hamster cells 2	-1.50
Gtse1	G two S phase expressed protein 1	-1.67
Stk24	serine/threonine kinase 24 (STE20 homolog, yeast)	-1.76

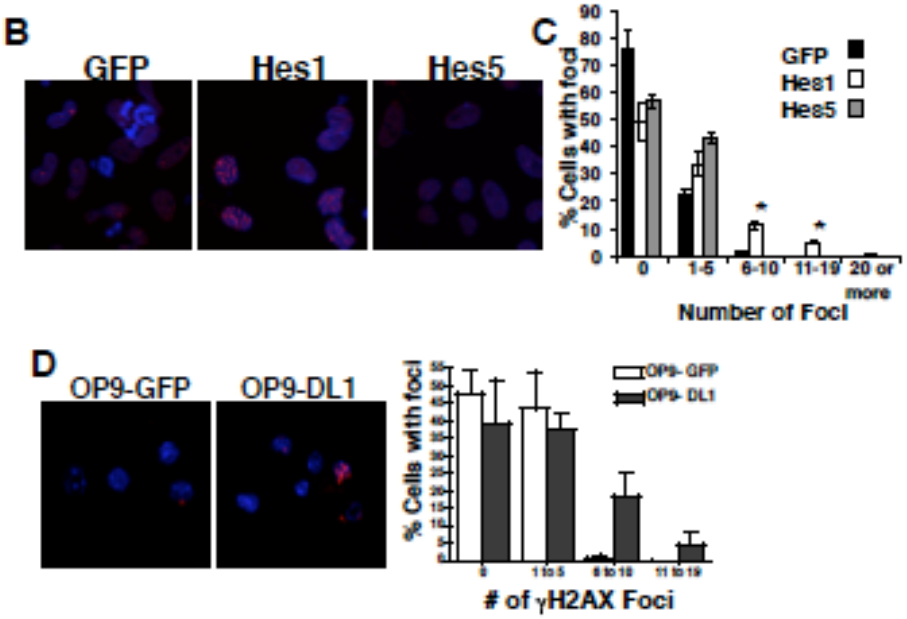

Figure 37. Inactivation of *Mtg16* alters the expression of DNA damage control genes, in particular, *Hes1*. (A) The LSK microarray results were cross-referenced with published screens that identified genes whose over expression or siRNA-mediated inactivation caused DNA damage (Lovejoy et al., 2009; Paulsen et al., 2009). The 7 genes that were mis-regulated in the *Mtg16*-null LSK cells that cause DNA damage are shown along with the level of change in wild type versus *Mtg16*-null LSK cells. FC stands for fold change compared to wild type. (B) Vector control (*GFP*), *Hes1* or *Hes5* were expressed in HeLa cells and DNA double strand breaks were identified using immunofluorescence with anti-53BP1. (C) Graphical representation of the percentage of cells containing the indicated number of 53BP1 positive foci. Data are expressed as mean ± SEM. An unpaired two-tailed *t* test indicated that over-expression of *Hes1* induced a statistically significant difference (marked with an *) in the number of 6-10 and 11-19 foci (6-10, P = 0.0004; 11-19, P = 0.003; n = 6). (D) Wild type LSK cells were sorted and cultured for 6 days on OP9-GFP or OP9-DL1 stromal cells and DNA double strand breaks were identified using immunofluorescence with anti-gH2AX. Graphical representation of the percentage of cells containing the indicated number of gH2AX positive foci. Data are expressed as mean ± SEM.

expressed caused DNA damage (*Hes1* and *Maff*, Fig. 37A) [161]. In addition, siRNA knockdown of 5 genes that were significantly under expressed in the *Mtg16*-null LSK cells caused DNA double strand breaks (Fig. 37A). Thus, changes in gene expression patterns are likely to contribute to the observed DNA damage found upon inactivation of *Mtg16*.

Although mis-expression of any one of these 7 genes was sufficient to cause DNA double strand breaks [161, 162], the coordinate mis-regulation of this group of genes likely contributes to the dramatic levels of DNA damage that we observed (Fig. 36). Nevertheless, we were particularly intrigued by *Hes1*, which was highly up regulated in the absence of *Mtg16* (Fig. 37A), because as a key target of Notch signaling it likely plays an important role in hematopoietic stem and progenitor cell maturation. In addition, MTG8 and Mtg16 can associate with CSL, a mediator of Notch signaling, as well as the Notch intracellular domain to regulate the expression of *Hes1* [48, 50]. We found that expression of *Hes1*, but not *GFP* or *Hes5*, caused an increase in 53BP1-containing foci, indicative of DNA double strand breaks (Fig. 37B, C). This experiment used retroviral expression of *Hes1* in HeLa cells, but to use a more physiological system, we co-cultured wild type FACS purified LSK cells with control OP9-GFP stromal cells or OP9-DL1 stromal cells that express the Delta-like 1 Notch ligand. The OP9-DL1 system transmits a constitutive Notch signal yielding a level of *Hes1* expression similar to that observed in the absence of *Mtg16* (6-8 fold) as measured by quantitative RT-PCR (data not shown). LSK cells cultured on OP9-DL1 stroma for 6 to 7 days displayed an increase in γH2AX foci as compared to LSK cells grown on control stroma (Fig. 37D).

Thus, mis-regulation of *Hes1* likely contributes to the DNA damage observed in the absence of *Mtg16*, but the mis-regulation of multiple genes is likely additive.

DNA damage triggers premature differentiation of stem/progenitor cells

Engineered mutations in mice or naturally occurring human mutations in DNA repair pathways cause genotoxic stress that results in impaired progenitor function and ultimately stem cell failure [153, 154, 157, 163, 164]. Our initial analysis found DNA damage in the lineage negative fraction of bone marrow cells (Fig. 36) that are mostly rapidly proliferating progenitor cells with less damage in maturing cells that are losing proliferative potential. Therefore, we FACS purified LSK/Flt3$^-$, LSK/Flt3$^+$, and Lineage negative/c-Kit$^+$/Sca1$^-$ myeloid progenitor (MP) cells to assess DNA damage in stem/early progenitor cells versus more highly proliferating myeloid progenitor cells. Neither of the LSK populations showed high levels of γH2AX foci, but the *Mtg16*-null myeloid progenitor cells displayed higher levels of DNA damage (Fig. 38A-D). Combined with our earlier analysis of more heterogeneous populations (Fig. 36), these data suggest that DNA damage may underlie the proliferative defects observed in *Mtg16*-deficient progenitor cells and suggest that cell cycle progression is required for this DNA damage.

Next, because the observed DNA damage was so closely linked with cell cycle progression, we reasoned that the rare entry of an HSC into the cell cycle to self-renew or produce progeny that will repopulate progenitor pools may cause DNA damage that would impair stem cell function over an extended period of time and lead to a reduction in stem cell number (Fig. 22). Moreover, because few LSK cells are cycling, this lower

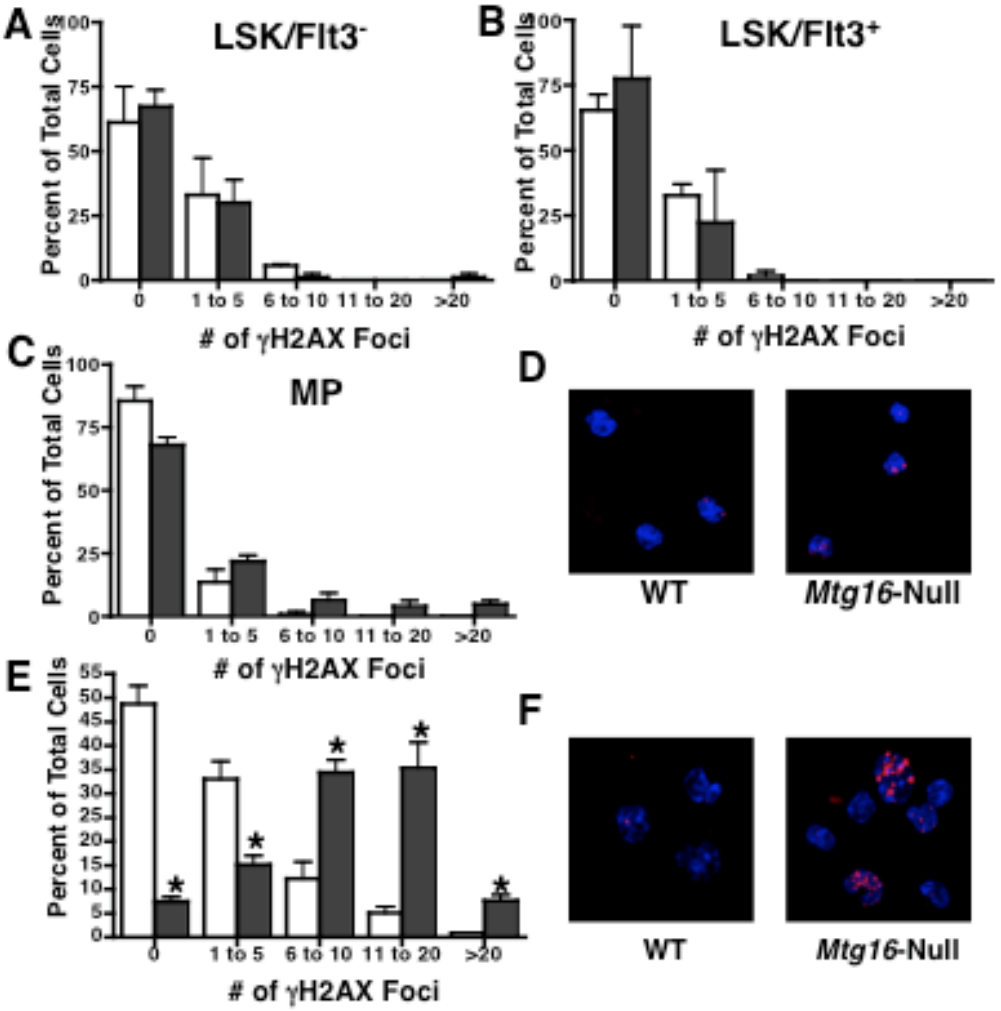

Figure 38. Cycling *Mtg16*-null progenitor cells contain hallmarks of DNA double strand breaks. Lineage negative bone marrow cells were FACS purified using anti-c-Kit, anti-Scal, and anti-Flt3 to assess DNA damage in stem/early progenitor cells (LSK/Flt3$^-$ or LSK/Flt3$^+$) versus more actively proliferating HPCs (Lineage negative/c-Kit$^+$/Sca1$^-$ myeloid progenitor, MP) and DNA double strand breaks were identified using immunofluorescence with anti-gH2AX. (A-C) Graphical representation of quantification of the percentage of cells containing the indicated number of gH2AX foci in sorted LSK Flt3- cells (A), LSK/Flt3+ cells (B) and MP cells (C). (D) Immunofluorescence analysis of the MP cells using anti-gH2AX (red) to detect DNA double strand breaks. DNA was counterstained with DAPI (blue) to display the nuclei. (E) 2,500 sorted LSK Flt3- bone marrow cells were cultured on an OP9-GFP stromal layer in IL6, SCF, and LIF and the number of gH2AX foci was quantified 7 days after harvesting the bone marrow cells. (F) Immunofluorescence analysis of the LSK Flt3- cultured cells using anti-gH2AX (red) to detect DNA double strand breaks. DNA was counterstained with DAPI (blue) to display the nuclei. These experiments were performed in triplicate and are representative of biological replicates. The data is expressed as the mean ± SEM. An unpaired two-tailed *t* test indicated these differences were statistically significant (marked with an *; 0, P = 0.004; 1-5, P = 0.0115; 6-10, P = 0.007; 11-20, P = 0.0052; >20, P = 0.0063; n=3).

level of DNA damage may not be detected under homeostatic conditions. Therefore, we FACS purified LSK/Flt3$^-$ cells and cultured them in IL6, SCF, and LIF (to suppress differentiation) for 7 days prior to assessing DNA damage. When these early progenitor cells were stimulated to cycle, they too accumulated DNA damage with *Mtg16*-null cells acquiring much more damage than control cells (Fig. 38E, F).

The levels of DNA double strand breaks found in the absence of *Mtg16* may trigger cell cycle checkpoints that cause cells to exit the cell cycle [165]. In the case of hematopoietic cells, exit from the cell cycle may cause loss of self-renewal potential and trigger differentiation. Both the methylcellulose serial replating and LTC-IC assays indicate that the *Mtg16*-null stem/progenitor cells have decreased self-renewal potential (Figure 29).

Given our identification of DNA damage in *Mtg16*-null progenitor cells and their premature differentiation/loss of self-renewal capacity (Fig. 29, 34, 36, and 38), we tested the effects of DNA damage on the self-renewal capacity of wild type stem cells using the LTC-IC assay (Fig. 39A). Irradiation of wild type bone marrow cells with 1 Gy of IR was sufficient to trigger a 3-4 fold loss of self-renewal (80% compared to only 25%) two weeks after IR treatment and by week 3 there were few CFU-C present (Fig. 39A and data not shown). This was similar to the effect of inactivating *Mtg16* (Fig. 29 and 39A). Thus, the relatively low levels of DNA damage observed in *Mtg16*-null cells are sufficient to impair self-renewal and may contribute to both the defect in progenitor cell proliferation and the loss of HSCs.

An *in vivo* test of stem cell self-renewal is the ability of the hematopoietic compartment to respond to repeated stress over an extended time frame. We treated

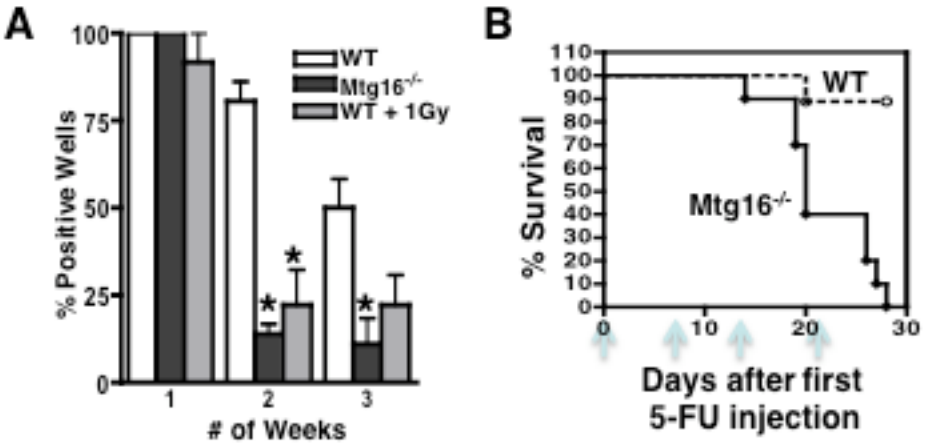

Figure 39. DNA damage contributes to a loss of hematopoietic self-renewal. (A) Graphical representation of the numbers of methylcellulose colonies formed at the indicated times from LTC-IC cultures of wild type (open bars), *Mtg16*-null (dark grey bars), and irradiated wild type (1Gy) bone marrow cells (light grey bars). Data are expressed as mean ± SEM. An unpaired two-tailed *t* test indicated the difference at week 2 and week 3 after culture (marked with an *) was statistically significant ($P<0.05$). Shown are representative results from three separate experiments. (B) Graphical representation of the survival of wild type (WT) or *Mtg16*-null mice treated with 5-FU weekly with 100 mg/kg to kill cycling progenitor cells and test for stem cell self-renwal (WT, $n = 9$; *Mtg16*-null, $n = 10$).

cohorts of mice with 5-fluorouracil (5-FU), which causes S phase-specific DNA damage. Control and *Mtg16*-null mice were serially injected with 100 mg/kg 5-FU (a moderate dose) once a week. Both sets of mice tolerated the first injection well, but within 5 days of the second dose of 5-FU the *Mtg16*-null mice began to show signs of distress and only half of the *Mtg16*-null cohort were healthy enough to receive the third injection (Fig. 39B). By 28 days after the first injection, the entire cohort of mice lacking *Mtg16* had to be humanely euthanized (Fig. 39B). By contrast, the majority of the control mice tolerated the 5-FU treatments well with only a single subject not surviving past 20 days (Fig. 39B). Thus, inactivation of *Mtg16* sensitized the mice to genotoxic stress due to the requirement of *Mtg16* to suppress DNA damage in actively cycling progenitors to prevent differentiation and loss of HSC self-renewal (Fig. 34, 36, and 39).

DNA damage triggers myeloid differentiation.

The levels of DNA double strand breaks found in the absence of *Mtg16* is often associated with cell death, but DNA damage can also trigger cell cycle checkpoints that cause cells to exit the cell cycle, and in the case of hematopoietic stem/progenitor cells, may cause them to differentiate [165]. Given that *Mtg16*-null progenitor cells displayed premature differentiation (Fig. 34-35), we tested whether a sub-lethal dose of irradiation might also trigger the differentiation of wild type progenitor cells. Wild type or *Mtg16*-null lineage negative cells were cultured in the presence of IL6, SCF, and LIF on OP9 stromal cells, and exposed to increasing amounts of ionizing radiation (IR). Consistent with our prior results (Fig. 34), even in the absence of IR the *Mtg16*-null cells showed reduced proliferation (Figure 40A). After IR, proliferation was further decreased

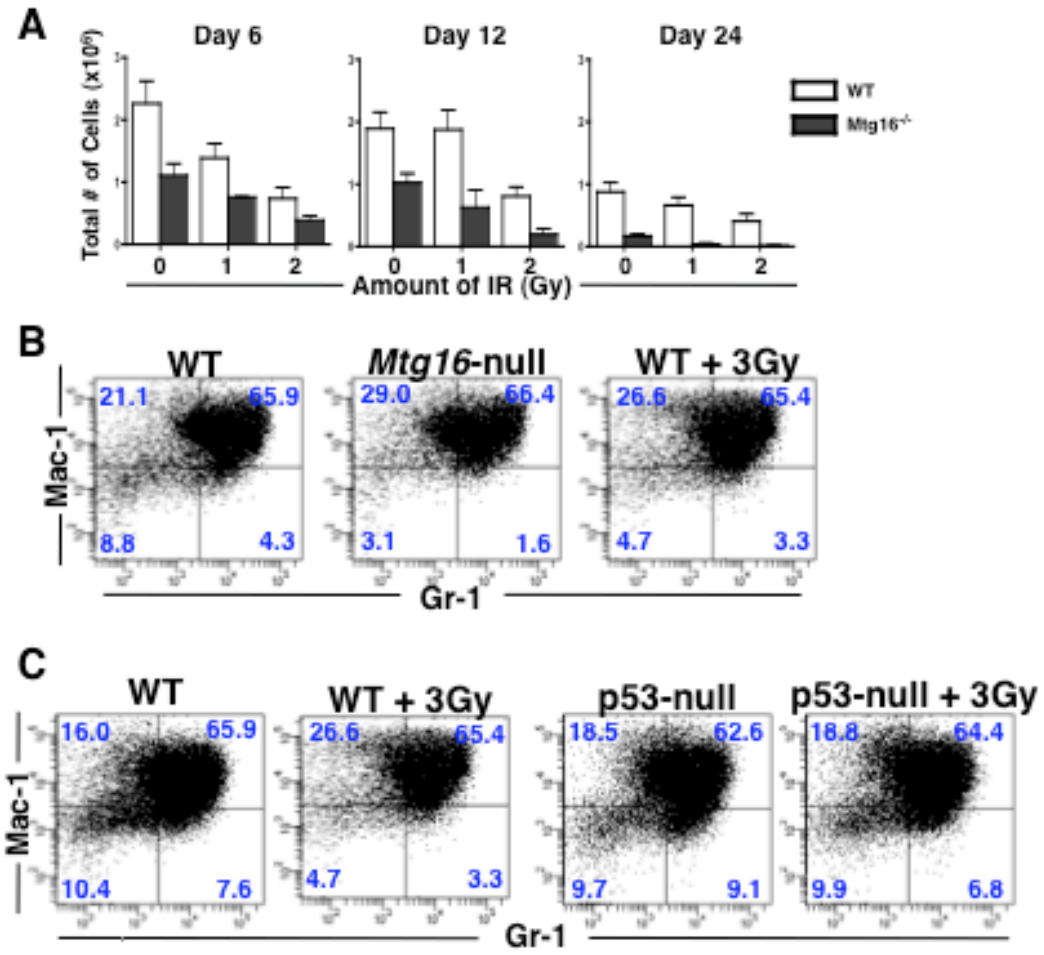

Figure 40. DNA damage triggers myeloid differentiation of hematopoietic progenitor cells. (A) Cells were cultured on OP9 stromal cells in media containing IL6, SCF, and LIF and treated with increasing amounts of ionizing radiation (0, 1, or 2, or 3 Gy). Cell proliferation was monitored by counting the total number of cells 6 to 18 days after harvesting the bone marrow cells. (B) Flow cytometric analysis using a combination of anti-Gr1 and anti-Mac1 to quantify myeloid cell differentiation. Control cells were compared to *Mtg16*-null or wild type cells treated with 3 Gy of IR 6 days prior to analysis. Graphical representation of the immature (double negative) cells in a flow cytometric analysis of myeloid cell differentiation using anti-Gr1 and anti-Mac1. Control cells were compared to *Mtg16*-null or wild type cells treated with 3 Gy of IR 15 days prior to analysis. (C) Flow cytometric analysis using a combination of anti-Gr1 and anti-Mac1 to quantify myeloid cell differentiation. Control Lineage negative bone marrow stem and progenitor cells taken from p53-null mice were compared to *Mtg16*-null or wild type cells not treated or treated with 3 Gy of IR 6 days prior to analysis.

relative to the control cells and by 12 days after IR most of the *Mtg16*-null progenitor cells receiving 2 Gy IR were eliminated (Fig. 40A). In fact, wild type cells receiving 1-3 Gy of IR, displayed similar growth profiles as *Mtg16*-null cells without treatment (Fig. 40A and data not shown).

The loss of proliferation of wild type hematopoietic stem/progenitor cells upon DNA damage (Fig. 40A) coincided with a reduction in the numbers of immature, Gr1/Mac1 double negative cells in these cultures (Fig. 40B, lower left quadrants; 8.8% vs. 4.7%). Flow cytometric analysis also indicated that in the absence of IR, *Mtg16*-null cells showed a propensity to differentiate into both Gr1/Mac1 double positive and Mac1 single positive cells (Fig. 40B). This loss of the double negative population and increase of $Mac1^{+}$ cells was phenocopied by wild type cells 6 days after exposure to 3 Gy of IR (Fig. 40B). To test whether the DNA damage checkpoint was required for the loss of the immature progenitor cells and the acquisition of myeloid cell markers, we treated *p53*-null stem and progenitor cells with 3 Gy of IR (Fig. 40C). In the absence of *p53*, irradiation did not trigger a loss of the Gr1/Mac1 double negative population or an accumulation of Mac1 single positive cells (Fig. 40C). We conclude that genotoxic stress caused by loss of *Mtg16* contributes to the loss of HSC self-renewal by triggering cell cycle exit and myeloid differentiation.

Discussion

Inactivation of *Mtg16* caused a reduction in stem cell numbers that was likely due to over active cycling in response to deficits in progenitor cell proliferation (Chapter IV and Figure 34). These defects could be caused by DNA damage that was found in

populations undergoing rapid expansion, but not in quiescent or post-mitotic cells and this damage accumulated with age (Fig. 36 and 38). Mechanistically, inactivation of Mtg16 caused the de-regulation of multiple genes linked to genomic stability, including *Hes1*. The defects found are reminiscent of mutations in DNA repair factors or other proteins that regulate genomic stability that lead to premature hematopoietic failure [153, 154]. Moreover, the emergence of DNA damage coincided with enhanced or accelerated differentiation, which may be a common feature in genetic hematopoietic failure syndromes [154, 157, 163, 164]. Low doses of ionizing radiation also caused a loss of stem cell self-renewal and phenocopied *Mtg16*-inactivation (Fig. 39-40). Thus, Mtg16 plays a central role in maintaining the potency of stem and progenitor cells, at least partly through its recruitment to the promoters of genes whose dys-regulation triggers genotoxic stress.

Although several genome maintenance genes were dys-regulated in *Mtg16*-null LSK cells (Fig. 37), *Hes1* is a particularly interesting target. MTG8 is recruited to *Hes1* through interactions with Sharp, a corepressor that contacts CSL, to repress *Hes1*. However, in the presence of a Notch signal, CSL activates *Hes1* through association with the Notch intracellular domain. Mtg16 associates with both the Notch intracellular domain and CSL, making it a key regulatory factor in this transcriptional switch [48, 50]. In terms of genome maintenance, *Hes1* was identified in a genomic screen of factors that cause DNA double strand breaks [161], and in a screen for genes that trigger p53 accumulation [166]. Given that *Hes1* is one of the best characterized targets of canonical Notch signaling and our findings that Notch signals are sufficient to induce hallmarks of DNA damage, one can speculate that this DNA damage or replication stress plays a

physiological role during hematopoiesis. Given that canonical Notch signaling is not required for hematopoietic stem cell self-renewal, but plays a role in differentiation and cell fate choices [167], it is possible that Notch signaling triggers cell cycle checkpoints to promote differentiation. In this model, the DNA damage found would be an extreme example of replication stress that could be very detrimental when Notch receptors are activated by mutation in T cell acute lymphocytic leukemia [168].

In general, the t(8;21) is viewed as a relatively weak oncogene as various human studies have suggested that patients can carry this translocation for several years before developing AML [151]. While the fusion protein can directly repress the expression of tumor suppressors, it also induces a DNA damage gene signature [24-26, 152, 169, 170]. In addition, expression of the fusion protein *in vitro* increased DNA damage and sensitized the cells to DNA damaging agents [169, 170]. These data suggest that the t(8;21) promotes immortalization of hematopoietic stem and progenitor cells by repressing tumor suppressor genes, while triggering a low level of DNA damage that increases the mutation rate to promote leukemia. It is possible that binding of the t(8;21) fusion protein to Mtg16 impairs the action of Mtg16 in genomic stability as in various mouse models the oligomerization domain is essential to the transforming ability of the fusion protein [39-41].

In support of our current results, we found that *Mtg8*-null murine embryonic fibroblasts also display genotoxic stress (DeBusk et al., in prep.), which suggests that MTG family members contribute to genomic stability in a variety of cell types. This is intriguing given the fact that two MTG family members are targeted by chromosomal translocations in acute myeloid leukemia and mutations of MTG family members have

been found in other types of cancers as well. Thus, a role in suppressing DNA damage or in maintaining genomic stability could explain why MTGs are so frequently targeted in cancer, as inactivation would cause more frequent DNA damage/repair cycles leading to an accumulation of additional mutations.

CHAPTER VI

HDAC3, AN MTG16 INTERACTING PROTEIN, IS ESSENTIAL FOR HEMATOPOIETIC STEM CELL FUNCTION

Background and Significance

We have shown that Mtg16 is an important regulator of hematopoietic stem and progenitor cell functions, however; Mtg16 is a scaffolding protein that links DNA binding transcription factors to various corepressor proteins [10, 11, 54]. Thus, the action of Mtg16 on the transcription factors it binds is imparted by the corepressors that Mtg16 links to them. Therefore, information about the function of the corepressors that bind to Mtg16 would help delineate which interactions are required for various functions of Mtg16. One of these main interacting proteins is histone deacetylase 3 (Hdac3), which is part of the NCoR/SMRT repression complex and contributes to both transcriptional repression and genomic stability [54, 171]. To delete *Hdac3* in hematopoietic stem cells we used the *Vav-Cre* transgenic allele to trigger recombination since deletion in the germline leads to embryonic lethality (Summers et al, in prep.). These mice were viable but showed a dramatic loss of lymphoid cells (both B and T cells), hypocellular bone marrow with myelosuppression and anemia. FACS analysis of the hematopoietic stem/early progenitor compartment suggested that *Hdac3* was required for the formation of the earliest lymphoid progenitor cells ($Lin^-/Sca1^+/c\text{-}Kit^+/Flt3^{hi}$), but not myeloid progenitor cells. Although $Hdac3^{-/-}$ bone marrow contained roughly half the normal complement of hematopoietic cells, they contained 4-5 times more stem/early progenitor

cells. However, the initial results of the impairment in lymphopoiesis implied that the HSCs that were present were defective. Thus, we set out to carefully examine the functions of hematopoietic stem cells in the absence of *Hdac3*. This information will be valuable further understanding of how loss of *Mtg16* leads to defects in HSCs. In addition, commonly used histone deacetylase inhibitors target Hdac3, and therefore this information could help provide a mechanism on how these drugs work.

Results

Hdac3 is required for the proliferation of hematopoietic progenitor cells.

To begin studying the stem cell functions, we assessed hematopoietic progenitor pool size in the *Vav-Hdac3*$^{-/-}$ mice using methylcellulose colony formation assays. When methylcellulose containing IL-6, IL-3, SCF, and Epo was used to examine myeloid progenitors, the number of colonies that formed from *Vav-Hdac3*$^{-/-}$ bone marrow was similar to that derived from control bone marrow, but the colonies were distinctly smaller suggesting a general proliferation defect (Fig. 41A). Nevertheless, we were able to identify the types of colonies and there were shifts within the most differentiated CFU-G populations with an absence of colonies that contained erythroid cells, including BFU-E and CFU-GEMM (Fig. 41B), which is consistent with the anemia observed in these mice. The lack of BFU-E was confirmed using methylcellulose containing only Epo (data not shown). Additionally, we examined B-cell formation using methylcellulose containing IL-7 and confirmed that Hdac3 is required for the formation of B-cells, as no colonies were present (Figure 41C).

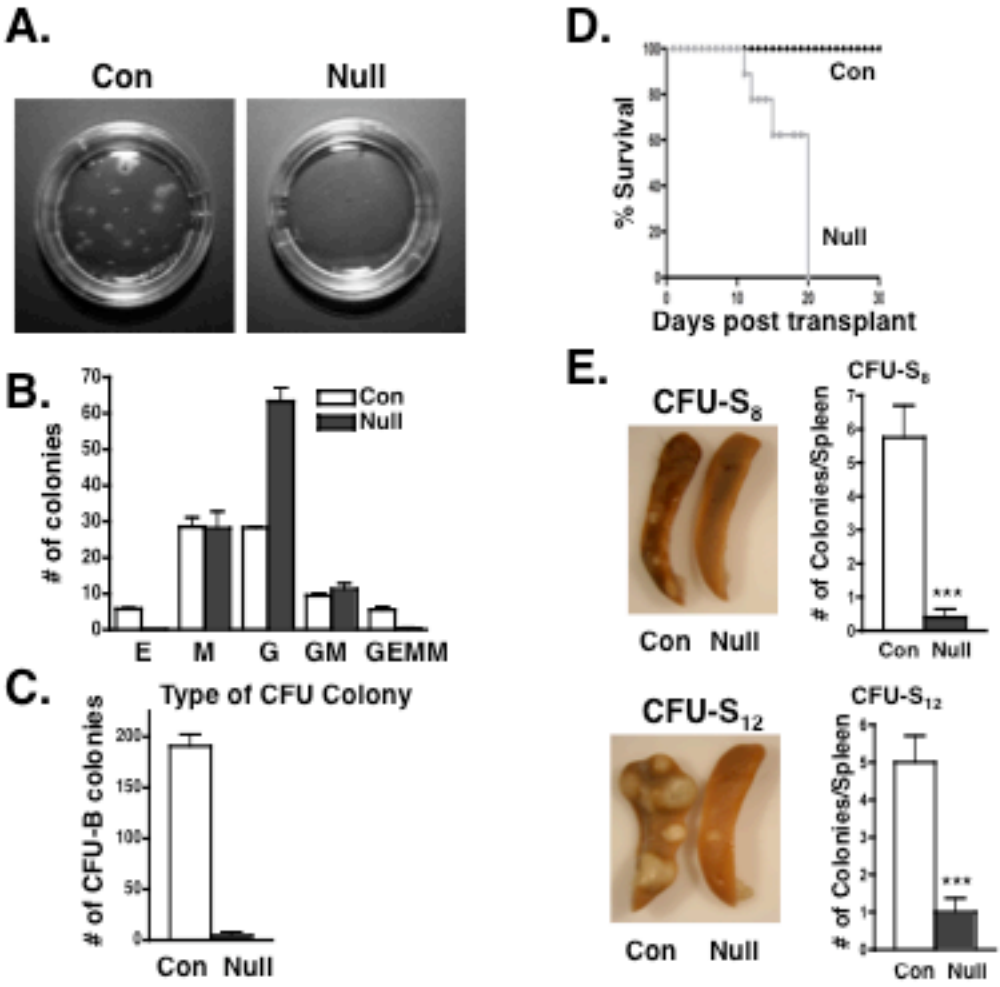

Figure 41. Loss of *Hdac3* disrupts hematopoietic progenitor and stem cell functions. Bone marrow (2.5×10^4) cells were plated in methylcellulose containing IL-3, IL-6, Epo, and SCF and colonies were quantified after 8-10 days in culture. Representative pictures of the plates are shown in (A) and quantification of each of the colony type (E, BFU-E; M, CFU-M; G, CFU-G; GM, CFU-GM; GEMM, CFU-GEMM) are shown in (B). (C) Bone marrow (7.5×10^4) cells were plated in methylcellulose containing IL-7 and colonies (CFU-pre-B) were quantified after 7 days in culture. (D) Survival curves of a transplant experiment using 1×10^6 wild type (black circles), or *Hdac3*-null bone marrow cells (grey circles). (E) CFU-S_8 and CFU-S_{12} were obtained for wild type and *Hdac3*-null bone marrow. Quantification of each CFU-S is calculated for the number of colonies per spleen and is shown to the right of each picture of representative spleens (wild type (n = 5), empty bars; *Hdac3*-null (n = 5), full bars). Data are expressed as mean ± the standard error of the mean (SEM). An unpaired two-tailed *t* test indicated that the changes observed in the number of cells were significant (***p = 0.0005).

Hdac3 is required for long-term stem cell function

Given that inactivation of *Hdac3* caused genomic instability and apoptosis in murine embryonic fibroblasts (MEFs) [171] and that hematopoietic progenitor cells displayed a growth defect, we functionally tested the HSC and progenitor cell populations. Bone marrow transplantation assays and competitive repopulation studies were used to assess the ability of stem cells to repopulate lethally irradiated mice. Remarkably, irradiated mice injected with a million *Hdac3*-null bone marrow cells had survival curves that matched that of the lethally irradiated control mice, whereas mice injected with control bone marrow cells were rescued by the transplant (Fig. 41D). Therefore, we performed spleen colony forming assays to quantitatively measure the response to hematopoietic stress after bone marrow transplantation. The *Hdac3*-null bone marrow yielded essentially no colonies at either 8 days post transplantation, which measures megakaryocyte and erythroid progenitor cells (MEPs), or at 12 days post injection when the colonies formed represent both MEPs and short term stem cells and multi-potent progenitor cells (Fig. 41E).

Given the dramatic growth defects of progenitor cells, we used competitive bone marrow transplantation (cBMT) assays to provide the null stem cells with wild type progenitor cells to measure the ability of the null long-term stem cells to compete with wild type stem cells. We injected a mixture of 90% *Vav:Hdac3*$^{-/-}$ bone marrow cells that express CD45.2 and 10% wild type CD45.1 cells into lethally irradiated mice. Only 3-weeks after transplantation into the CD45.1 recipient mice, we observed a prominent decline in the numbers of CD45.2^{+} *Hdac3*-null bone marrow cells in the peripheral blood (Figure 42A). FACS analysis of the bone marrow 3 weeks after transplant showed that

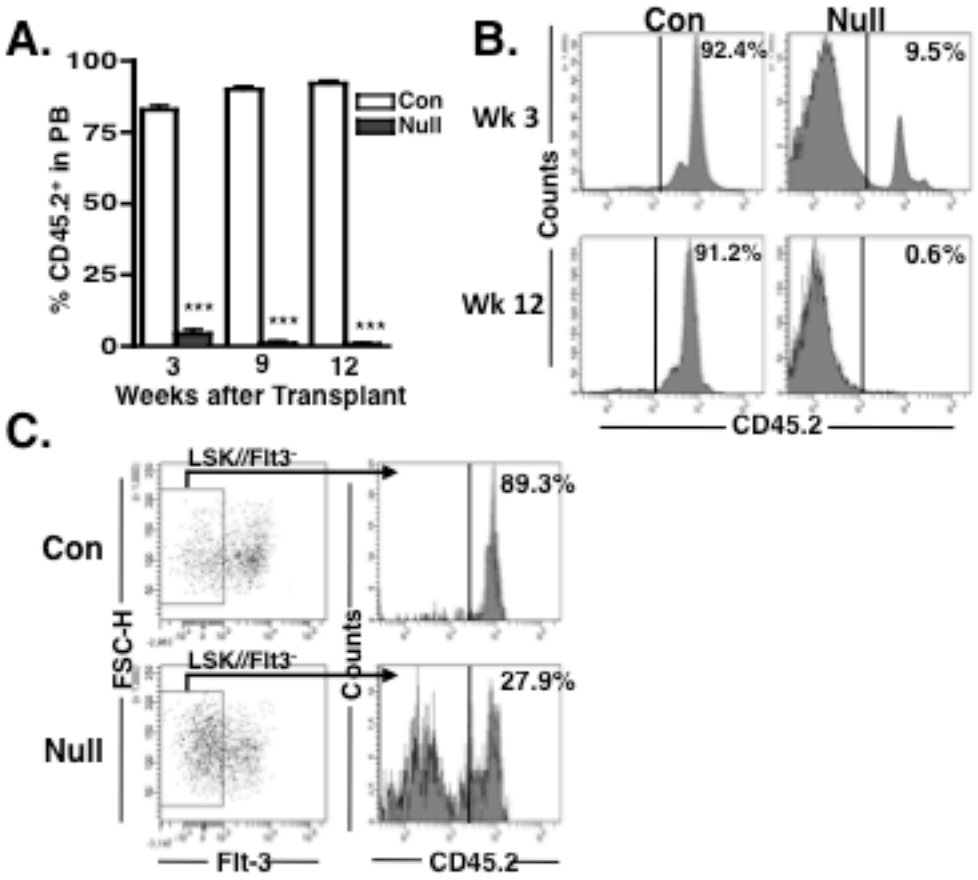

Figure 42. *Hdac3* is required for survival in a competitive bone marrow transplant. (A) Competitive repopulation assay where 90% control (filled bars) or *Hdac3*-null (empty bars) CD45.2$^+$ bone marrow cells were co-injected with 10% wild type CD45.1$^+$ cells. The contribution of each population to long-term reconstitution of the bone marrow was assessed by flow cytometry using anti-CD45.1 and anti-CD45.2 to enumerate cells in the peripheral blood. Data are expressed as mean ± SEM at different times after transplantation. An unpaired two-tailed *t* test indicated the difference at all weeks after transplant were statistically significant (***$p \leq 0.0001$; $n = 4$). (B) Flow cytometry analysis of whole bone marrow to determine the percentage of CD45.2 that had repopulated the bone marrow 3 or 12 weeks after a competitive repopulation assay. (C) Flow cytometry analysis of the LSK/Flt3$^-$ compartment to determine the percentage of CD45.2 that had repopulated this population 3 weeks after competitive bone marrow transplantation.

only about 10% of the cells were generated from *Hdac3*-null bone marrow cells (Figure 42B). Interestingly, when we looked at the number of LSK/Flt3$^-$ LT-HSCs that were CD45.2$^+$, the percentage was three times higher than the percentage in the total bone marrow (about 30% compared to 10%; Figure 42C). This data corresponds with the fact that the *Vav:Hdac3*$^{-/-}$ mice have an increased number of LSK/Flt3$^-$ cells but deficits in more mature cells. However, by 12 weeks after transplant, essentially all of the *Hdac3*$^{-/-}$ cells were out-competed by the 10% of wild type marrow (Fig. 42B). Thus, *Hdac3* is required for the function of stem and progenitor cells and is essential for the formation of lymphoid-primed progenitor cells that give rise to B and T cells.

Hdac3 is required for stem cell self-renewal.

Inactivation of *Hdac3* caused an accumulation of LSK/Flt3$^-$ stem cells (Summers et al, in prep.), yet these cells were dramatically ineffective at reconstituting hematopoiesis after bone marrow transplantation (Fig. 41D). Therefore, we injected *Vav:Hdac3*$^{-/-}$ and control mice with BrdU to assess the number of LSK/Flt3$^-$ stem cells that were in S phase. Remarkably, nearly twice as many stem cells were cycling in *Vav:Hdac3*$^{-/-}$ mice as in wild type control mice (Fig. 43A), suggesting that this population was actively cycling, rather than entering a quiescent state. This inappropriate cycling could be due to defects in progenitor cell proliferation (Fig. 41A), or it could be due to impaired stem cell self-renewal. However, because the *Vav:Hdac3*$^{-/-}$ stem cells were defective after transplant, we were unable to use this system to address this issue. Therefore, we used *in vitro* long-term culture of initiating cell (LTC-IC) assays to measure stem cell activity. Cultures of cells lacking *Hdac3* rapidly lost self-renewal

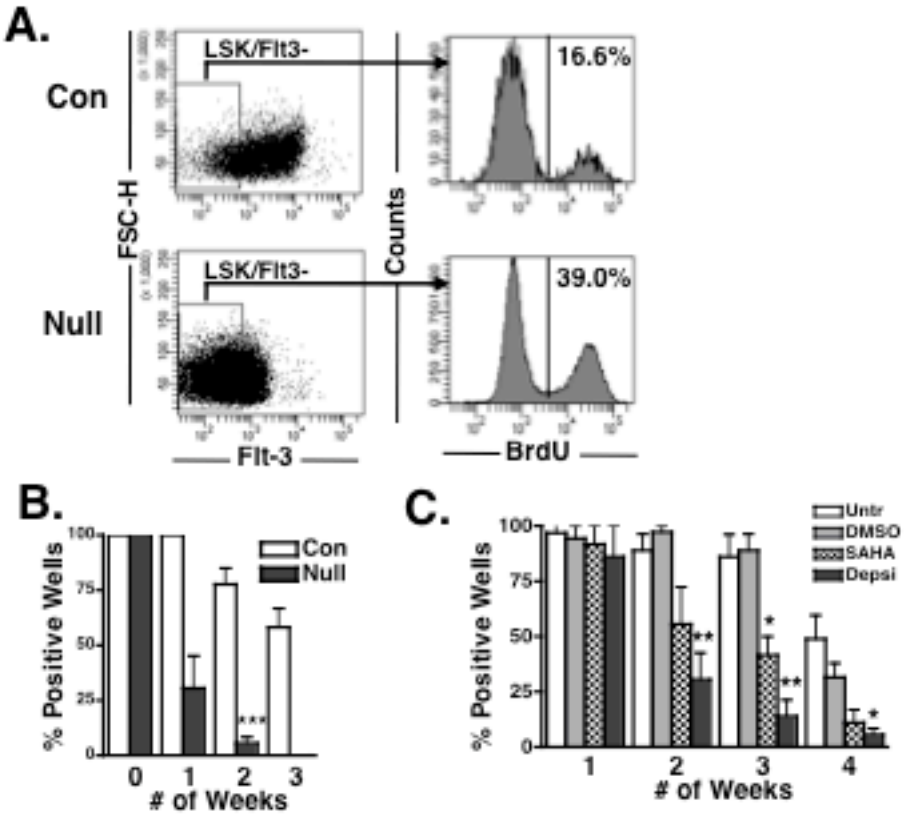

Figure 43. *Hdac3*-null stem cells are hyperproliferative leading to a loss of stem cell self-renewal. (A) Cell cycle status of LSK/Flt3$^-$ cells was analyzed using BrdU. Shown is a representative FACS plot from an experiment performed with 4 mice that is consistent with other biological replicates. (B) Graphical representation of the numbers of methylcellulose colonies formed at the indicated times from LTC-IC cultures of wild type (open bars) and *Hdac3*-null (full bars) bone marrow cells. Data are expressed as mean ± SEM. An unpaired two-tailed *t* test indicated the difference at week 2 after culture (marked with an *) was statistically significant ($p = 0.0008$; $n = 3$). Shown are representative results from two separate experiments. (B) Graphical representation of the numbers of methylcellulose colonies formed at the indicated times from LTC-IC cultures of wild type bone marrow cells treated with DMSO, SAHA, or Depsi for 48 hours before plating in the LTC-IC assay. Data are expressed as mean ± SEM. An unpaired two-tailed *t* test indicated the difference for SAHA (marked with an *) was statistically significant (Wk 3, $p = 0.0131$; $n = 3$), and the differences for Depsi at week 2, 3 and 4 weeks after culture (marked with an *) were statistically significant (Wk 2, $p = 0.0058$; Wk 3, $p = 0.002$; Wk 4, $p = 0.0192$; $n = 3$).

capacity, whereas control cells retained multi-lineage potential for multiple weeks (Fig. 43B). This defect in null stem cell function was similar to the effect of a 48 hr pre-treatment of control cultures with the histone deacetylase inhibitors SAHA (Vorinostat) or Depsipeptide, (Fig. 43C), suggesting that the defect could be related to precocious differentiation, impaired cell cycle progression, or both.

To further define the effect of *Hdac3* inactivation in stem cell functions, we cultured LSK/Flt3^{-} cells from *Vav:Hdac3*$^{-/-}$ mice on OP9 stromal cells with media containing IL6, SCF, and LIF. We noted a profound defect in the expansion of this population in culture, as compared to wild type control cells (Fig. 44A), which is consistent with the overall hypocellular bone marrow defect *in vivo* (Summers et al, in prep.). Likewise, the majority of these cells remained negative for lineage markers, suggesting a major defect in proliferation rather than precocious differentiation (Figure 44B). These data also suggest that the expansion of LSK cells *in vivo* (Summers et al, in prep.) is not a response to the lack of erythropoiesis, but that inactivation of *Hdac3* may impair stem cell differentiation. However, the cells that did differentiate in these cultures were primarily Gr1^{+}/Mac1^{+} or Mac1^{+} with a loss of the Gr1^{+} cells (Fig. 44B). This is similar to the effects observed when wild type LSK cells were treated with SAHA, which caused a skewing towards Mac1^{+} cells and few Gr1^{+} cells (Fig. 44C). Intriguingly, Depsipeptide, which is somewhat more selective for Hdac1 and Hdac2 over Hdac3, impaired proliferation, but did not cause the same type of skewing toward Mac1^{+} cells. Thus, Hdac3 may be a key target for the action of SAHA in hematopoietic malignancies by affecting stem cell action, proliferation, and myeloid differentiation.

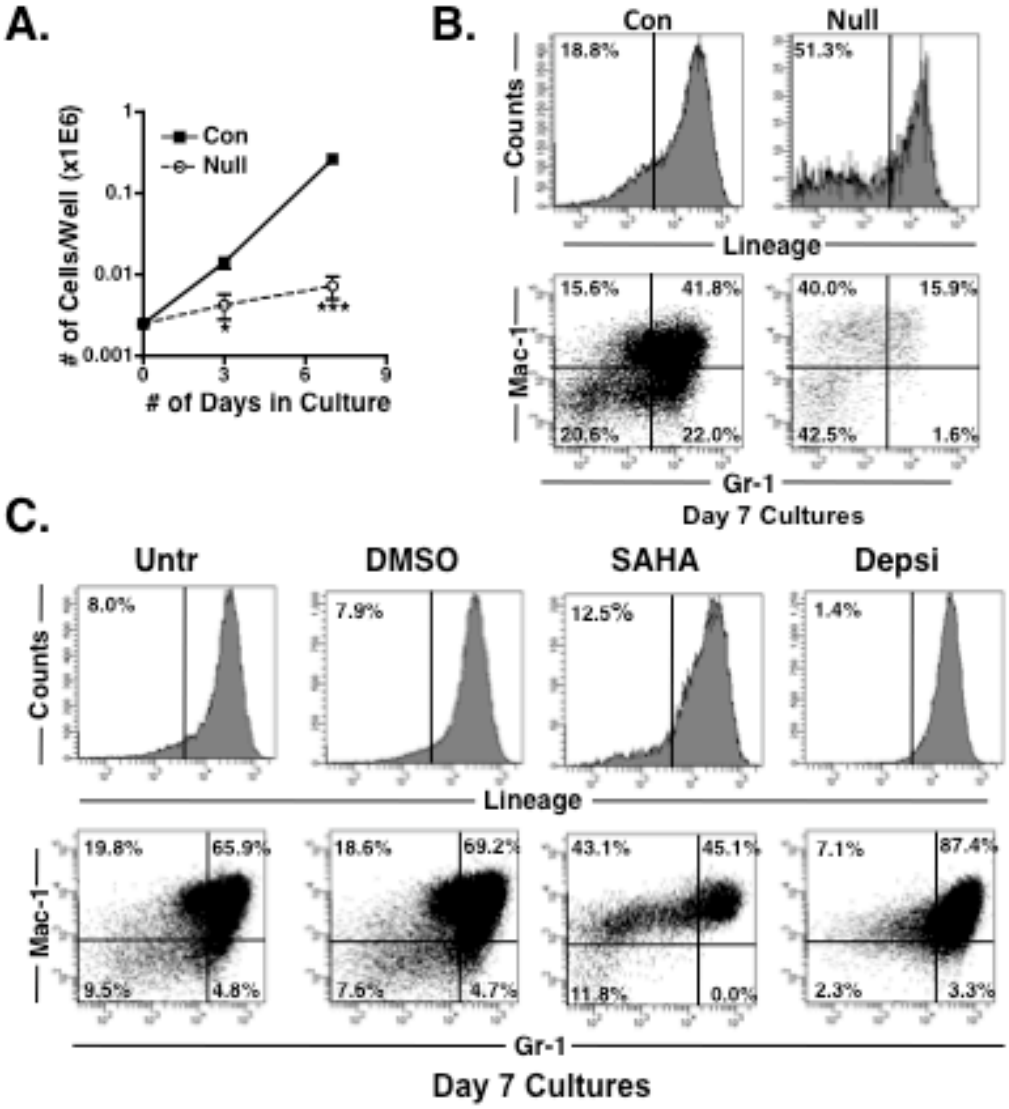

Figure 44. Inactivation of *Hdac3* impairs progenitor cell proliferation *in vitro* without causing differentiation while HDIs promote myeloid differentiation *in vitro*. (A) 2,500 wild type or *Hdac3*-null LSK/Flt3$^-$ bone marrow cells were cultured on an OP9-GFP stromal layer in IL6, SCF, and LIF and the proliferation in liquid culture was monitored by counting the total number of cells 3 to 7 days after harvesting the bone marrow cells. Data are expressed as mean ± SEM. An unpaired two-tailed *t* test indicated these differences were statistically significant (day 3, $p = 0.0256$; day 7, $p \leq 0.0001$; $n = 3$). (B) Flow cytometry analysis of day 7 cultures (from A) using a combination of anti-Cd3, anti-B220, anti-Gr1, anti-Mac1, and anti-Ter119 to distinguish mature cells from immature progenitor cells (top panel) or a combination of anti-Gr1 and anti-Mac1 to quantify myeloid cell differentiation (bottom panel). (C) Flow cytometry analysis of wild type LSK cells treated with DMSO, SAHA, or Depsi after 7 days in culture. Representative plots are shown using a combination of anti-Cd3, anti-B220, anti-Gr1, anti-Mac1, and anti-Ter119 to distinguish mature cells from immature progenitor cells (top panel) or a combination of anti-Gr1 and anti-Mac1 to quantify myeloid cell differentiation (bottom panel).

Discussion

In order for stem cells to repopulate the bone marrow they must yield progeny that can undergo massive proliferation and at the same time self renew to maintain the stem cell pool. In bone marrow transplantation assays, in CFU-S assays, and *in vitro*, *Hdac3* was essential for the proliferation of stem and multi-potential progenitor cells and the production of mature erythroid cells that are needed for mice to thrive (Figures 41, 42 and 43). Remarkably, these mice survived even though nearly 40% of their LSK/Flt3$^-$ stem cells were in S phase (Figure 43). This failure of the stem cells to self-renew and quiesce and to continue to cycle is a harbinger of major stem cell defects, which were observed in bone marrow transplantation assays and LTC-IC assays (Figure 42 and 43). Importantly, competitive bone marrow reconstitution assays demonstrated a dramatic loss of *Hdac3*-null stem cell functions in the presence of complementing wild type progenitor cells (Figure 42). The combination of these data suggests that *Hdac3* is required for cell intrinsic stem cell functions, which might be attributed to cell cycle defects when the HSC enters the cell cycle.

Given how similar the defects are between the loss of *Mtg16* and *Hdac3*, this suggests that *Hdac3* is likely one of the main interacting proteins that drives *Mtg16* functions in HSCs. However, the fact that the phenotypes are much more severe in the absence of *Hdac3* implies that other factors must be able to partially compensate for the loss of *Mtg16*. Our data also hint at how inhibiting Hdac3 may be beneficial for the treatment of hematopoietic malignancies. By inhibiting the earliest lymphoid progenitor cell it would be expected that inhibition of Hdac3 would impair any stem-like tumor initiating cells within lymphoma, and cutaneous T cell lymphoma is responsive to SAHA

[172]. Moreover, by affecting stem cell self-renewal, inhibition of Hdac3 might represent a targeted therapy towards myeloid leukemia, especially those that show characteristics of immature myeloid progenitor cells (e.g., M0, M1, and M2). Finally, for those cells that escaped the proliferation defects and matured into myeloid progenitor cells, these cells preferentially differentiated into $Mac1^{+}$ cells. Thus, Hdac3 selective inhibitors may be useful in myeloid leukemia as both anti-proliferative agents and as differentiation agents.

CHAPTER VII

SUMMARY AND FUTURE DIRECTIONS

The myeloid translocation gene proteins have been defined as transcriptional corepressors, particularly through interactions with NCoR/SMRT, mSin3A/3B, and histone deacetylases. As expected for transcriptional corepressors, MTG family members are recruited by many site-specific DNA binding proteins, including Gfi1, Gfi1B, TAL1/SCL, the "E proteins" E2A and HEB, BTB-POZ domain factors BCL6 and PLZF, and mediators of Wnt and Notch signaling (TCF4 and CSL) [42-50]. Given the breadth of cellular functions these transcription factors are known to regulate, it is not surprising that MTG family members have been linked to stem cell functions and the development of cancers in various tissues [3-5]. However, the cellular consequences of their corepressor functions must be defined to further delineate how disruption of the MTG proteins leads to cancer. Since two MTG family members, MTG8 and MTG16, are targeted by chromosomal translocations in AML, the t(8;21) and t(16;21) respectively, and many of the transcription factors the MTG family bind regulate hematopoietic stem and progenitor cell function, it is assumed that this family must play an important role in hematopoiesis. Knockout mouse models of *Mtg8* and *Mtgr1* show defects in the gut, where both genes are highly expressed; however, they have yet to show any defects in the hematopoietic compartment [56, 103]. Since MTG16 is the most highly expressed family member in the hematopoietic compartment, *Mtg16*-deficient mice were generated to determine if this family member was an important regulator of hematopoiesis (Figure 9).

Since Mtg16 binds transcription factors that are involved in almost every stage of hematopoiesis [44-48, 50, 147], a comprehensive look at all lineages was performed, and we initially any overt defects caused by deletion of *Mtg16*, as discussed in Chapter 3. Upon gross examination of the mice, they appeared normal without a complete block in the development of any mature hematopoietic lineage; however, there were significant changes in various compartments, such as reductions in lymphoid and erythroid cells and increases in myeloid cells (Figure 11), which stemmed from each of their corresponding progenitor populations. Strikingly, these skewed lineage allocations were even more pronounced after the bone marrow system was stressed. In addition to skewed lineage allocation, *Mtg16*-null progenitor cells were also impaired in their ability to rapidly proliferate in response to stress, as shown by the absence of colonies in the CFU-S assay, which could be rescued by the over expression of *c-myc* (Figure 21).

Given that two of the DNA binding factors that recruit MTG family members, Gfi1b and TAL1/Scl, are required for erythropoiesis, as shown by the fact that deletion of either of these transcription factors results in embryonic lethality due to defective erythropoiesis [72, 127, 128], we set out to characterize the effects loss of *Mtg16* had on erythropoiesis as well. Although there was only a slight reduction in red blood cells under homeostasis, the erythroid progenitors were defective in responding to any kind of stimulus that required them to rapidly make more erythroid cells, as shown in erythroid-specific methylcellulose assays (in response to EPO alone), PHZ treatment (a hemolytic agent), or CFU-S assays (Figures 11, 13, and 20). The PHZ treatment resulted in death of the *Mtg16*-null mice due to acute anemia, which appeared to be caused by a failure of erythropoietic expansion in the spleen. This proliferation defect of the MEPs was further

emphasized in the methylcellulose and CFU-S assays, in that the *Mtg16*-null bone marrow cells were completely unable to generate any colonies in either of those assays. Although some of these erythroid defects must stem from aberrant transcriptional activity of Scl or Gfi1b in the absence of *Mtg16*, another explanation for the lack of erythroid expansion is the drastic reduction of expression in the erythropoietin receptor (EpoR) in the LSK population (>6-10 fold reduction, Figure 30). It is well documented that erythropoietin (EPO) is an important cytokine for basal and stress erythropoiesis, and that its level increases up to 1000-fold during stress situations [173]. Therefore, stress erythropoiesis requires considerably higher expression of EpoR than is necessary to maintain basal erythropoiesis. This is further exemplified by the fact that mice that express only one *EpoR* have a normal basal hematocrit, but are deficient in their response to stress. In light of this, *Mtg16*-null mice express sufficient EpoR to generate red blood cells under homeostasis, albeit at reduced amounts; however, the decreased level of expression of EpoR is not enough to mount the proper response during stress erythropoiesis.

In addition to the exacerbated defects in erythropoiesis in response to stress, the skewing from lymphoid lineages toward granulocyte/monocyte lineages was amplified in stress conditions as well. Other work from our lab has shown that T-cell development is greatly impaired in the absence of *Mtg16* in the context of an OP9-delta-like1 (DL1) assay, which is a stromal cell line that overexpresses the DL1 ligand of the Notch signaling cascade. In this assay, sorted BM cells are grown in IL7 and Flt3L with the constitutive Notch signal, which drives T-cell development *in vitro* within 3 weeks of culture. However, *Mtg16*-null cells are incapable of making T-cells in this assay, but

showed an increase in production of Gr-1^{+}/Mac-1^{+} cells, even in the presence of the lymphoid signals [61]. This skewing toward myelopoiesis and away from lymphopoiesis was especially evident after competitive bone marrow transplantation. After a competitive transplant, there was drastic reduction in total reconstitution from the *Mtg16*-null cells. However, the cells that did manage to survive were mostly comprised of granulocytes and monocytes, while T and B cells were almost non-existent after transplantation (Figures 23-24; Hunt et al., unpublished data; [61]). Mechanistically, this altered lineage allocation when *Mtg16* is deleted is best explained by changes in gene expression patterns due to the loss of repressive transcription on the hematopoietic regulators that normally interact with MTGs. Indeed, the T-cell defect could be reconstituted in the OP9-DL1 assay by retroviral expression of *Mtg16*; however, two mutants that disrupted Notch or E-protein (E2A, HEB) interactions with Mtg16 abrogated this reconstitution [61]. Overall, both during homeostasis, and more dramatically after stress, the loss of *Mtg16* shows a similar phenotype, namely enhanced myelopoiesis, as compared to that caused by the expression of AML1-ETO.

In addition to the lack of response to cytokine signaling and altered lineage skewing caused by gene expression changes, *Mtg16*-null cells also display cell proliferation problems, which appear to be cell type dependent. It is important to note that almost all of the progenitor cell populations have impaired proliferation. For example, the MEPs and ST-HSCs/MPPs could not proliferate in the CFU-S assay and required the expression of *c-Myc* to form colonies. Similarly, when B cell progenitors are grown in methylcellulose with IL7, they are able to form colonies, but they are fewer in number and much smaller in size, also suggesting a proliferation defect (Hunt et al. in

prep.). In addition, *MTG8*-null MEFs grow much more slowly than WT MEFs *in vitro* (DeBusk et al. in prep.). This is especially interesting because the AML1-ETO fusion protein also impairs proliferation. In contrast to the impaired proliferation in progenitor populations, our analysis of the stem cells in Chapter 4, showed that LT-HSCs were actually hyperproliferative, as shown by increased BrdU incorporation. This increased cycling of the stem cells caused a loss of self-renewal, which ultimately led to stem cell exhaustion, as shown by their inability to perform in a secondary transplant. We found that *E2F2*, a transcription factor that regulates the cell cycle, was up regulated in *Mtg16*$^{-/-}$ LSK cells. In addition, Mtg16 robustly associated with an enhancer-like sequence in the first intron of *E2F2*, suggesting that *E2F2* is a direct target for Mtg16-mediated repression. The increased cycling in the HSCs was similar to the inappropriate cycling of the stem/progenitor cells in the crypts of the small intestine in *Mtgr1*$^{-/-}$ mice after treatment with DSS [57]. Thus, the effect on proliferation changes that are evident in the absence of *Mtg16* appears to be different between stem and progenitor cell populations. However, it must be noted that the increase in BrdU in the HSCs does not necessarily mean they do not have problems going through the cell cycle, it simply shows that more cells have entered into S phase. This might be more evident in the HSC population simply because the stem cells are normally quiescent and not cycling, therefore any increase in cycling would be more noticeable as compared to the context of the progenitors that are required to rapidly proliferate to keep up with the high demand for new blood cells. In fact, impaired progression through the cell cycle could also explain the loss of HSC self-renewal in the LTC-IC and CRAs. Thus, more work must

be done to delineate exactly how the proliferation defects affect the *Mtg16*-null HSC loss of self-renewal.

Given that genotoxic stress is closely associated with hematopoietic failure syndromes, we tested whether the loss of *Mtg16* caused genotoxic stress [154, 157]. Indeed, we observed a slight increase in DNA double-strand breaks (as indicated by γH2AX foci) in lineage-negative cells, and this DNA damage increased with age (Figure 36). Further analysis with FACS purified stem and progenitor cells showed very low levels of γH2AX foci in the HSCs, but the *Mtg16*-null myeloid progenitor cells displayed higher levels of DNA damage (Figure 38). More importantly, we also showed that when wild type lineage negative cells are exposed to low doses of IR *in vitro*, they have similar proliferation kinetics to *Mtg16*-null cells and also display premature differentiation (Figure 40), which led to a loss of HSC self-renewal (Figure 39). These data suggest that DNA damage may underlie the proliferative defects observed in *Mtg16*-deficient progenitor cells and suggest that cell cycle progression is required for this DNA damage. Similarly, *MTG8*-null MEFs also display increased DNA damage when compared to WT MEFs (DeBusk et al. in prep.), which suggests that MTG family members contribute to genomic stability in a variety of cell types. If these proteins have a fundamental role in the maintenance of genome stability, this could explain why the MTG family members are frequently mutated in various types of cancer. However, much more work is needed to determine the mechanism by which loss of *Mtg16* causes genomic instability. One such mechanism to test would be to determine if *Mtg16*-null HSCs contain higher levels of reactive oxygen species (ROS), as ROS have been linked to genomic instability and a

knockout mouse model of *FoxO1/3a/4*$^{-/-}$ has elevated ROS and displays a very similar phenotype as the *Mtg16*-null mouse [156].

Another possible mechanism to be explored is whether Mtg16 involves DNA damage pathway proteins for its regulation of genomic stability. Given that the effect of a low dose of IR on the wild type cells *in vitro* required p53 (Figure 40C), this protein and p21, one of its major effector proteins, would be likely candidates of action for Mtg16 function. These proteins are also both involved in cell cycle regulation and have been shown to be required for HSC functions [153, 174]. To test if these proteins had an impact on Mtg16 hematopoietic stem and progenitor cell functions, we crossed our *Mtg16*-null mice with *p21*-null or *p53*-null mice and determined the effect that deletion of either of those genes had on the hematopoietic compartment of *Mtg16*-null mice. In context of the deletion of p21, there did not appear to be any changes in myeloid progenitor cell numbers as assessed by methylcellulose containing IL6, IL3, SCF, and EPO assays or by FACS analysis (Figure 45A and data not shown). Similarly, the loss of *p21* did not restore erythroid progenitor cell functions as shown by the absence of BFU-E colonies from the *Mtg16*-null/*p21*-null cells in methylcellulose assays containing EPO or by the CFU-S_{12} assay (Figure 45B, C). This was a bit surprising considering the *Mtg16*-null MEP microarray showed an up-regulation of p21, but this might highlight the importance that loss of EPOR has on the erythroid cell functions. Finally, we tested the function of the long-term stem cells in a competitive repopulation assay and again no difference between the *Mtg16*-null bone marrow and the *Mtg16*-null/*p21*-null bone marrow was observed (Figure 45D). Taken together, these data show that the loss of *p21*

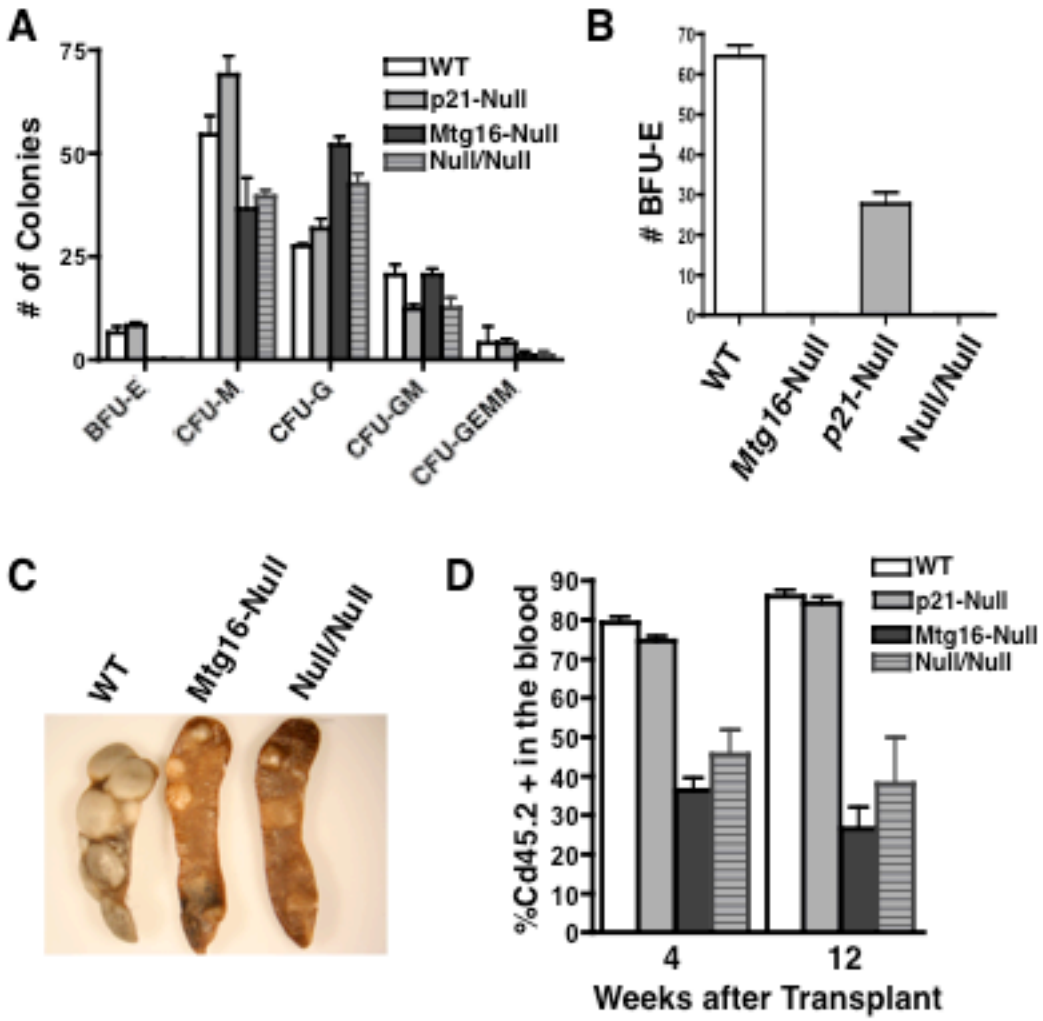

Figure 45. Loss of *p21* does not restore hematopoietic progenitor and stem cell functions in *Mtg16*-null mice. Bone marrow (2.5×10^4) cells were plated in methylcellulose containing IL-3, IL-6, Epo, and SCF and colonies were quantified after 8-10 days in culture. Quantification of each of the colony type (E, BFU-E; M, CFU-M; G, CFU-G; GM, CFU-GM; GEMM, CFU-GEMM) are shown in (A). (B) Bone marrow (5×10^5) cells were plated in methylcellulose containing EPO and colonies (BFU-E) were quantified after 14 days in culture. (C) CFU-S_{12} were obtained for wild type, *Mtg16*-null, and *Mtg16*-null/*p21*-null bone marrow. D) Competitive repopulation assay where 90% test CD45.2$^+$ bone marrow cells of each genotype were co-injected with 10% wild type CD45.1$^+$ cells. The contribution CD45.2$^+$ cells in the peripheral blood was assessed. Data are expressed as mean ± SEM at different times after transplantation.

does not have an effect, either positively or negatively, on the defects that are seen in the absence of *Mtg16*.

Though the loss of *p21* in the context of the *Mtg16*-null did not appear to have an effect on hematopoiesis, it is still important to determine the effects of the loss of *p53* since p53 has so many different functions independent of p21. Though these results are very preliminary, it does not appear that the loss of *p53* has any major effect on myeloid progenitor cell functions by flow cytometry, methylcellulose assays, or CFU-S assays (data not shown). However, in contrast to the loss of *p21*, the *Mtg16*-null/*p53*-null cells appear to have restored B cell progenitor function. As previously mentioned, *Mtg16*-null B cell progenitors are defective in their ability to grow in methylcellulose with IL7, as shown by fewer numbers of colonies that are much smaller in size (Hunt et al. in prep.; and Figure 47A, B). The defect in B cell progenitors is even more pronounced after bone marrow transplantation, where in contrast to increased $Gr1^+/Mac1^+$ cell production after transplant, the Mtg16-null B cell progenitors are almost incapable of producing mature $B220^+$ cells after transplant (Figure 46), showing that *Mtg16* is definitively required for B cell progenitor function. Thus, we looked at the ability of *Mtg16*-null B cell progenitors to form B cell colonies in *in vitro* methylcellulose assays containing IL7. Strikingly, the loss of *p53* was able to restore both total B cell colony numbers and the size of the colonies as shown by the increase in total cell number (Figure 47A, B). The loss of colony number and size in Mtg16-null cells is in part due to an increase in apoptosis as shown by an increase in Annexin V^+ cells; however, the loss of *p53* decreased the amount of apoptosis, which is likely contributing to the restoration of colony number and size in the *Mtg16*-null/*p53*-null cells (Figure 47C, D). Preliminary results have shown that the

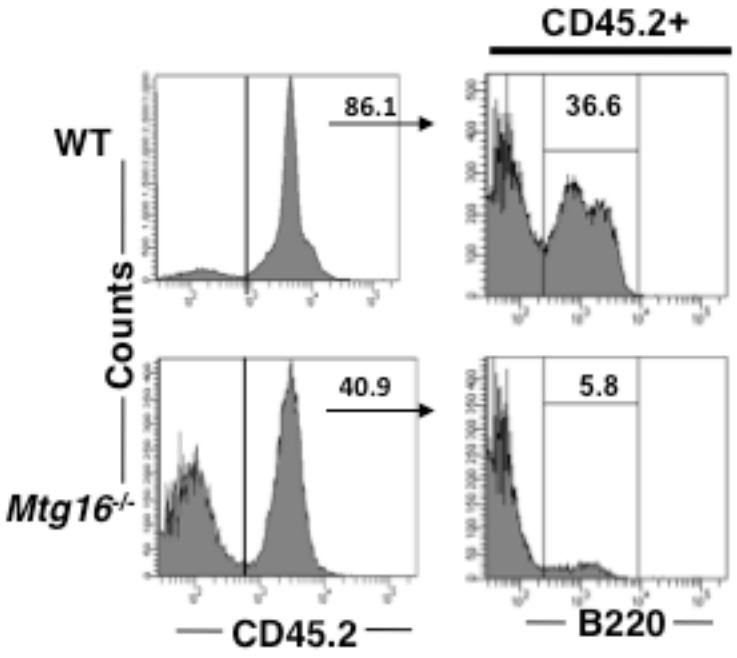

Figure 46. Inactivation of Mtg16 leads to decreased B220⁺ cell production after competitive bone marrow transplantation. Flow cytometry analysis of CD45.2 cells that were B220⁺ 12 weeks after a competitive repopulation assay. Shown is a representative plot from an experiment performed in triplicate that is consistent with other biological replicates.

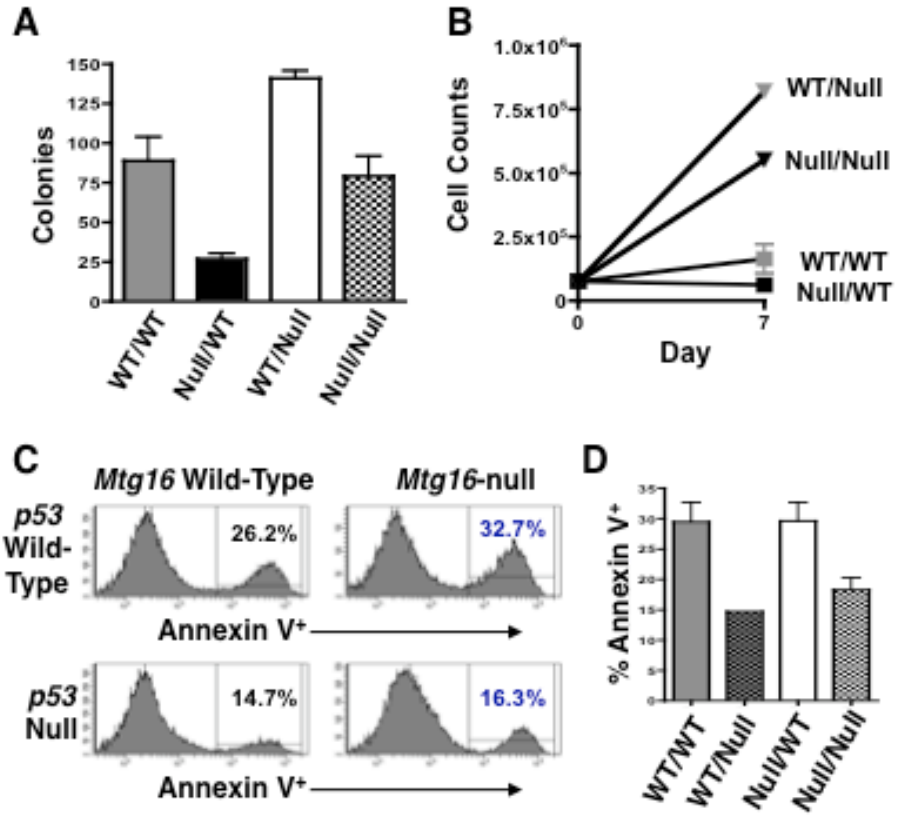

Figure 47. Loss of *p53* in *Mtg16*-null cells restores B cell formation *in vitro* through inhibiting apoptosis. (A) Bone marrow (7.5×10^4) cells were plated in methylcellulose containing IL-7 and colonies (CFU-pre-B) were quantified after 7 days in culture. (B) Quantification of the total number of cells that were counted after harvesting the plates from (A). (C) Flow cytometry plots showing the amount of Annexin V+ cells after 7 days in culture, which is quantified in (D). The genotypes displayed are in reference to *Mtg16/p53* status, respectively.

Mtg16-null BFU-E cells have an increased amount of γH2AX DNA damage foci, which could be triggering the apoptotic pathway through p53. This would explain why apoptosis is not activated in the absence of *p53*. However, experiments assessing the number of γH2AX DNA damage foci need to be performed before any conclusion can be made about how p53 is regulating Mtg16 function. In addition, experiments need to be performed to determine if the loss of *p53* will inhibit Mtg16-null premature differentiation in the *in vitro* cultures, and thereby possibly restore HSC self-renewal in the LTC-IC assay. Though it is exciting to think the loss of *p53* may be able to restore some of the *Mtg16*-null defects, much more work needs to be done to ensure the deletion of *p53* does not have an effect on other cell functions, and that the complementation seen in the BFU-E cells is not simply due to a generalized effect of inhibiting apoptosis. Also, the Mtg16/p53 mice provide a useful model system to test whether the loss of *Mtg16* might contribute to tumor formation. Since the *p53*-null mice succumb to various tumors (most commonly T cell lymphomas) [175], we can assess if the *p53*-null or *p53*-het mice get tumors at a different rate or different types of tumors when *Mtg16* is deleted. Altogether, the analysis of the effect of the loss of *p53* on Mtg16 functions will give us valuable insight on the mechanism by which Mtg16 is functioning in various cells.

Aside from DNA damage, another mechanism of action to be explored is the role of Mtg16 in transcriptional elongation. MTG16 was recently found in a proteomic screen to be in a complex with Tif1γ, which is required for transcriptional elongation, so it is plausible that Mtg16 is also involved in this process [149]. This concept is intriguing because Mixed Lineage Leukemia (MLL), one of the other four most common genes

involved in chromosomal translocations in AML [8], is also required for transcriptional elongation. In fact, we have data in our lab that shows that Mtg16 and MLL interact (DeBusk et al. in prep.). Linkage of both of these proteins to transcriptional elongation is important because it suggests that despite the variation in gene expression of the AML-associated fusion proteins, they might all converge on similar pathways to transform myeloid cells. Although this has yet to be proven, this is an attractive hypothesis with respect to therapeutic treatment of AMLs.

Overall, deletion of *Mtg16* in a murine model resulted in numerous hematopoietic defects, such as altered lineage cell fate decisions, proliferation defects of various hematopoietic cells, and ultimately, loss of functional integrity of the HSCs. It is clear from the data that the requirement for Mtg16 is different between homeostasis and stress conditions. For example, under homeostasis, there is a reduction in HSCs, but they are capable of forming all lineages of the blood (Figure 48A). Though all lineages are formed, there are consistent reductions in lymphopoiesis (both B and T cells), and erythroid cells, with a generalized skewing towards the granulocyte/monocyte lineages. Even with these alterations in lineage allocation, the mice appear normal with no apparent complications during aging. Though these results imply a modest role for Mtg16 in hematopoiesis, the severe hematopoietic defects and failure that occur during stress conditions highlights the important roles Mtg16 plays in maintaining hematopoiesis. In contrast to homeostatic conditions, *Mtg16*-null cells almost completely fail to make T, B, or erythroid cells during stress hematopoiesis (Figure 48B). Interestingly, the Mtg16-null cells retain the ability to make granulocyte/monocyte cells even under stress conditions. However, the loss of Mtg16 in the stem cells greatly

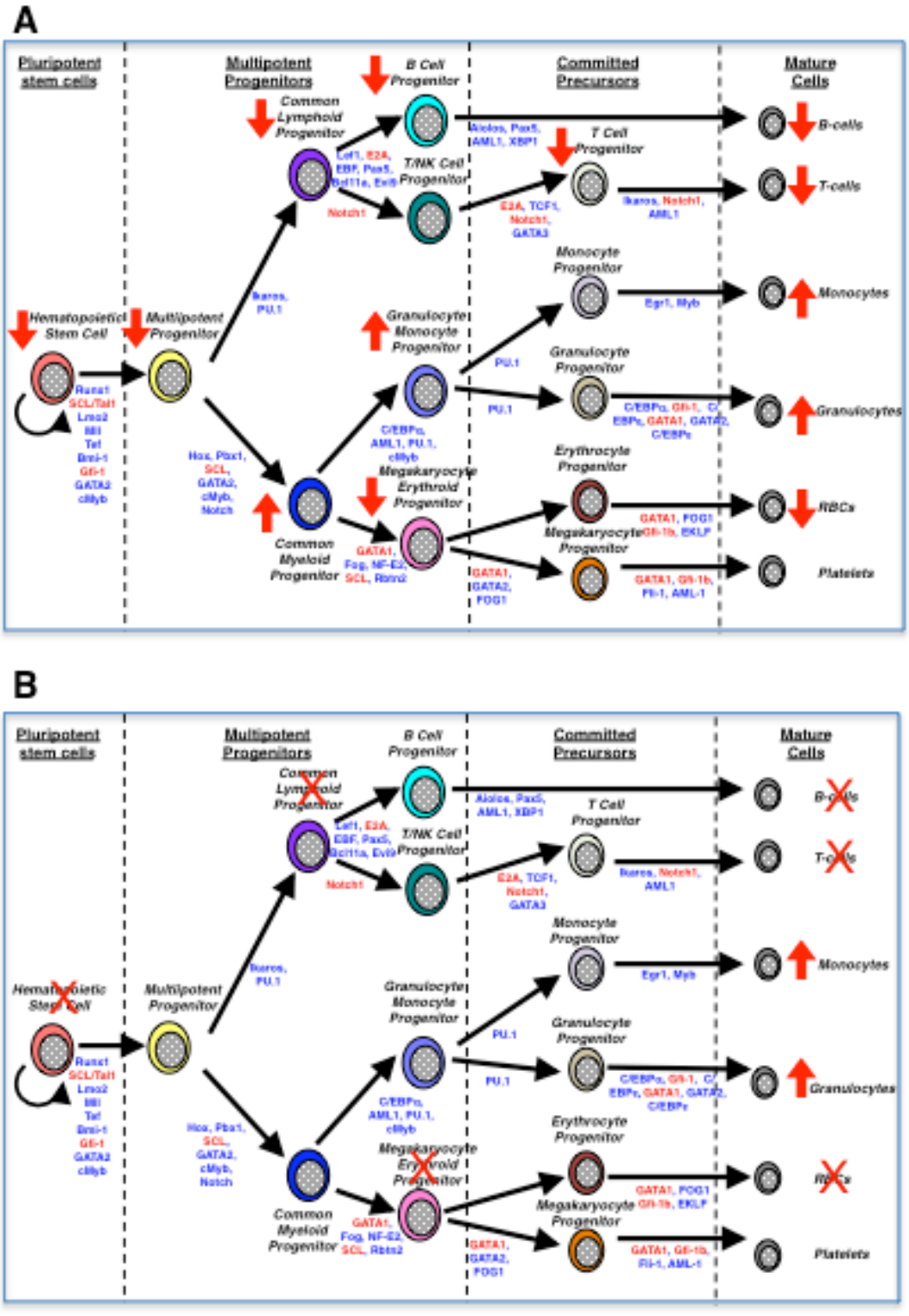
A
Pluripotent stem cells
Multipotent Progenitors
B Cell Progenitor
Committed Precursors
Mature Cells
Common Lymphoid Progenitor
T Cell Progenitor
T/NK Cell Progenitor
B-cells
T-cells
Monocyte Progenitor
Monocytes
Granulocyte Monocyte Progenitor
Granulocyte Progenitor
Granulocytes
Hematopoietic Stem Cell
Multipotent Progenitor
Erythrocyte Progenitor
RBCs
Megakaryocyte Erythroid Progenitor
Common Myeloid Progenitor
Megakaryocyte Progenitor
Platelets
B
Pluripotent stem cells
Multipotent Progenitors
B Cell Progenitor
Committed Precursors
Mature Cells
Common Lymphoid Progenitor
T Cell Progenitor
T/NK Cell Progenitor
Monocyte Progenitor
Monocytes
Granulocyte Monocyte Progenitor
Granulocyte Progenitor
Granulocytes
Hematopoietic Stem Cell
Multipotent Progenitor
Erythrocyte Progenitor
Megakaryocyte Erythroid Progenitor
Common Myeloid Progenitor
Megakaryocyte Progenitor
Platelets

Figure 48. Mtg16 regulates hematopoietic stem cell functions and cell fate decisions during homeostasis and under stress conditions. Schematic diagram showing the hematopoietic defects observed in mice with deletion of *Mtg16* under homeostasis (A) and stress conditions (B). (A) Under homeostasis, there are consistent reductions in the HSC, T, B, and erythroid compartments, but all lineages are present, with an enhanced generation of granulocyte/ monocyte cells. The HSCs are less quiescent and the progenitors have defects in proliferation, but overall, the mice survive normally with no apparent defects during aging. (B) Under stress conditions, the defects that are found during homeostasis, are greatly exaggerated with severe defects in lymphopoiesis and erythropoiesis. While the production of granulocytes/monocytes is initially retained, the HSCs eventually lose their self-renewal potential and exhaust resulting in complete bone marrow failure.

impairs their self-renewal capacity through exhaustive replication of the HSC compartment, which ultimately leads to bone marrow failure of all lineages in a secondary transplant (Figure 48B). Also, the fact that the HSC, lymphoid, and erythroid compartments are the compartments most affected by the loss of Mtg16 implies that Scl/Tal1, E proteins, Gfi1, GATA1, and Notch interaction with Mtg16 is critically required for their function in controlling these lineage decisions. One hypothesis to explain the differences between homeostasis and acute conditions is that the homologous family member, MtgR1, can compensate some of the function of Mtg16. Though MtgR1 is expressed at lower levels than Mtg16 in the bone marrow, the amount may be sufficient to help some of the cells get through their proliferation defects under homeostasis where there is not a great demand. However, this level of MtgR1 expression might not be enough to compensate for the loss of *Mtg16* under stress conditions when there is a much higher demand for hematopoietic production. In concordance with possible complementation by MtgR1, *Mtg16/MtgR1* double knockout mice display embryonic lethality at approximately day e14, however the cause of this embryonic lethality needs to be further defined to determine if this is due to impaired hematopoiesis. To circumvent the embryonic lethality, a conditional deletion of *Mtg16* could be generated so that when crossed with an *MtgR1*-null mouse, *Mtg16* could be specifically deleted after adult hematopoiesis is established. This model could then be used to determine if the combined loss of *Mtg16* and *MtgR1* displays defects that are similar to normal *Mtg16*-null mice or if they are much more severe, which would imply there is compensation between family members. In addition, the striking similarities between the deletion of *Mtg16* and *Hdac3* (Chapter 6), or of the various transcription factors that bind

Mtg16, imply the requirement of each of these complex proteins for proper hematopoietic regulation. Taken together, these phenotypes seen during homeostasis and stress conditions suggest that Mtg16 is indeed a master regulator of hematopoiesis (Figure 48).

Our work may also provide a mechanism for the role of MTG/ETO factors in leukemogenesis. In general, the t(8;21) is viewed as a relatively weak oncogene, as various human studies have suggested that patients can carry this translocation for several years before developing AML [151]. However, the fact that the oligomerization domain, which also binds to endogenous Mtg16/Eto2 and Mtgr1, is essential to the transforming ability of the t(8;21) fusion protein in mouse models supports the importance of the endogenous functions of these proteins for the formation of leukemia [39-41]. Therefore, it is possible that binding of the AML1-ETO fusion protein to Mtg16 impairs the action of Mtg16 and causes the HSC to enter the cell cycle. While the fusion protein can directly repress the expression of tumor suppressors, it also induces a DNA damage gene signature [24-26, 152, 169, 170]. Additionally, expression of the fusion protein *in vitro* increased DNA damage and sensitized the cells to DNA damaging agents [169, 170]. These data suggest that the t(8;21) could promote immortalization of hematopoietic stem and progenitor cells by repressing tumor suppressor genes, while triggering proliferation by activating genes such as *E2F2* and promoting a modest level of DNA damage that increases the mutation rate resulting in the development of leukemia after the accumulation of a '2nd hit'(Figure 49).

Ultimately, the work presented in this dissertation has provided valuable insight into the normal function of Mtg16 in hematopoiesis, and described potential mechanisms in which disruption of this gene could lead to development of leukemia by the AML1-

ETO fusion protein. Moreover, the MTG family members are highly homologous and interact with similar binding partners. Thus, this knowledge can be used to help decipher a common mechanism for MTG disruption to cause cancer in various tissue types.

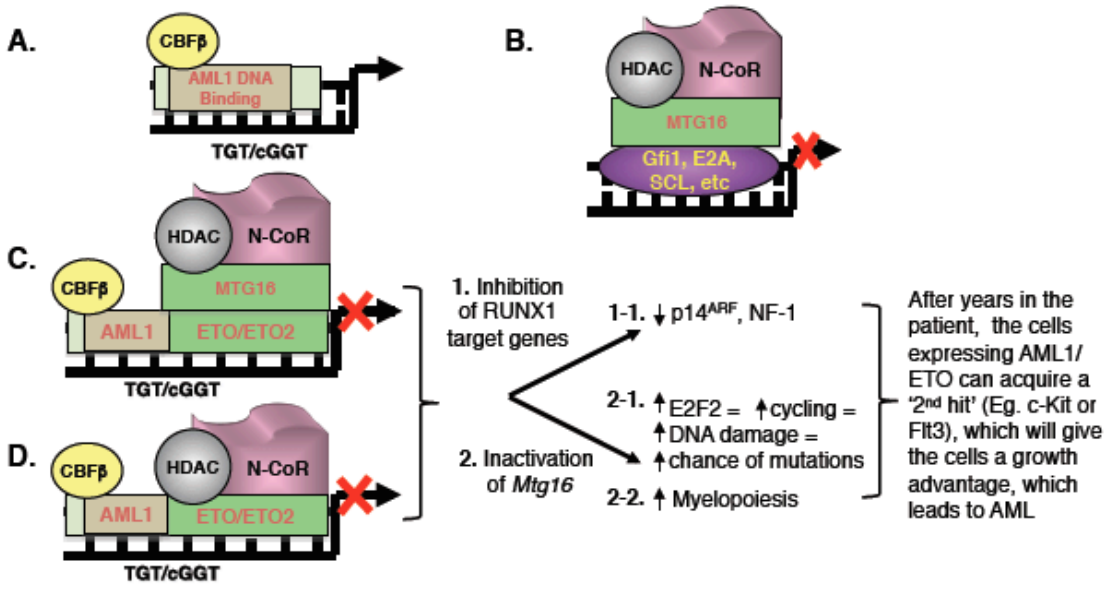

Figure 49. Model for how AML1/ETO can cause leukemia by disrupting *Mtg16* functions. A. AML1 DNA binding is enhanced by CBFβ and activates transcription of the genes it binds. B. Mtg16 interacts with various transcription factors and recruits co-repressors to repress transcription. The AML1/ETO fusion protein can disrupt *Mtg16* function by (C) its ability to bind endogenous *Mtg16* and recruit it away from its normal binding partners, or (D) recruiting away its cofactors so that the endogenous *Mtg16* will not be able to link co-repressors to the TF it binds. This in turn can lead to leukemia in two ways, (1) inhibiting RUNX1 targets such as the tumor suppressor genes $p14^{ARF}$ and NF-1 (1-1), and (2) inactivating *Mtg16*, which causes increased cell cycling and therefore the chance of acquiring additional mutations (2-1) and enhanced myelopoiesis (2-2). Thus, over time, the cell can acquire a 2^{nd} hit and cause AML in the patient. AML, acute myeloid leukemia; TF, transcription factor.

REFERENCES

1. Hope, K.J., L. Jin, and J.E. Dick, *Human acute myeloid leukemia stem cells.* Arch Med Res, 2003. **34**(6): p. 507-14.

2. Rowley, J.D., *The role of chromosome translocations in leukemogenesis.* Semin Hematol, 1999. **36**(4 Suppl 7): p. 59-72.

3. Sjoblom, T., et al., *The consensus coding sequences of human breast and colorectal cancers.* Science, 2006. **314**(5797): p. 268-74.

4. Kochetkova, M., et al., *CBFA2T3 (MTG16) is a putative breast tumor suppressor gene from the breast cancer loss of heterozygosity region at 16q24.3.* Cancer Res, 2002. **62**(16): p. 4599-604.

5. Kan, Z., et al., *Diverse somatic mutation patterns and pathway alterations in human cancers.* Nature, 2010. **466**(7308): p. 869-73.

6. Lowenberg, B., J.R. Downing, and A. Burnett, *Acute myeloid leukemia.* N Engl J Med, 1999. **341**(14): p. 1051-62.

7. Muller, A.M., et al., *Complementing mutations in core binding factor leukemias: from mouse models to clinical applications.* Oncogene, 2008. **27**(44): p. 5759-73.

8. Martens, J.H. and H.G. Stunnenberg, *The molecular signature of oncofusion proteins in acute myeloid leukemia.* FEBS Lett, 2010. **584**(12): p. 2662-9.

9. Meyers, S., J.R. Downing, and S.W. Hiebert, *Identification of AML-1 and the (8;21) translocation protein (AML-1/ETO) as sequence-specific DNA-binding proteins: the runt homology domain is required for DNA binding and protein-protein interactions.* Molecular & Cellular Biology, 1993. **13**(10): p. 6336-45.

10. Davis, J.N., L. McGhee, and S. Meyers, *The ETO (MTG8) gene family.* Gene, 2003. **303**: p. 1-10.

11. Davis, J.N., et al., *ETO-2, a new member of the ETO-family of nuclear proteins.* Oncogene, 1999. **18**(6): p. 1375-83.

12. Gelmetti, V., et al., *Aberrant recruitment of the nuclear receptor corepressor-histone deacetylase complex by the acute myeloid leukemia fusion partner ETO.* Mol Cell Biol, 1998. **18**(12): p. 7185-91.

13. Erickson, P., et al., *Identification of breakpoints in t(8;21) acute myelogenous leukemia and isolation of a fusion transcript, AML1/ETO, with similarity to Drosophila segmentation gene, runt.* Blood, 1992. **80**(7): p. 1825-31.

14. Kitabayashi, I., et al., *The AML1-MTG8 leukemic fusion protein forms a complex with a novel member of the MTG8(ETO/CDR) family, MTGR1.* Mol Cell Biol, 1998. **18**(2): p. 846-58.

15. Miyoshi, H., et al., *The t(8;21) translocation in acute myeloid leukemia results in production of an AML1-MTG8 fusion transcript.* Embo J, 1993. **12**: p. 2715-2721.

16. Miyoshi, H., et al., *t(8;21) breakpoints on chromosome 21 in acute myeloid leukemia are clustered within a limited region of a single gene, AML1.* Proc Natl Acad Sci U S A, 1991. **88**: p. 10431-10434.

17. Gamou, T., et al., *The partner gene of AML1 in t(16;21) myeloid malignancies is a novel member of the MTG8(ETO) family.* Blood, 1998. **91**(11): p. 4028-37.

18. Okuda, T., et al., *AML1, the target of multiple chromosomal translocations in human leukemia, is essential for normal fetal liver hematopoiesis.* Cell, 1996. **84**: p. 321-330.

19. Wang, Q., et al., *Disruption of the Cbfa2 gene causes necrosis and hemorrhaging in the central nervous system and blocks definitive hematopoiesis.* Proc Natl Acad Sci U S A, 1996. **93**(8): p. 3444-9.

20. Ichikawa, M., et al., *AML-1 is required for megakaryocytic maturation and lymphocytic differentiation, but not for maintenance of hematopoietic stem cells in adult hematopoiesis.* Nat Med, 2004. **10**(3): p. 299-304.

21. Growney, J.D., et al., *Loss of Runx1 perturbs adult hematopoiesis and is associated with a myeloproliferative phenotype.* Blood, 2005.

22. Meyers, S., N. Lenny, and S.W. Hiebert, *The t(8;21) fusion protein interferes with AML-1B-dependent transcriptional activation.* Mol Cell Biol, 1995. **15**(4): p. 1974-82.

23. Lutterbach, B., et al., *The MYND motif is required for repression of basal transcription from the multidrug resistance-1 promoter by the t(8;21) fusion protein.* Mol. Cell. Biol., 1998. **18**: p. 3601-3611.

24. Linggi, B., et al., *The t(8;21) fusion protein, AML1 ETO, specifically represses the transcription of the p14(ARF) tumor suppressor in acute myeloid leukemia.* Nat Med, 2002. **8**(7): p. 743-50.

25. Yang, G., et al., *Transcriptional Repression of the Neurofibromatosis-1 Tumor Suppressor by the t(8;21) Fusion Protein.* Mol Cell Biol, 2005. **25**(14): p. 5869-79.

26. Vangala, R.K., et al., *The myeloid master regulator transcription factor PU.1 is inactivated by AML1-ETO in t(8;21) myeloid leukemia.* Blood, 2003. **101**(1): p. 270-7.

27. Zhang, D.E., et al., *CCAAT enhancer-binding protein (C/EBP) and AML1 (CBF alpha2) synergistically activate the macrophage colony-stimulating factor receptor promoter.* Mol Cell Biol, 1996. **16**(3): p. 1231-40.

28. Okuda, T., et al., *Expression of a knocked-in AML1-ETO leukemia gene inhibits the establishment of normal definitive hematopoiesis and directly generates dysplastic hematopoietic progenitors.* Blood, 1998. **91**(9): p. 3134-43.

29. Yergeau, D.A., et al., *Embryonic lethality and impairment of haematopoiesis in mice heterozygous for an AML-ETO fusion gene.* Nature Genetics, 1997. **15**: p. 303-306.

30. Rhoades, K.L., et al., *Analysis of the role of AML1-ETO in leukemogenesis, using an inducible transgenic mouse model.* Blood, 2000. **96**(6): p. 2108-15.

31. Yuan, Y., et al., *AML1-ETO expression is directly involved in the development of acute myeloid leukemia in the presence of additional mutations.* Proc Natl Acad Sci U S A, 2001. **98**(18): p. 10398-403.

32. Higuchi, M., et al., *Expression of a conditional AML1-ETO oncogene bypasses embryonic lethality and establishes a murine model of human t(8;21) acute myeloid leukemia.* Cancer Cell, 2002. **1**(1): p. 63-74.

33. Grisolano, J.L., et al., *An activated receptor tyrosine kinase, TEL/PDGFbetaR, cooperates with AML1/ETO to induce acute myeloid leukemia in mice.* Proc Natl Acad Sci U S A, 2003. **100**(16): p. 9506-11.

34. Zheng, X., et al., *Cooperation between constitutively activated c-Kit signaling and leukemogenic transcription factors in the determination of the leukemic phenotype in murine hematopoietic stem cells.* Int J Oncol, 2009. **34**(6): p. 1521-31.

35. Schessl, C., et al., *The AML1-ETO fusion gene and the FLT3 length mutation collaborate in inducing acute leukemia in mice.* J Clin Invest, 2005. **115**(8): p. 2159-68.

36. Nishida, S., et al., *AML1-ETO rapidly induces acute myeloblastic leukemia in cooperation with the Wilms tumor gene, WT1.* Blood, 2006. **107**(8): p. 3303-12.

37. Schwieger, M., et al., *AML1-ETO inhibits maturation of multiple lymphohematopoietic lineages and induces myeloblast transformation in synergy with ICSBP deficiency.* J Exp Med, 2002. **196**(9): p. 1227-40.

38. Peterson, L.F., M. Yan, and D.E. Zhang, *The p21Waf1 pathway is involved in blocking leukemogenesis by the t(8;21) fusion protein AML1-ETO.* Blood, 2007. **109**(10): p. 4392-8.

39. Yan, M., et al., *A previously unidentified alternatively spliced isoform of t(8;21) transcript promotes leukemogenesis.* Nat Med, 2006. **12**(8): p. 945-9.

40. Yan, M., et al., *Deletion of an AML1-ETO C-terminal NcoR/SMRT-interacting region strongly induces leukemia development.* Proc Natl Acad Sci U S A, 2004. **101**(49): p. 17186-91.

41. Yan, M., et al., *RUNX1/AML1 DNA-binding domain and ETO/MTG8 NHR2-dimerization domain are critical to AML1-ETO9a leukemogenesis.* Blood, 2009. **113**(4): p. 883-6.

42. Melnick, A.M., et al., *The ETO protein disrupted in t(8;21)-associated acute myeloid leukemia is a corepressor for the promyelocytic leukemia zinc finger protein.* Mol Cell Biol, 2000. **20**(6): p. 2075-86.

43. McGhee, L., et al., *Gfi-1 attaches to the nuclear matrix, associates with ETO (MTG8) and histone deacetylase proteins, and represses transcription using a TSA-sensitive mechanism.* J Cell Biochem, 2003. **89**(5): p. 1005-18.

44. Chevallier, N., et al., *ETO protein of t(8;21) AML is a corepressor for Bcl-6 B-cell lymphoma oncoprotein.* Blood, 2004. **103**(4): p. 1454-63.

45. Zhang, J., et al., *E protein silencing by the leukemogenic AML1-ETO fusion protein.* Science, 2004. **305**(5688): p. 1286-9.

46. Schuh, A.H., et al., *ETO-2 associates with SCL in erythroid cells and megakaryocytes and provides repressor functions in erythropoiesis.* Mol Cell Biol, 2005. **25**(23): p. 10235-50.

47. Goardon, N., et al., *ETO2 coordinates cellular proliferation and differentiation during erythropoiesis.* Embo J, 2006. **25**(2): p. 357-66.

48. Salat, D., et al., *ETO, but not leukemogenic fusion protein AML1/ETO, augments RBP-Jkappa/SHARP-mediated repression of notch target genes.* Mol Cell Biol, 2008. **28**(10): p. 3502-12.

49. Moore, A.C., et al., *Myeloid translocation gene family members associate with T-cell factors (TCFs) and influence TCF-dependent transcription.* Mol Cell Biol, 2008. **28**(3): p. 977-87.

50. Engel, M.E., et al., *Myeloid translocation gene 16 (MTG16) interacts with Notch transcription complex components to integrate Notch signaling in hematopoietic cell fate specification.* Mol Cell Biol, 2010. **30**(7): p. 1852-63.

51. Amann, J.M., et al., *ETO, a target of t(8;21) in acute leukemia, makes distinct contacts with multiple histone deacetylases and binds mSin3A through its oligomerization domain.* Mol Cell Biol, 2001. **21**(19): p. 6470-83.

52. Lutterbach, B., et al., *The MYND motif is required for repression of basal transcription from the multidrug resistance 1 promoter by the t(8;21) fusion protein.* Mol Cell Biol, 1998. **18**(6): p. 3604-11.

53. Lutterbach, B., et al., *ETO, a target of t(8;21) in acute leukemia, interacts with the N-CoR and mSin3 corepressors.* Mol Cell Biol, 1998. **18**(12): p. 7176-84.

54. Amann, J.M., et al., *ETO, a target of t(8;21) in acute leukemia, makes distinct contacts with multiple histone deacetylases and binds mSin3A through its oligomerization domain.* Mol Cell Biol, 2001. **21**(19): p. 6470-83.

55. Calabi, F., R. Pannell, and G. Pavloska, *Gene targeting reveals a crucial role for MTG8 in the gut.* Mol Cell Biol, 2001. **21**(16): p. 5658-66.

56. Amann, J.M., et al., *Mtgr1 is a transcriptional corepressor that is required for maintenance of the secretory cell lineage in the small intestine.* Mol Cell Biol, 2005. **25**(21): p. 9576-85.

57. Martinez, J.A., et al., *Deletion of Mtgr1 sensitizes the colonic epithelium to dextran sodium sulfate-induced colitis.* Gastroenterology, 2006. **131**(2): p. 579-88.

58. Fracchiolla, N.S., et al., *EHT, a new member of the MTG8/ETO gene family, maps on 20q11 region and is deleted in acute myeloid leukemias.* Blood, 1998. **92**(9): p. 3481-4.

59. Barrett, C.W., et al., *MTGR1 is required for tumorigenesis in the murine AOM/DSS colitis-associated carcinoma model.* Cancer Res, 2011. **71**(4): p. 1302-12.

60. Lindberg, S.R., et al., *The Leukemia-associated ETO homologues are differently expressed during hematopoietic differentiation.* Exp Hematol, 2005. **33**(2): p. 189-98.

61. Hunt, A., et al., *Mtg16/Eto2 contributes to murine T-cell development.* Mol Cell Biol, 2011. **31**(13): p. 2544-51.

62. Deneault, E., et al., *A functional screen to identify novel effectors of hematopoietic stem cell activity.* Cell, 2009. **137**(2): p. 369-79.

63. Hock, H., et al., *Intrinsic requirement for zinc finger transcription factor Gfi-1 in neutrophil differentiation.* Immunity, 2003. **18**(1): p. 109-20.

64. Hock, H., et al., *Gfi-1 restricts proliferation and preserves functional integrity of haematopoietic stem cells.* Nature, 2004. **431**(7011): p. 1002-7.

65. Zeng, H., et al., *Transcription factor Gfi1 regulates self-renewal and engraftment of hematopoietic stem cells.* Embo J, 2004. **23**(20): p. 4116-25.

66. Khandanpour, C., et al., *Evidence that growth factor independence 1b regulates dormancy and peripheral blood mobilization of hematopoietic stem cells.* Blood, 2010. **116**(24): p. 5149-61.

67. Saleque, S., S. Cameron, and S.H. Orkin, *The zinc-finger proto-oncogene Gfi-1b is essential for development of the erythroid and megakaryocytic lineages.* Genes Dev, 2002. **16**(3): p. 301-6.

68. Shivdasani, R.A., E.L. Mayer, and S.H. Orkin, *Absence of blood formation in mice lacking the T-cell leukaemia oncoprotein tal-1/SCL.* Nature, 1995. **373**(6513): p. 432-4.

69. Porcher, C., et al., *The T cell leukemia oncoprotein SCL/tal-1 is essential for development of all hematopoietic lineages.* Cell, 1996. **86**(1): p. 47-57.

70. Robb, L., et al., *The scl gene product is required for the generation of all hematopoietic lineages in the adult mouse.* Embo J, 1996. **15**(16): p. 4123-9.

71. Robb, L., et al., *Absence of yolk sac hematopoiesis from mice with a targeted disruption of the scl gene.* Proc Natl Acad Sci U S A, 1995. **92**(15): p. 7075-9.

72. Mikkola, H.K., et al., *Haematopoietic stem cells retain long-term repopulating activity and multipotency in the absence of stem-cell leukaemia SCL/tal-1 gene.* Nature, 2003. **421**(6922): p. 547-51.

73. Lacombe, J., et al., *Scl regulates the quiescence and the long-term competence of hematopoietic stem cells.* Blood, 2010. **115**(4): p. 792-803.

74. Dey, S., et al., *The TAL1/SCL transcription factor regulates cell cycle progression and proliferation in differentiating murine bone marrow monocyte precursors.* Mol Cell Biol, 2010. **30**(9): p. 2181-92.

75. Yang, Q., B. Esplin, and L. Borghesi, *E47 regulates hematopoietic stem cell proliferation and energetics but not myeloid lineage restriction.* Blood, 2011. **117**(13): p. 3529-38.

76. Semerad, C.L., et al., *E2A proteins maintain the hematopoietic stem cell pool and promote the maturation of myelolymphoid and myeloerythroid progenitors.* Proc Natl Acad Sci U S A, 2009. **106**(6): p. 1930-5.

77. Seita, J. and I.L. Weissman, *Hematopoietic stem cell: self-renewal versus differentiation.* Wiley Interdiscip Rev Syst Biol Med, 2010. **2**(6): p. 640-53.

78. Till, J.E. and C.E. Mc, *A direct measurement of the radiation sensitivity of normal mouse bone marrow cells.* Radiat Res, 1961. **14**: p. 213-22.

79. Morrison, S.J., N.M. Shah, and D.J. Anderson, *Regulatory mechanisms in stem cell biology.* Cell, 1997. **88**(3): p. 287-98.

80. Challen, G.A., et al., *Mouse hematopoietic stem cell identification and analysis.* Cytometry A, 2009. **75**(1): p. 14-24.

81. Spangrude, G.J., S. Heimfeld, and I.L. Weissman, *Purification and characterization of mouse hematopoietic stem cells.* Science, 1988. **241**(4861): p. 58-62.

82. Warr, M.R., E.M. Pietras, and E. Passegue, *Mechanisms controlling hematopoietic stem cell functions during normal hematopoiesis and hematological malignancies.* Wiley Interdiscip Rev Syst Biol Med, 2011.

83. Purton, L.E. and D.T. Scadden, *Limiting factors in murine hematopoietic stem cell assays.* Cell Stem Cell, 2007. **1**(3): p. 263-70.

84. Orford, K.W. and D.T. Scadden, *Deconstructing stem cell self-renewal: genetic insights into cell-cycle regulation.* Nat Rev Genet, 2008. **9**(2): p. 115-28.

85. Kiel, M.J., et al., *SLAM family receptors distinguish hematopoietic stem and progenitor cells and reveal endothelial niches for stem cells.* Cell, 2005. **121**(7): p. 1109-21.

86. Adolfsson, J., et al., *Upregulation of Flt3 expression within the bone marrow Lin(-)Sca1(+)c-kit(+) stem cell compartment is accompanied by loss of self-renewal capacity.* Immunity, 2001. **15**(4): p. 659-69.

87. Christensen, J.L. and I.L. Weissman, *Flk-2 is a marker in hematopoietic stem cell differentiation: a simple method to isolate long-term stem cells.* Proc Natl Acad Sci U S A, 2001. **98**(25): p. 14541-6.

88. Na Nakorn, T., et al., *Myeloerythroid-restricted progenitors are sufficient to confer radioprotection and provide the majority of day 8 CFU-S.* J Clin Invest, 2002. **109**(12): p. 1579-85.

89. Orkin, S.H. and L.I. Zon, *Hematopoiesis: an evolving paradigm for stem cell biology.* Cell, 2008. **132**(4): p. 631-44.

90. Galloway, J.L. and L.I. Zon, *Ontogeny of hematopoiesis: examining the emergence of hematopoietic cells in the vertebrate embryo.* Curr Top Dev Biol, 2003. **53**: p. 139-58.

91. Rhodes, J., et al., *Interplay of pu.1 and gata1 determines myelo-erythroid progenitor cell fate in zebrafish.* Dev Cell, 2005. **8**(1): p. 97-108.

92. Passegue, E., et al., *Normal and leukemic hematopoiesis: are leukemias a stem cell disorder or a reacquisition of stem cell characteristics?* Proc Natl Acad Sci U S A, 2003. **100 Suppl 1**: p. 11842-9.

93. Lapidot, T., et al., *A cell initiating human acute myeloid leukaemia after transplantation into SCID mice.* Nature, 1994. **367**(6464): p. 645-8.

94. Stubbs, M.C. and S.A. Armstrong, *Therapeutic implications of leukemia stem cell development.* Clin Cancer Res, 2007. **13**(12): p. 3439-42.

95. Elrick, L.J., et al., *Punish the parent not the progeny.* Blood, 2005. **105**(5): p. 1862-6.

96. Tybulewicz, V.L., et al., *Neonatal lethality and lymphopenia in mice with a homozygous disruption of the c-abl proto-oncogene.* Cell, 1991. **65**(7): p. 1153-63.

97. Bilousova, G., et al., *Impaired DNA replication within progenitor cell pools promotes leukemogenesis.* PLoS Biol, 2005. **3**(12): p. e401.

98. Wang, X. and B. Seed, *A PCR primer bank for quantitative gene expression analysis.* Nucleic Acids Res, 2003. **31**(24): p. e154.

99. Boggs, D.R., *The total marrow mass of the mouse: a simplified method of measurement.* Am J Hematol, 1984. **16**(3): p. 277-86.

100. Dalla-Favera, R., et al., *Human c-myc onc gene is located on the region of chromosome 8 that is translocated in Burkitt lymphoma cells.* Proc Natl Acad Sci USA, 1982. **79**: p. 7824-7827.

101. Graninger, W.B., et al., *Expression of Bcl-2 and Bcl-2-Ig fusion transcripts in normal and neoplastic cells.* J Clin Invest, 1987. **80**(5): p. 1512-5.

102. Linggi, B.E., et al., *Translating the histone code into leukemia.* J Cell Biochem, 2005. **96**(5): p. 938-50.

103. Calabi, F., R. Pannell, and G. Pavloska, *Gene targeting reveals a crucial role for MTG8 in the gut.* Mol Cell Biol, 2001. **21**(16): p. 5658-66.

104. Brown, G.E. and G.M. Roth, *The Reduction of Hypercalcemia in Cases of Polycythemia Vera by Phenylhydrazine.* J Clin Invest, 1928. **6**(1): p. 159-69.

105. Duan, Z. and M. Horwitz, *Targets of the transcriptional repressor oncoprotein Gfi-1.* Proc Natl Acad Sci U S A, 2003. **100**(10): p. 5932-7.

106. Ivins, S., et al., *Regulation of Hoxb2 by APL-associated PLZF protein.* Oncogene, 2003. **22**(24): p. 3685-97.

107. Jegalian, A.G. and H. Wu, *Regulation of Socs gene expression by the proto-oncoprotein GFI-1B: two routes for STAT5 target gene induction by erythropoietin.* J Biol Chem, 2002. **277**(3): p. 2345-52.

108. Shaffer, A.L., et al., *BCL-6 represses genes that function in lymphocyte differentiation, inflammation, and cell cycle control.* Immunity, 2000. **13**: p. 199-212.

109. Schwartz, R., et al., *Gene expression patterns define novel roles for E47 in cell cycle progression, cytokine-mediated signaling, and T lineage development.* Proc Natl Acad Sci U S A, 2006. **103**(26): p. 9976-81.

110. Metcalf, D., et al., *Gigantism in mice lacking suppressor of cytokine signalling-2.* Nature, 2000. **405**(6790): p. 1069-73.

111. Marine, J.C., et al., *SOCS3 is essential in the regulation of fetal liver erythropoiesis.* Cell, 1999. **98**(5): p. 617-27.

112. Porse, B.T., et al., *Loss of C/EBP alpha cell cycle control increases myeloid progenitor proliferation and transforms the neutrophil granulocyte lineage.* J Exp Med, 2005. **202**(1): p. 85-96.

113. Gery, S., et al., *C/EBPepsilon interacts with retinoblastoma and E2F1 during granulopoiesis.* Blood, 2004. **103**(3): p. 828-35.

114. Porse, B.T., et al., *E2F repression by C/EBPalpha is required for adipogenesis and granulopoiesis in vivo.* Cell, 2001. **107**(2): p. 247-58.

115. Yang, L., et al., *Identification of Lin(-)Sca1(+)kit(+)CD34(+)Flt3- short-term hematopoietic stem cells capable of rapidly reconstituting and rescuing myeloablated transplant recipients.* Blood, 2005. **105**(7): p. 2717-23.

116. Bryder, D., D.J. Rossi, and I.L. Weissman, *Hematopoietic stem cells: the paradigmatic tissue-specific stem cell.* Am J Pathol, 2006. **169**(2): p. 338-46.

117. Karsunky, H., et al., *Inflammatory reactions and severe neutropenia in mice lacking the transcriptional repressor Gfi1.* Nat Genet, 2002. **30**(3): p. 295-300.

118. Person, R.E., et al., *Mutations in proto-oncogene GFI1 cause human neutropenia and target ELA2.* Nat Genet, 2003. **34**(3): p. 308-12.

119. Duprez, E., et al., *C/EBPbeta: a major PML-RARA-responsive gene in retinoic acid-induced differentiation of APL cells.* Embo J, 2003. **22**(21): p. 5806-16.

120. Pabst, T., et al., *Dominant-negative mutations of CEBPA, encoding CCAAT/enhancer binding protein-alpha (C/EBPalpha), in acute myeloid leukemia.* Nat Genet, 2001. **27**(3): p. 263-70.

121. O'Hagan, R.C., et al., *Myc-enhanced expression of Cul1 promotes ubiquitin-dependent proteolysis and cell cycle progression.* Genes Dev, 2000. **14**(17): p. 2185-91.

122. Yang, W., et al., *Repression of transcription of the p27(Kip1) cyclin-dependent kinase inhibitor gene by c-Myc.* Oncogene, 2001. **20**(14): p. 1688-702.

123. Leone, G., et al., *Myc and Ras collaborate in inducing accumulation of active cyclin E/Cdk2 and E2F.* Nature, 1997. **387**(6631): p. 422-6.

124. Look, A.T., *Oncogenic transcription factors in the human acute leukemias.* Science, 1997. **278**(5340): p. 1059-64.

125. Shroyer, N.F., et al., *Gfi1 functions downstream of Math1 to control intestinal secretory cell subtype allocation and differentiation.* Genes Dev, 2005. **19**(20): p. 2412-7.

126. Rochford, J.J., et al., *ETO/MTG8 is an inhibitor of C/EBPbeta activity and a regulator of early adipogenesis.* Mol Cell Biol, 2004. **24**(22): p. 9863-72.

127. Hall, M.A., et al., *The critical regulator of embryonic hematopoiesis, SCL, is vital in the adult for megakaryopoiesis, erythropoiesis, and lineage choice in CFU-S12.* Proc Natl Acad Sci U S A, 2003. **100**(3): p. 992-7.

128. Curtis, D.J., et al., *SCL is required for normal function of short-term repopulating hematopoietic stem cells.* Blood, 2004. **103**(9): p. 3342-8.

129. Duan, Z. and M. Horwitz, *Gfi-1 oncoproteins in hematopoiesis.* Hematology, 2003. **8**(5): p. 339-44.

130. Hall, M.A., et al., *Functional but abnormal adult erythropoiesis in the absence of the stem cell leukemia gene.* Mol Cell Biol, 2005. **25**(15): p. 6355-62.

131. Ibanez, V., et al., *AML1-ETO decreases ETO-2 (MTG16) interactions with nuclear receptor corepressor, an effect that impairs granulocyte differentiation.* Cancer Res, 2004. **64**(13): p. 4547-54.

132. Yergeau, D.A., et al., *Embryonic lethality and impairment of haematopoiesis in mice heterozygous for an AML1-ETO fusion gene.* Nature Genetics, 1997. **15**(3): p. 303-6.

133. Strom, D.K., et al., *Expression of the AML-1 oncogene shortens the G(1) phase of the cell cycle.* J Biol Chem, 2000. **275**(5): p. 3438-45.

134. Burel, S.A., et al., *Dichotomy of AML1-ETO functions: growth arrest versus block of differentiation.* Mol Cell Biol, 2001. **21**(16): p. 5577-90.

135. Santaguida, M., et al., *JunB protects against myeloid malignancies by limiting hematopoietic stem cell proliferation and differentiation without affecting self-renewal.* Cancer Cell, 2009. **15**(4): p. 341-52.

136. Shizuru, J.A., R.S. Negrin, and I.L. Weissman, *Hematopoietic stem and progenitor cells: clinical and preclinical regeneration of the hematolymphoid system.* Annu Rev Med, 2005. **56**: p. 509-38.

137. Chyla, B.J., et al., *Deletion of Mtg16, a target of t(16;21), alters hematopoietic progenitor cell proliferation and lineage allocation.* Mol Cell Biol, 2008. **28**(20): p. 6234-47.

138. Miller, C.L., B. Dykstra, and C.J. Eaves, *Characterization of mouse hematopoietic stem and progenitor cells.* Curr Protoc Immunol, 2008. **Chapter 22**: p. Unit 22B 2.

139. Thomas, P.D., et al., *PANTHER: a library of protein families and subfamilies indexed by function.* Genome Res, 2003. **13**(9): p. 2129-41.

140. Buitenhuis, M., et al., *Differential regulation of granulopoiesis by the basic helix-loop-helix transcriptional inhibitors Id1 and Id2.* Blood, 2005. **105**(11): p. 4272-81.

141. Lin, Y.C., et al., *A global network of transcription factors, involving E2A, EBF1 and Foxo1, that orchestrates B cell fate.* Nat Immunol, 2010. **11**(7): p. 635-43.

142. DeGregori, J., et al., *Distinct roles for E2F proteins in cell growth control and apoptosis.* Proc Natl Acad Sci U S A, 1997. **94**(14): p. 7245-50.

143. Plevin, M.J., et al., *The acute myeloid leukemia fusion protein AML1-ETO targets E proteins via a paired amphipathic helix-like TBP-associated factor homology domain.* Proc Natl Acad Sci U S A, 2006. **103**(27): p. 10242-7.

144. Guo, C., et al., *Multivalent binding of the ETO corepressor to E proteins facilitates dual repression controls targeting chromatin and the basal transcription machinery.* Mol Cell Biol, 2009. **29**(10): p. 2644-57.

145. Park, S., et al., *Structure of the AML1-ETO eTAFH domain-HEB peptide complex and its contribution to AML1-ETO activity.* Blood, 2009. **113**(15): p. 3558-67.

146. Hamlett, I., et al., *Characterization of megakaryocyte GATA1-interacting proteins: the corepressor ETO2 and GATA1 interact to regulate terminal megakaryocyte maturation.* Blood, 2008. **112**(7): p. 2738-49.

147. Cai, Y., et al., *Eto2/MTG16 and MTGR1 are heteromeric corepressors of the TAL1/SCL transcription factor in murine erythroid progenitors.* Biochem Biophys Res Commun, 2009. **390**(2): p. 295-301.

148. Fujiwara, T., et al., *Building multifunctionality into a complex containing master regulators of hematopoiesis.* Proc Natl Acad Sci U S A, 2010. **107**(47): p. 20429-34.

149. Bai, X., et al., *TIF1gamma controls erythroid cell fate by regulating transcription elongation.* Cell, 2010. **142**(1): p. 133-43.

150. Capron, C., et al., *The SCL relative LYL-1 is required for fetal and adult hematopoietic stem cell function and B-cell differentiation.* Blood, 2006. **107**(12): p. 4678-86.

151. Peterson, L.F. and D.E. Zhang, *The 8;21 translocation in leukemogenesis.* Oncogene, 2004. **23**(24): p. 4255-62.

152. Pabst, T., et al., *AML1-ETO downregulates the granulocytic differentiation factor C/EBPalpha in t(8;21) myeloid leukemia.* Nat Med, 2001. **7**(4): p. 444-51.

153. Cheng, T., et al., *Hematopoietic stem cell quiescence maintained by p21cip1/waf1.* Science, 2000. **287**(5459): p. 1804-8.

154. Nijnik, A., et al., *DNA repair is limiting for haematopoietic stem cells during ageing.* Nature, 2007. **447**(7145): p. 686-90.

155. Yang, L., et al., *Rho GTPase Cdc42 coordinates hematopoietic stem cell quiescence and niche interaction in the bone marrow.* Proc Natl Acad Sci U S A, 2007. **104**(12): p. 5091-6.

156. Tothova, Z., et al., *FoxOs are critical mediators of hematopoietic stem cell resistance to physiologic oxidative stress.* Cell, 2007. **128**(2): p. 325-39.

157. Rossi, D.J., et al., *Deficiencies in DNA damage repair limit the function of haematopoietic stem cells with age.* Nature, 2007. **447**(7145): p. 725-9.

158. Rogakou, E.P., et al., *DNA double-stranded breaks induce histone H2AX phosphorylation on serine 139.* J Biol Chem, 1998. **273**(10): p. 5858-68.

159. Barlow, J.H., M. Lisby, and R. Rothstein, *Differential regulation of the cellular response to DNA double-strand breaks in G1.* Mol Cell, 2008. **30**(1): p. 73-85.

160. Zierhut, C. and J.F. Diffley, *Break dosage, cell cycle stage and DNA replication influence DNA double strand break response.* Embo J, 2008. **27**(13): p. 1875-85.

161. Lovejoy, C.A., et al., *Functional genomic screens identify CINP as a genome maintenance protein.* Proc Natl Acad Sci U S A, 2009. **106**(46): p. 19304-9.

162. Paulsen, R.D., et al., *A genome-wide siRNA screen reveals diverse cellular processes and pathways that mediate genome stability.* Mol Cell, 2009. **35**(2): p. 228-39.

163. Cohn, M.A. and A.D. D'Andrea, *Chromatin recruitment of DNA repair proteins: lessons from the fanconi anemia and double-strand break repair pathways.* Mol Cell, 2008. **32**(3): p. 306-12.

164. Prasher, J.M., et al., *Reduced hematopoietic reserves in DNA interstrand crosslink repair-deficient Ercc1-/- mice.* EMBO J, 2005. **24**(4): p. 861-71.

165. Hoeijmakers, J.H., *DNA damage, aging, and cancer.* N Engl J Med, 2009. **361**(15): p. 1475-85.

166. Huang, Q., et al., *Identification of p53 regulators by genome-wide functional analysis.* Proc Natl Acad Sci U S A, 2004. **101**(10): p. 3456-61.

167. Maillard, I., et al., *Canonical notch signaling is dispensable for the maintenance of adult hematopoietic stem cells.* Cell Stem Cell, 2008. **2**(4): p. 356-66.

168. Weng, A.P., et al., *Activating mutations of NOTCH1 in human T cell acute lymphoblastic leukemia.* Science, 2004. **306**(5694): p. 269-71.

169. Krejci, O., et al., *p53 signaling in response to increased DNA damage sensitizes AML1-ETO cells to stress-induced death.* Blood, 2008. **111**(4): p. 2190-9.

170. Alcalay, M., et al., *Acute myeloid leukemia fusion proteins deregulate genes involved in stem cell maintenance and DNA repair.* J Clin Invest, 2003. **112**(11): p. 1751-61.

171. Bhaskara, S., et al., *Deletion of histone deacetylase 3 reveals critical roles in S phase progression and DNA damage control.* Mol Cell, 2008. **30**(1): p. 61-72.

172. O'Connor, O.A., et al., *Clinical experience with intravenous and oral formulations of the novel histone deacetylase inhibitor suberoylanilide hydroxamic acid in patients with advanced hematologic malignancies.* J Clin Oncol, 2006. **24**(1): p. 166-73.

173. Socolovsky, M., *Molecular insights into stress erythropoiesis.* Curr Opin Hematol, 2007. **14**(3): p. 215-24.

174. Liu, Y., et al., *The p53 tumor suppressor protein is a critical regulator of hematopoietic stem cell behavior.* Cell Cycle, 2009. **8**(19): p. 3120-4.

175. Jacks, T., et al., *Tumor spectrum analysis in p53-mutant mice.* Curr Biol, 1994. **4**(1): p. 1-7.